

**UNIVERSITY OF CALGARY**

**Forecasting Shear Strength  
and Skier-Triggered Avalanches  
for Buried Surface Hoar Layers**

**By**

**Thomas S. Chalmers**

**A THESIS**

**SUBMITTED TO THE FACULTY OF GRADUATE STUDIES  
IN PARTIAL FULFILLMENT OF THE REQUIREMENTS FOR THE  
DEGREE OF MASTER OF SCIENCE**

**DEPARTMENT OF CIVIL ENGINEERING**

**CALGARY, ALBERTA**

**SEPTEMBER, 2001**

**© Thomas Scott Chalmers 2001**



**National Library  
of Canada**

**Acquisitions and  
Bibliographic Services**

**385 Wellington Street  
Ottawa ON K1A 0N4  
Canada**

**Bibliothèque nationale  
du Canada**

**Acquisitions et  
services bibliographiques**

**385, rue Wellington  
Ottawa ON K1A 0N4  
Canada**

*Your file Votre référence*

*Our file Notre référence*

**The author has granted a non-exclusive licence allowing the National Library of Canada to reproduce, loan, distribute or sell copies of this thesis in microform, paper or electronic formats.**

**The author retains ownership of the copyright in this thesis. Neither the thesis nor substantial extracts from it may be printed or otherwise reproduced without the author's permission.**

**L'auteur a accordé une licence non exclusive permettant à la Bibliothèque nationale du Canada de reproduire, prêter, distribuer ou vendre des copies de cette thèse sous la forme de microfiche/film, de reproduction sur papier ou sur format électronique.**

**L'auteur conserve la propriété du droit d'auteur qui protège cette thèse. Ni la thèse ni des extraits substantiels de celle-ci ne doivent être imprimés ou autrement reproduits sans son autorisation.**

**0-612-65149-5**

**Canada**

## **Abstract**

Surface hoar crystals grow on the snow surface and can form a persistent weak layer in the snowpack when buried. Skiers may trigger slab avalanches on such layers, which can be difficult to predict.

During the winters 1992-2001, measurements of snowpack and surface hoar layers were collected at study sites in the Columbia Mountains. This data was used to develop three models to predict the shear strength of buried surface hoar layers. The Interval model accounts for 72% of the variability in the data, and forecasts shear strength to within 18% of measured values.

Snowpack measurements were used to calculate a skier stability index for a number of buried surface hoar layers. It was shown that this index is a predictor of regional skier-triggered avalanche activity on these layers. A shear strength model was used to forecast this stability index, which may be useful for operational avalanche forecasting.

## **Acknowledgements**

This project would not have been possible without Dr. Bruce Jamieson, who provided training, guidance, advice, funding, proofreading, and patient answers to many questions.

For financial support, I thank the Natural Sciences and Engineering Research Council of Canada.

For collecting the data for this study, I owe thanks to all of the technicians employed by the University of Calgary Applied Snow and Avalanche Research Group from the years 1992-2001. Special thanks to Michelle Gagnon, Jill Hughes, Ben Crane Johnson, Greg Johnson, Alan Jones, Kalle Kronholm, Paul Langevin, and Kyle Stewart.

I thank Mike Wiegele Helicopter Skiing and Canadian Mountain Holidays for providing avalanche occurrence data.

For daily advice, support, and many good snow talks, I thank the Avalanche Control Section of Glacier National Park: David Skjonsberg, Bruce McMahon, Jeff Goodrich, John Kelly, Eric Dafoe, Dean Flick, Edwin Knox, Johan Schleiss, and Steve Thomas.

For supplying snowboard equipment and clothing, I thank Burton Snowboards and RED Corp.: Chris Mask, Scott Oliver, David Van Mullen, Scott Taylor, and Kristin Geishecker.

Finally, I would like to thank my family, friends, and backcountry partners, for encouragement, places to sleep, and many unforgettable days in the mountains. Special thanks to Darlene Chalmers for being a good listener.

## **Table of Contents**

Approval page.....	ii
Abstract.....	iii
Acknowledgements.....	iv
Table of contents.....	v
List of tables.....	viii
List of figures.....	ix
Notation.....	x
1 Introduction.....	1
1.1 Snow avalanches.....	1
1.2 The mountain snowpack.....	1
1.3 Avalanche formation.....	2
1.4 Weak layers in the snowpack.....	4
1.5 Surface hoar.....	5
1.6 Snowpack metamorphism.....	7
1.7 Snowpack observations.....	7
1.8 The role of the avalanche forecaster.....	8
1.9 Objectives.....	10
1.10 Overview of this study.....	11
2 Literature review.....	12
2.1 Introduction.....	12
2.2 Surface hoar.....	12
2.2.1 Surface hoar forms and orientations.....	12
2.2.2 Meteorological conditions favoring surface hoar growth.....	13
2.2.3 Conditions for surface hoar to form a persistent weak layer.....	13
2.2.4 Surface hoar and slab avalanches.....	14
2.2.5 Bonding of surface hoar to adjacent layers.....	14
2.2.6 Changes in structure of buried surface hoar crystals.....	16
2.2.7 Changes in structure of buried surface hoar layers.....	17
2.2.8 Inclination of buried surface hoar layers.....	17
2.2.9 Density of surface hoar deposits.....	18
2.2.10 Thinning of buried surface hoar layers.....	18
2.2.11 Rate of strength change of buried surface hoar layers.....	20
2.2.12 Observing texture of buried surface hoar layers.....	20
2.2.13 Snowpack factors associated with strength change of buried surface hoar.....	21
2.2.14 Physically-based snowpack models and surface hoar weak layer evolution.....	24
2.3 Stability indices.....	24
2.4 Extrapolated study plot measurements for avalanche forecasting.....	26
2.5 Summary.....	27

<b>3 Methods</b> .....	<b>28</b>
3.1 Study areas and co-operating organisations.....	28
3.2 Sites for snowpack observations.....	30
3.2.1 Study plots and slopes.....	30
3.2.2 Study sites with automated meteorological stations.....	30
3.2.3 Airbox study sites.....	31
3.3 Equipment.....	32
3.3.1 Manual snow study equipment.....	32
3.3.2 Automated meteorological equipment.....	34
3.4 Measurement procedures.....	34
3.4.1 Snowpack properties.....	34
3.4.2 Photographic techniques.....	37
3.5 Avalanche activity.....	38
<b>4 Predicting shear strength of buried surface hoar layers</b> .....	<b>39</b>
4.1 Introduction.....	39
4.1.1 Goals of a shear strength prediction model.....	39
4.1.2 Snowpack and shear strength measurement variables.....	39
4.1.3 Shear strength of buried surface hoar layers in the Columbia Mountains.....	40
4.2 Shear Strength—Power Law model.....	44
4.2.1 Introduction.....	44
4.2.2 Dataset.....	45
4.2.3 Parameter fitting for individual time series.....	45
4.2.4 Description of parameter values.....	49
4.2.5 Snowpack factors influencing model parameters.....	51
4.2.6 Results.....	55
4.3 Shear Strength—Interval model.....	56
4.3.1 Introduction.....	56
4.3.2 Dataset.....	57
4.3.3 Distribution of measured data.....	57
4.3.4 Snowpack variables.....	61
4.3.5 Initial regression.....	65
4.3.6 Refinement via outlier analysis.....	67
4.3.7 Refinement via variable selection.....	70
4.3.8 Simplified regression.....	72
4.3.9 Comparison of initial and simplified regression.....	72
4.3.10 Residual analysis.....	74
4.3.11 Model formula.....	78
4.4 Shear Strength—Lagged Load model.....	79
4.4.1 Introduction.....	79
4.4.2 Dataset.....	80
4.4.3 Formulation and construction.....	81
4.4.4 Determining lag effects.....	82
4.4.5 Model formula.....	84

4.5 Model testing .....	85
4.5.1 Introduction.....	85
4.5.2 Fit to model-building dataset .....	86
4.5.3 Test layers .....	89
4.5.4 Selecting the best model .....	89
4.6 Summary .....	91
5 Forecasting skier-triggered avalanches.....	93
5.1 Introduction.....	93
5.2 Dataset.....	94
5.3 Extrapolated skier stability index.....	95
5.4 Extrapolated model skier stability index.....	100
6 Conclusions.....	101
6.1 Conclusions.....	101
6.2 Suggestions for further research .....	102
References.....	104
Appendix.....	108

## List of Tables

No.	Title	Page
3.1	Study sites .....	28
4.1	Snowpack variables and units .....	40
4.2	Time series of surface hoar layers 1992-2001 .....	42
4.3	Time series with 4 or more measurements during the first 30 days of burial .....	46
4.4	Descriptive statistics for $\Sigma_1$ and $A$ .....	49
4.5	General forms of snowpack variables for Power Law model .....	51
4.6	Spearman rank correlations of $\Sigma_1$ and $A$ with snowpack variables .....	52
4.7	Results of regression for $\Sigma_1$ with $\sigma_1$ .....	54
4.8	Results of regression for $A$ with $\sigma_1$ .....	54
4.9	Surface hoar layers used in Interval model .....	58
4.10	Descriptive statistics for $\Sigma_i$ and $(\Delta\Sigma/\Delta t)_{ij}$ .....	57
4.11	General forms of snowpack variables for Interval model .....	61
4.12	Spearman rank correlations between variables in Interval model .....	62
4.13	Results of initial multiple stepwise least-squares regression on $(\Delta\Sigma/\Delta t)_{ij}$ .....	66
4.14	Results of initial multiple stepwise least-squares regression on $\Sigma_i$ .....	66
4.15	Outliers of initial regression on $(\Delta\Sigma/\Delta t)_{ij}$ and $\Sigma_i$ .....	67
4.16	Cross correlations between predictor variables, initial regression .....	72
4.17	Results of simplified multiple stepwise regression on $(\Delta\Sigma/\Delta t)_{ij}$ .....	73
4.18	Results of simplified multiple stepwise regression on $\Sigma_i$ .....	73
4.19	Surface hoar series for the Lagged load model .....	81
4.20	Results of fitting Lagged load model .....	83
4.21	Results of testing fit of model to model-building data .....	86
4.22	Results of model forecasting for test layers .....	89
5.1	Surface hoar time series used in forecasting application .....	94
5.2	Contingency table for testing $Sk_{38}$ .....	95
5.3	Master contingency table and results of testing $Sk_{38}$ .....	99

## List of Figures

No.	Title	Page
1.1	A loose snow avalanche.....	2
1.2	A slab avalanche.....	2
1.3	Schematic of a typical slab avalanche.....	3
1.4	Surface hoar on the snow surface.....	6
1.5	A layer of buried surface hoar.....	6
1.6	A snow profile.....	9
1.7	Collecting data in a snow pit.....	9
1.8	Performing the shear frame test.....	9
3.1	Study areas in the Columbia Mountains.....	29
3.2	Folding ruler, crystal screen and magnifier in use.....	33
3.3	Pit wall photography.....	33
4.1	Shear strength of the surface hoar layer buried 20-January-2001.....	41
4.2	Residuals of regression on untransformed Equation 4.1.....	48
4.3	Residuals of regression on transformed Equation 4.2.....	48
4.4	Distribution of $\Sigma_1$ values from Table 4.3.....	50
4.5	Distribution of A values from Table 4.3.....	50
4.6	Distribution of $(\Delta\Sigma/\Delta t)_{ij}$ .....	60
4.7	Distribution of $\Sigma_i$ .....	60
4.8	Distribution of residuals of initial regression on $(\Delta\Sigma/\Delta t)_{ij}$ .....	68
4.9	Distribution of residuals of initial regression on $\Sigma_i$ .....	68
4.10	Surface hoar disaggregated from 23-January-1999 weak layer.....	71
4.11	Surface hoar disaggregated from 30-December-1999 weak layer.....	71
4.12	Scatter of residuals of simplified regression on $(\Delta\Sigma/\Delta t)_{ij}$ .....	76
4.13	Scatter of residuals of simplified regression on $\Sigma_i$ .....	76
4.14	Distribution of residuals of simplified regression on $(\Delta\Sigma/\Delta t)_{ij}$ .....	77
4.15	Distribution of residuals of simplified regression on $\Sigma_i$ .....	77
4.16	Shear strength and daily load on the layer of surface hoar buried 20-January-2001.....	80
4.17	Observed vs. predicted shear strength, Power Law model.....	87
4.18	Observed vs. predicted shear strength, Interval model.....	87
4.19	Observed vs. predicted shear strength, Lagged Load model.....	87
4.20	Testing model fit to model-building data.....	88
4.21	Testing model forecast shear strength for test layers.....	90
5.1	Skier stability index $Sk_{38}$ and associated skier-triggered avalanche activity..	96

## **Notation**

$\Sigma$	Shear strength of a layer of buried surface hoar
$\sigma$	Overburden stress (load) on a layer of buried surface hoar
$\rho$	Density of snow layer
A	Exponential shear strength growth term
$E_{min}$	Minimum characteristic crystal size of a layer of buried surface hoar
$E_{max}$	Maximum characteristic crystal size of a layer of buried surface hoar
g	Acceleration due to gravity
h	Thickness (measured vertically) of a snowpack layer
H	Thickness of slab (measured vertically) overlying a layer of buried surface hoar
HS	Height of snowpack
m	Mass of snow slab core sample
N	Number of observation/measurement days of a buried surface hoar layer
$Sk_{38}$	Skier stability index
t	Time (days) since burial of a surface hoar layer by snowfall
$T_{wl}$	Temperature in the middle of a layer of buried surface hoar
TG	Magnitude of temperature gradient (measured vertically) through a layer of buried surface hoar
Thick	Thickness of a layer of buried surface hoar

## **1. INTRODUCTION**

### **1.1 Snow avalanches**

In mountainous regions throughout the world, snow avalanches are the rule, and not the exception. Snow avalanches affect tourism, construction, and transportation industries by causing death, injury, property damage, as well as closure and delays on mountainous roads. Although the number of Canadian avalanche fatalities involving buildings, roads, and work sites shows a decreasing trend in the last forty years, the number of recreational fatalities does not show signs of decrease as backcountry winter activities become increasingly popular (Jamieson and Geldsetzer, 1996, pp. 8-9). Understanding factors in the snowpack that lead to avalanche activity is the role of both avalanche forecaster and researcher; better understanding can help save lives in the backcountry.

### **1.2 The mountain snowpack**

A typical mountain snowpack will, over the course of a given winter, exhibit a layered stratigraphy of different snow forms. Each of these layers will have different properties, including constituent snow grains, density, hardness, liquid water content, etc. Often the snowpack includes a slab of several strong layers overlying a weak layer. This weak layer can act as the failure plane for slab avalanches.

The mountain snowpack characteristically exhibits considerable spatial variability in its makeup within a given region and across individual slopes. Such variability is due to factors including wind exposure, aspect to incoming solar radiation, ground cover characteristics, elevation, incline, and others.

### 1.3 Avalanche formation

In speaking of avalanches, it is common practice to divide them into two distinct categories, based on the mechanism of release: point release (loose snow) avalanches and slab avalanches (e.g. Canadian Avalanche Association, 1995). A point release avalanche (Figure 1.1) occurs when a small amount of cohesionless snow releases from the surface of a slope and sets other snow in motion. This produces a characteristic triangular pattern of snow release, with the original release point at the apex. A slab avalanche (Figure 1.2) occurs when a slab of cohesive snow is released in a block by a failure at depth, and is characterised by a fracture line or crown at the top of the avalanche. Slab avalanches are typically larger than loose snow avalanches and start in a weak layer below the constituent layers of the snow slab (e.g. McClung, 1987).



**Figure 1.1:** A loose snow avalanche.  
B. Jamieson photo.

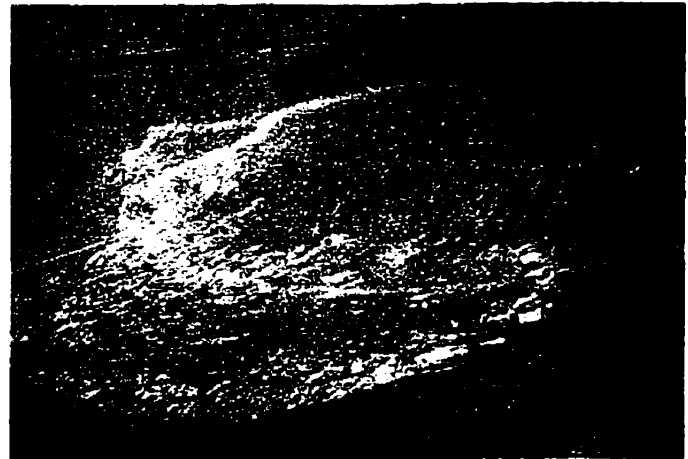


**Figure 1.2:** A slab avalanche.  
B. Jamieson photo.

This study undertakes to gain greater understanding of slab avalanches on weak layers of buried surface hoar crystals.

Slab avalanches can be either triggered (by skiers, explosives, over-snow machines, cornice fall, etc.) or release naturally (spontaneously). In the case of rapid loading, such as that by a skier, slab avalanches release when the stress on the snowpack (due to the weight of slab plus triggers if applicable) is greater than the strength of the weak layer underlying the slab. Release is thus a function of the properties of the overlying slab and of the weak layer, in addition to any applicable triggers.

Skier-induced stresses on the snowpack decrease with increasing slab thickness, and skiers are not usually effective triggers on slabs thicker than one meter (e.g. Föhn, 1987; Schweizer and Jamieson, 2001).

Slab avalanche failure and release (Figure 1.3) is often described as a shear failure in a weak layer (which causes tension in the overlying slab), followed by a propagat-

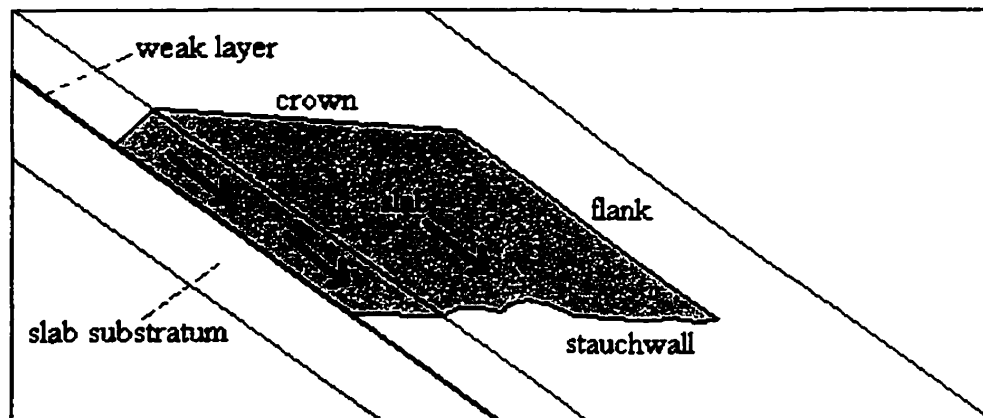


**Figure 1.3:** Schematic of a typical slab avalanche (after McClung and Schaerer, 1993, p.75).

ing shear fracture in the weak layer, then a tensile fracture at the crown (upper horizontal wall) of the avalanche, then shear failure at the flanks (sidewalls) (McClung and Schaerer, 1993, pp. 80-83).

#### **1.4 Weak layers in the snowpack**

Weak layers in the snowpack can be termed either persistent or non-persistent. Non-persistent weak layers, also called new snow or storm instabilities, usually take the form of a low density layer of large precipitation particles that exhibits lower strength than adjacent layers of new snow particles. Non-persistent weak layers generally stabilise within a few days of forming (Jamieson, 1995, p. 10). Jamieson and Johnston (1992) found that non-persistent weak layers commonly play a role in fatal backcountry avalanches involving amateur (recreational) decision makers, but not with professional decision-makers.

Persistent weak layers can remain unstable in the snowpack for a month or more when buried and are made of one of three crystal types: facets, depth hoar, and surface hoar. Facets and surface hoar can form on or near the snow surface and can become the failure planes for slab avalanches once buried by snowfall. Facets can also form within the snowpack. Depth hoar is an advanced form of faceted crystals typically found close to ground in shallower snowpacks. A persistent weak layer may vary quite considerably over a local region, such that they are quite capable of surprising professional decision-makers in the backcountry (Jamieson and Geldsetzer, 1999). These persistent weak layers account for most of the slab avalanche fatalities in Canada from 1972 to 1992 (Jamieson and Johnston, 1992). Studies have shown that thin (i.e. less than 10 mm

thick) persistent weak layers are most important to slab avalanche failure (e.g. Föhn, 1992), and therefore are of considerable importance in avalanche forecasting.

Based on reports of 93 fatal slab avalanches in Canada between 1972 and 1991, Jamieson and Johnston (1992) estimate that persistent weak layers of surface hoar, facets, or depth hoar were involved in 91% of fatal slab avalanches and “almost all” avalanche accidents involving snow professionals. In a survey of 153 experienced western Canadian avalanche professionals (Jamieson and Geldsetzer, 1999), 71% of unexpected skier-triggered avalanches involved the aforementioned persistent weak layers, 55% of which were surface hoar.

### **1.5 Surface hoar**

Surface hoar or “hoarfrost” consists of highly faceted crystal forms, which grow on the snow surface (Figure 1.4) by the deposition of water vapour from the air above the snow surface (e.g. Colbeck, 1987; Lang et al., 1984). This occurs most often during clear, cold, fairly calm nights when the air near the snow surface cools to its dewpoint. Once buried by snowfall (Figure 1.5), surface hoar layers are characteristically weak due to few intercrystalline bonds within the layer and poor bonding to over- and underlying layers in the snowpack (e.g. Lang et al., 1984; Colbeck, 1987). These weak layers may remain reactive as a failure plane for slab avalanches for several weeks or more (e.g. Föhn, 1992). Even when no longer a factor in avalanche occurrences, a surface hoar layer can remain visible in the snowpack for an extended period, such that, “a dramatic change in snowpack conditions...is required to completely destroy a hoar layer,” (Lang et al., 1984).



**Figure 1.4:** Surface hoar on the snow surface. Applied Snow and Avalanche Research Consortium (ASARC) photo.

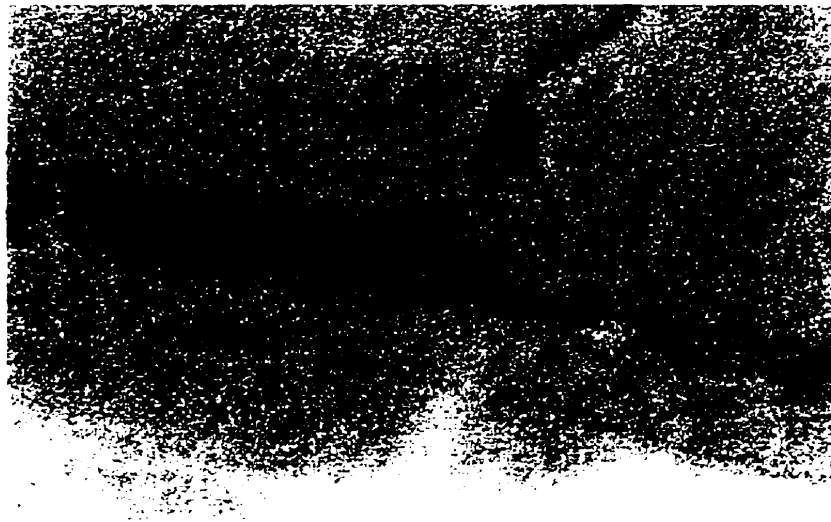


**Figure 1.5:** A layer of buried surface hoar. Region on right displaced due to failure of surface hoar layer. ASARC photo.

Once a shear fracture has been initiated under a snow slab, it can propagate within surface hoar layers, through areas where the surface hoar could not be triggered by a skier (Jamieson, 1995, pp. 185-194). Thus, when triggered at an isolated weakness in the snowpack, surface hoar may allow fractures through regions of the snowpack that were apparently stable, making such events surprising and dangerous to avalanche professionals.

### **1.6 Snowpack metamorphism**

In a dry mountain snowpack (below 0°C), there are two processes affecting the metamorphism of the snow crystals, rounding (equilibrium) and faceting (kinetic). The dominant process depends on the magnitude of the temperature gradient, measured vertically in the snowpack. Rounding metamorphism occurs when the temperature gradient is less than 10°C m<sup>-1</sup> in magnitude, and is associated with more rapid bonding between crystals and strength gain. Rounding will tend to occur in areas with thicker snowpacks and warmer temperatures. Faceting metamorphism occurs when the temperature gradient is greater than 10°C m<sup>-1</sup> in magnitude, and is associated with little bonding between crystals and slower strength gain. Faceting will tend to occur in areas with thinner snowpacks and colder temperatures (e.g. Akitaya, 1974; Colbeck, 1987).

### **1.7 Snowpack observations**

Snowpack observations for this project were made at fixed study sites in the Columbia Mountains of British Columbia.

Fixed study sites enable the collection of consistent, temporally continuous snowpack data; the evolution of specific layers may be monitored throughout the winter.

The snow profile is a depthwise cross-section of the snowpack (Figure 1.6). The profile represents data collected from a snow pit (Figure 1.7) dug at an undisturbed site. The important layers in the snowpack are identified, recording the grain type and size, hand hardness (resistance to penetration), density, and liquid water content of each layer, as well as a temperature profile of the snowpack. More detail on snow profiles can be found in the *Observation Guidelines and Recording Standards for Weather, Snowpack and Avalanches* (Canadian Avalanche Association, 1995).

Once identified in the snow profile, the strength of a buried surface hoar layer can be measured with a shear frame test (Jamieson and Johnston, 2001). This involves placing a sheet metal frame in the snow directly above the weak layer and pulling manually with a force gauge to cause a brittle shear failure in the weak layer (Figure 1.8). The shear strength of the layer is the maximum force read on the gauge divided by the area of the frame. The details of this technique will be discussed in Chapter 3.

### **1.8 The role of the avalanche forecaster**

Performing a snow stability evaluation in order to assess the avalanche hazard in an area has long been the role of the avalanche forecaster (e.g. McClung and Schaerer, 1993, p.164). The parameters observed by forecasters or their staff in the course of their duties are divided into Class I, II, and III factors (McClung and Schaerer, 1993, p.125). The lower the class number, the more directly the factor relates to avalanche release.



Class I factors include avalanche activity and mechanical tests of snow stability (such as explosive and ski testing, Rutschblock and compression tests). Class II factors are snowpack factors, which come from within the snow cover (such as shear strength of layers, snowpack stratigraphy, hardness of layers, temperatures, densities, grain types of layers, etc.). Class III factors are meteorological data (such as wind, precipitation, temperature, solar radiation). Weather (Class III) begets the snowpack (Class II) which begets avalanches (Class I) (LaChapelle, 1980; McClung and Schaerer, 1993, pp. 124-150).

Some Class I and II factors are based on point observations of the snowpack and therefore subject to spatial variability, a consideration that limits interpretation.

### **1.9 Objectives**

Class I factors are the most direct indicators of snow stability. Class I factors such as avalanche activity and mechanical stability tests are commonly used by the forecaster, but quantitative tests of weak layer strength are not. This is because such tests, like the shear frame test, require special equipment and training, and thus are not commonly used operationally.

The goal of this study is to develop a model that relates the strength of a buried weak layer of surface hoar to commonly observed (Class II) snowpack factors. Thus, standard observation techniques may be used to estimate the strength of a buried surface hoar layer in the Columbia Mountains. Furthermore, this study also aims to construct a model for predicting future changes in the shear strength of a buried surface hoar layer.

If such a model is successful, not only will the avalanche forecaster have knowledge of another means of evaluating snow stability, but also will have access to a new forecasting tool for the Columbia Mountains.

### **1.10 Overview of this study**

Chapter 1 of this study introduces the role of buried surface hoar as a persistent weak layer in the mountain snowpack and outlines the means by which an avalanche forecaster evaluates snow stability. The merit of a model to predict the strength of buried surface hoar layers is presented. Chapter 2 reviews the literature on buried surface hoar layers, stability indices, and the extrapolation of study site measurements for forecasting avalanche activity. Chapter 3 discusses the methods and locations of data collection for this study. In Chapter 4, several models to predict the strength of buried surface hoar layers are developed and evaluated. Chapter 5 examines an application of a shear strength prediction model for regional avalanche forecasting. Chapter 6 presents conclusions from this study and provides some suggestions for further research.

## **2. LITERATURE REVIEW**

### **2.1 Introduction**

This chapter reviews the literature on surface hoar in Section 2.2, stability indices and avalanche forecasting in Section 2.3, and extrapolation of study plot measurements for avalanche forecasting in Section 2.4. The results of the literature review are summarised in Section 2.5.

### **2.2 Surface hoar**

#### **2.2.1 Surface hoar forms and orientations**

In general, the shape and growth rate of surface hoar crystals depends on environmental factors at the time of formation, such as temperature, degree of supersaturation of the water vapour, and wind (e.g. Kobayashi, 1961). Surface hoar is commonly seen as “hexagonal plate-type crystals” (Lang et al., 1984); these wedge shapes, or sector plates, are the most frequent form of surface hoar in snow profiles and failure layers of slab avalanches in the Columbia Mountains of western Canada (Jamieson and Schweizer, 2000). However, a number of different one, two, and three dimensional forms have been observed, such that Jamieson and Johnston (1997) and Jamieson and Schweizer (2000) propose some subclasses of surface hoar type crystals: wedges (sector plates), feathers (dendritic forms), spikes/needles, cups, and combinations of such growth forms in a single grain.

Surface hoar can range in size from a few millimetres to a few centimetres (Jamieson and Schweizer, 2000). Most surface hoar crystals grow wider as they grow upward (Lang et al., 1984; Breyfogle, 1986).

Surface hoar, especially sector plates, usually grows oriented within a few degrees of the snow surface normal, but dendritic forms and rimed needles have been observed to grow with a range of orientations within sixty degrees of the surface normal (Lang et al., 1984).

Many surface hoar layers exhibit crystals with faces aligned parallel. Colbeck (1988) argues that they are aligned by near-surface winds, which play a role in the formation of the crystals.

### **2.2.2 Meteorological conditions favouring surface hoar growth**

Surface hoar growth is generally favoured during fairly calm, clear nights with high relative humidity (70% or greater) in the air near the snow surface (Breyfogle, 1986; Hachikubo and Akitaya, 1998). Surface hoar formation begins when the snow surface temperature cools, via outgoing long-wave radiation, to the dewpoint of the overlying saturated air mass and water vapour deposition from the air to the surface is possible (e.g. Lang et al., 1984).

### **2.2.3 Conditions for surface hoar to form a persistent weak layer**

In order for a given surface hoar layer to become an effective persistent weak layer (i.e. prone to act as a failure layer for slab avalanches for more than a week after burial), it must be buried intact (relatively unaffected by destructive forces such as high winds, warm temperatures, or rain) following its growth on the surface (e.g. Breyfogle, 1986). Ideally, this entails burial soon after its formation by a snowfall of low intensity

and density with large precipitation particles (Breyfogle, 1986). Such snowfall has little erosive effect on the surface hoar crystals and does not fill in the spaces between crystals with precipitation particles that will form bonds within the surface hoar layer.

#### **2.2.4 Surface hoar and slab avalanches**

Skier-triggered slab avalanches on layers of buried surface hoar occur mostly within the first 15 to 20 days after a layer is buried (Chalmers and Jamieson, in press). Accidental skier-triggered avalanches which occur later in this period are less frequent and often larger, and more difficult to predict. The transition of buried surface hoar layers from unstable to stable conditions is difficult for avalanche professionals to forecast (Chalmers and Jamieson, in press).

#### **2.2.5 Bonding of surface hoar to adjacent layers**

Wedge or sector plate forms comprise the largest percentage of surface hoar failure layers of slab avalanches in the Columbia Mountains (Jamieson and Johnston, 1997), suggesting that this form is especially effective at forming persistent weak layers prone to releasing avalanches. Jamieson and Schweizer (2000) report many observations of surface hoar wedges in the failure layers of slab avalanches, but have never observed surface hoar needles in such layers.

Wedges are much wider at the top of the crystals than the bottom, which can create an “umbrella” effect when new snow buries the layer, which presumably prevents new snow grains from falling between and forming bonds to adjacent surface hoar crystals (Davis et al., 1996). This umbrella effect is greater when the surface hoar crystals

have grown over a range of orientations than when they have grown oriented in a single direction, such as surface normal (Jamieson and Schweizer, 2000). Varying orientations will create far more contact area between the surface hoar crystals and the adjoining upper layer than at the lower layer, which most likely results in larger and more numerous bonds at the top of the surface hoar layer and smaller bonds at the bottom of the layer (Geldsetzer et al., 1997). No measurements of these bonds have yet been made to corroborate this idea. Snowpack tests support this idea; surface hoar crystals are often stuck to the overlying slab following fracture tests, but are rarely found stuck to the layer below (Jamieson and Johnston, 1997; Jamieson and Schweizer, 2000).

The proposed smaller bonds and fewer bonds per unit area at the base of a surface hoar layer, compared to the top of the layer, should result in differentially lower shear strength, such that the failure of a surface hoar layer will typically depend on failure of the bonds at the base of the layer (e.g. Jamieson and Johnston, 1997, Jamieson and Schweizer, 2000). An increase in bonding over time between the surface hoar layer and the layer below has been proposed as a mechanism accompanying strength increase of the weak layer (Davis et al., 1996; Jamieson and Schweizer, 2000).

Although bonds between surface hoar and adjacent layers have been postulated to be of primary importance to the strength of buried surface hoar layers, there are no quantitative physical or mechanical models of bonding between surface hoar and adjacent layers in the snowpack.

### **2.2.6 Changes in structure of buried surface hoar crystals**

Just subsequent to burial, observations of disaggregated crystals from surface hoar layers in the Columbia Mountains show a minimum size from 2-20 mm (average 4 mm) and a maximum size from 3-30 mm (average 10 mm) (Jamieson and Schweizer, 2000). As time passes following burial, whole surface hoar crystals show little size decrease, even over periods as long as two or more months (Jamieson and Johnston, 1997), although such a size decrease has been reported by field workers who observe disaggregated, often broken crystals (Jamieson and Schweizer, 2000). During this time, the strength of the buried surface hoar layer may increase dramatically, such that, “change in size of disaggregated crystals is probably a poor indicator of strength (of the weak layer),” (Davis et al., 1996).

The initial size of the constituent crystals of a given surface hoar layer may be important to the strength of the layer. As suggested by Jamieson and Johnston (1997), “(a layer of) large surface hoar tends to have lower initial strength and be slower to stabilise than (a layer of) smaller crystals.” In one study, most avalanches involving a buried surface hoar layer had a fairly large mean crystal size of 7 mm (Breyfogle, 1986), which corroborates this idea, although smaller surface hoar cannot be ruled out as a failure layer.

Surface hoar crystals often initially have striations and sharp edges, but following burial said crystals “often lose sharp edges and become rounded,” (Colbeck, 1991), and small grains will cluster and bond to the crystals (Geldsetzer et al., 1997), both of which are observable by field workers (Jamieson and Schweizer, 2000). These processes of rounding and clustering appear to be associated with strengthening of the surface hoar

layer (Geldsetzer et al., 1997), which may in turn be associated with increased bonding at the bases of the surface hoar crystals (Jamieson and Johnston, 1997). This effect has not been measured nor quantified, but observed temperature gradients across buried surface hoar layers in the Columbia Mountains fall in the range which is indicative of such rounding (equilibrium) metamorphism and sintering of snow grains (Jamieson and Schweizer, 2000).

### **2.2.7 Changes in structure of buried surface hoar layers**

Jamieson and Schweizer (2000) used microphotography of surface hoar layers in-situ to make observations on the regular arrangement of the constituent surface hoar grains. Chalmers and Jamieson (in press) used the same technique and found that surface hoar layers do not necessarily have a regular arrangement of grains, concluding that changes in layer strength are not consistently indicated by changes in structure that are observable with this technique.

### **2.2.8 Inclination of buried surface hoar layers**

Buried surface hoar crystals are often observed to be inclined past slope normal (e.g. Davis et al., 1998). Jamieson and Schweizer (2000) calculated that this inclination of the crystals over time indicated a strain rate in the buried surface hoar layer which is 4 to 12 times greater than that of “settled” snow layer on a slope. This strain concentration in the relatively thin buried weak layer could contribute to slab avalanche failure. This supports the idea that thin persistent weak layers and interfaces are most important to slab avalanche failure (e.g. Föhn, 1992). This inclination of crystals is difficult to ob-

serve in the field, however, and is of limited use in describing a surface hoar layer.

### **2.2.9 Density of surface hoar deposits**

The number of surface hoar crystals deposited over a given area will vary considerably due to prevailing meteorological conditions at the time they are formed (Breyfogle, 1986; Schweizer et al; 1996). Geldsetzer and others (1997) suggested that higher deposit densities can result in greater strength of buried surface hoar layers, probably due to the larger number of bonds per unit area at the base. No field methods exist to measure deposit density, nor is there a physical model to explain the number of bonds per unit area.

Colbeck (1991) noted that, “buried surface hoar layers are usually uniform over distances hundreds of times the thickness of the snow cover.” However, it is important to realise that surface hoar deposition can be so variable as to leave isolated pockets of surface hoar over large avalanche start zones (Breyfogle, 1986). Furthermore, the texture of a buried surface hoar layer may also exhibit considerable spatial variability. This can make the existence and extent of a buried surface hoar layer difficult to predict based on point observations of the snowpack in avalanche start zones.

### **2.2.10 Thinning of buried surface hoar layers**

Soon after burial, a layer of surface hoar has a thickness approximately equal to the measured size of the larger crystals in the layer (Jamieson and Schweizer, 2000), and will become about 20-44% thinner in the first ten to twenty days subsequent to burial (Chalmers and Jamieson, in press; Davis et al., 1996). The initial rapid thinning of the

layer is accompanied by a marked increase in the strength of the layer (Geldsetzer et al., 1997). Over the two months after burial, a surface hoar layer can decrease in thickness 40 to 70% (Jamieson and Schweizer, 2000), which is accompanied by a gradual strengthening of the layer. The decrease in thickness of a buried surface hoar layer is measurable in the field (Jamieson and Schweizer, 2000), and is associated with increasing shear strength and stability (e.g. Chalmers and Jamieson, in press).

It has been postulated that thinning of the layer, and not some form of crystal metamorphism within the layer, is responsible for the often (qualitatively) observed densification of buried surface hoar layers (Davis et al., 1996). It should be noted that the density of surface hoar layers is not practically measured in the field, but plane sections of two surface hoar layers, obtained 7 and 10 days after burial show a density of about  $160 \text{ kg m}^{-3}$  (Davis et al., 1996).

Jamieson and Schweizer (2000) proposed that the thinning of buried surface hoar layers is due to the surface hoar crystals being pushed into the layers above and below as the weight of the overlying slab increases. This is augmented by concurrent rearrangement and metamorphosis of the grains in the surrounding layers. This process should be especially dominant at the base of the surface hoar crystals; the narrower base of the wedge forms is driven into the layer below, resulting in a broader part of the crystal contacting the interface with the layer below. This broader contact forms greater bond area, and thus the shear strength of the weak layer should increase (Davis et al., 1996; Jamieson and Johnston, 1997; Geldsetzer et al., 1997). Surface hoar on top of a harder surface, such as a crust, will not penetrate as easily and therefore will be slower to gain strength (Jamieson and Schweizer, 2000). If left for a sufficient length of time,

the surface hoar crystals will penetrate to the point that the two adjacent layers make contact and form bonds, whereupon the surface hoar layer will have ceased to exist in the snowpack (Jamieson and Schweizer, 2000).

It can thus be seen that the mechanics of thinning buried surface hoar have been qualitatively theorised, but not quantitatively modelled. However, empirical field measurements of layer thinning are associated with increased strength of buried surface hoar layers.

#### **2.2.11 Rate of strength change of buried surface hoar layers**

The shear strength of a buried surface hoar layer will most often increase between 0 and 200 Pa d<sup>-1</sup> (Jamieson and Johnston, 1999), with rates of 25 to 55 Pa d<sup>-1</sup> being typical over the course of monitoring periods of 50 to 100 days (Jamieson and Schweizer, 2000).

#### **2.2.12 Observing texture of buried surface hoar layers**

Some studies (e.g. Shapiro et al., 1997) emphasised the importance of the relationship between the texture (size, number, and type of bonds) and strength of a buried snowpack layer. Jamieson and Schweizer (2000) stated that, "...without a field method to objectively characterise the buried surface hoar layers at the time of measurement (of the layer's shear strength), it is impossible to relate the observed shear strength changes to changes in texture (of the layer)."

To characterise the texture of a layer, the bonds must be left intact; observation or preservation of disaggregated crystals involves breaking the bonds, so neither method

is suitable. Plane and serial section analysis of a preserved layering enables observation of texture (Perla, 1982; Davis et al., 1996), yet neither is possible in the field and too time consuming to be suitable for operational avalanche forecasting (Jamieson and Schweizer, 2000). Jamieson and Schweizer (2000) saw some promise in in-situ photography of a buried surface hoar layer to characterise its texture, although Chalmers and Jamieson (in press) found that this was not of use for two surface hoar layers studied over time.

The literature therefore indicates that a physically based texture characterisation of buried surface hoar layers is not possible with present field observational techniques.

### **2.2.13 Snowpack factors associated with strength change of buried surface hoar**

Jamieson and Johnston (1999) ranked a number of measured and calculated snowpack (predictor) variables against the average rate of change of shear strength of a surface hoar layer (response variable). They regarded this as, “a first step towards developing a model for predicting strength changes based on measurements that are easier to make than repeatedly measuring the shear strength of the layers with the shear frame,” (Jamieson and Johnston, 1999). The data set for their study included over 300 measured strength changes of buried surface hoar in the Columbia Mountains. It was found that the average rate of change of shear strength over intervals of 3-8 days was not normally distributed, so Kendall tau rank correlations were used.

Jamieson and Johnston (1999) listed the top ten predictors of the rate of change of shear strength of a buried surface hoar layer. Additionally, they included possible associations with physical processes and other snowpack variables. These predictors are

listed below, in order of decreasing significance:

**Snowpack depth (HS).** Larger values of strength increase were associated with a deeper snowpack, which in turn was associated with greater slab thickness (H) and more load (see below), and weakly associated with smaller magnitudes of temperature gradient across the weak layer.

**Maximum crystal size of the surface hoar ( $E_{max}$ ).** Layers with larger crystals were slower to gain strength (Section 2.9).

**Slab depth overlying the weak layer (H).** A thicker slab was associated with more load overlying the weak layer, which caused more contacts and bonds (via layer thinning, Section 2.12), in turn causing strength to increase. It was also plausible that a thicker slab caused a lower temperature gradient (TG) across the weak layer and therefore more rounding/bonding.

**Weak layer temperature gradient divided by weak layer temperature ( $TG/T_{wl}$ ).** Larger values of ( $TG/T_{wl}$ ) were associated with slower rates of strength change, because of a shallow snowpack (HS), thinner slabs (H), and higher magnitudes of temperature gradient (TG).

**Temperature of the surface hoar weak layer ( $T_{wl}$ ).** Colder surface hoar layers were associated with lower rates of strength increase, because layers were colder in shallower snowpacks (HS) where temperature gradients (TG) were larger and less conducive to rounding of crystals and strengthening of the layers.

**Minimum crystal size of the surface hoar layer ( $E_{min}$ ).** Layers with larger crystals were slower to gain strength (Section 2.9), compared to layers of smaller crystals.

**Load on the weak layer ( $\sigma$ ).** Increase load probably pushed crystals into adjacent

layers, which caused increased bonding and strength (Section 2.12).

Range of crystal size of the surface hoar ( $E_{max}-E_{min}$ ). A larger range of crystal sizes was correlated with larger maximum crystal size, which were slower to gain strength (Section 2.9).

Strength at the start of an interval ( $\Sigma_o$ ). Strong layers gained strength faster. Strong layers were associated with heavy loads (Load and H) in deep snowpacks (HS).

Air temperature ( $T_a$ ). Faster strength increases took place at higher elevations, where temperatures ( $T_a$ ) were colder, snowpacks deeper (HS), slabs thicker (H), and loads greater.

Jamieson and Johnston (1999) also noted a weak positive correlation of rate of strength change with temperature gradient across the surface hoar layer, consistent with the idea of increased bonding and strength with lower magnitudes of the temperature gradient. There was no correlation between the rate of strength change and the thickness of the surface hoar layer, although the association between the rate of strength change and the rate of change of the thickness of the surface hoar layer was not examined. There was also no correlation between the rate of strength change and the average temperature gradient of the snowpack.

Jamieson and Johnston (1999) suggested that the strong correlation of snow depth, slab thickness, and maximum crystal size with the rate of strength change imply that, "microstructure (of the surface hoar layer) and bond-stress may be important to understanding and modelling strength changes of buried surface hoar layers." To date, no studies of surface hoar microstructure and bond-stress have been made.

The work of Jamieson and Johnston (1999) indicates that that an empirical

model to predict the shear strength of buried surface hoar layers from observable snowpack factors may be more readily found than a model based on physical strengthening mechanisms.

#### **2.2.14 Physically-based snowpack models and surface hoar weak layer evolution**

At present, there exist two complex, physically-based models which simulate the evolution of the mountain snowpack, including the microstructure of layers, based on meteorological inputs. These are called Snowpack and Crocus. Neither Snowpack nor Crocus includes surface hoar as a grain type (Fierz and Gauer, 1998; Meteo France, 1996). Attempts have been made to input layers of buried surface hoar in these models as layers of large faceted crystals, with inconclusive results on their ability to simulate the evolution of such layers (e.g. Fierz and Gauer, 1998).

### **2.3 Stability indices**

As discussed in Chapter 1, the stability - susceptibility to slab avalanching - of buried weak layers in the snowpack may be assessed by direct indicators such as observations of other slab avalanches or snowpack stability (Class 1 factors), by less direct indicators such as snowpack factors (Class 2 factors), or weather observations (Class 3 factors).

Stability ratios or indices based on shear frame measurements are such Class 1 factors. Schleiss and Schleiss (1970) introduced a snow “stability factor” or Stability Ratio, SF (Canadian Avalanche Association, 1995), which is the shear strength of a weak layer divided by the load (weight per unit area above the weak layer). This has

been used since c. 1960 at the Mount Fidelity study plot to extrapolate snowpack stability for natural avalanches in the Rogers Pass highway corridor, but not for skier-triggered avalanche activity.

Roch (1966) introduced a stability index  $S$ , the ratio of shear strength to shear stress on the weak layer, and Föhn (1987) produced a stability index incorporating skier loading,  $S'$ . Both Roch (1966) and Föhn (1987) made their shear strength measurements on or near avalanche slopes. These indices were corrected for the effects of normal load and shear frame size. Föhn and Camponovo (1996) showed that the shear strength of weak layers strongly correlated with the skier stability index.

To apply the stability index  $S$  to slopes of differing angles over a geographical region (up to 30 km), Jamieson and Johnston (1993) obtained  $S_{35}$ , based on a typical inclination of 35 degrees for avalanche start zones. They found a band of transitional stability (1.6-1.8) between stable and unstable snowpack conditions. Jamieson and Johnston (1993) found that  $SF$  and  $S_{35}$  were effective regional predictors of unstable and marginal natural avalanche stability on 75-87% of days, but this study did not include extrapolated regional stability for skier-triggered avalanches.

Jamieson and Johnston (1994) refined the skier triggering stability index  $S'$ , as  $Sk$ , to include the effects of ski penetration. In order to use this index for slopes within 15 km, it was applied to a slope angle of 35 degrees as  $Sk_{35}$ . Jamieson (1995, pp. 148-156), applying a slope angle of 38 degrees, excluded normal load effects for persistent weak layers and presented daily  $Sk_{38}$  values for nine buried surface hoar layers in the Columbia mountains. Most layers in that study showed a slowing of skier-triggered slab avalanche activity when  $Sk_{38}$  exceeded approximately 0.5 and a cessation of observed

skier-triggered slab avalanche activity when  $Sk_{38}$  was 1-1.5.  $Sk$  was further refined in Jamieson and Johnston (1998) for tests done on or adjacent to avalanche slopes. However, to date, only Chalmers and Jamieson (in press) have attempted to apply study plot measurements, including stability indices, to extrapolate the regional-scale stability of a buried weak layer in regards to skier-triggered avalanche activity. They found that an  $Sk_{38}$  value of 1-1.5 indicated a transition between unstable and stable regional skier stability of buried surface hoar layers.

The stability index  $Sk$  assumes that a buried weak layer of surface hoar fails in shear and not in compression. Although a mixed mode of failure cannot be ruled out, buried surface hoar layers are generally thin (< 10 mm thickness), and shear failure is assumed (Jamieson and Schweizer, 2000).

#### **2.4 Extrapolated study plot measurements for avalanche forecasting**

Föhn and Camponovo (1996) found that the stability of weak layers in the snowpack was proportional to the strength of the layer. Several studies have measured strength changes of buried surface hoar layers, with stability trends of the layers and associated avalanche activity (Jamieson and Johnston, 1994; Jamieson, 1995, pp. 125-138, 149-156; Schweizer et al., 1998). These studies considered a study area of approximately 10-15 km around the snow study plot. Chalmers and Jamieson (in press) related study plot measurements of buried surface hoar layers to the skier-triggered avalanche activity on these layers in a surrounding region (up to about 100 km away). Some studies have addressed observable changes in buried surface hoar layer properties (Davis et al., 1996; Jamieson and Schweizer, 2000; Chalmers and Jamieson, in press). Chalmers

and Jamieson (in press) found that shear strength, layer thickness, and load on the weak layer, all had measurable values that were associated with the regional stability of buried surface hoar layers. Specifically, a shear strength of approximately 1 kPa, a load of approximately 1 kPa, and a thinning of initial layer thickness by 20-44%, all appear to be important indicators of the skier stability of a buried surface hoar layer. Chalmers and Jamieson (in press) also concluded that observable changes in layer texture, from photography of buried surface hoar layers, cannot readily be applied to regional stability forecasting.

## **2.5 Summary**

The literature on surface hoar shows that the trends in the strength of a buried surface hoar layer are related to observable characteristics of the layer and the surrounding snowpack. Physical mechanisms such as layer texture are perceived as important to the strength of buried surface hoar layers, but have yet to be extensively documented or quantitatively explained. Modelling the strength of buried surface hoar layers based on observable snowpack characteristics appears to be more promising than a physically-based model.

It appears that stability indices and study plot measurements may both be extrapolated to forecast regional skier-triggered avalanche activity where the snowpack in the study plot is similar to that in surrounding starting zones.

### 3. METHODS

#### 3.1 Study areas and co-operating organisations

Data for this study were collected at study sites in the Columbia Mountains (Figure 3.1, Table 3.1) of western Canada from the years 1992-2001. Study sites were located in areas used by Mike Wiegele Helicopter Skiing (1993-2000) and Canadian Mountain Holidays Bobbie Burns (1992-1998), and in Glacier National Park (1999-2001). Additional skier-triggered avalanche observation data were collected from Canadian Mountain Holidays Adamants, Gothics, Monashees, and Revelstoke (1999-2001).

The Columbia Mountains have a transitional snow climate, between maritime and continental conditions (see McClung and Schaerer, 1993, pp. 17-18), although maritime conditions have been observed to be the more influential in the region (e.g. Schweizer et al., 1998).

**Table 3.1: Study sites.**

<b>Organisation</b>	<b>Study site</b>	<b>Elevation (m)</b>	<b>Aspect</b>	<b>Slope (°)</b>
Canadian Mountain Holidays Bobbie Burns	Elk	2300	NE	5 to 24
	Middle Moose	2100	NW	8 to 21
	North Moose	1900	NW	20 to 34
	North Moose Log Cut	1950	NW	27 to 34
	Pygmy Run	2000	E	24 to 31
	Vermont	1600	N	0 to 6
	Vermont Airbox	1600	N	0
Parks Canada Glacier Nat. Park	Cheops	1600	ENE	4 to 28
	Fidelity	1890	N to E	15 to 30
Mike Wiegele Helicopter Skiing	Tower	1890	E	34 to 39
	Mt. St. Anne Airbox	1900	E	0
	Mt. St. Anne Cutblock	1600	E	23 to 32
	Mt. St. Anne Landing	1390	S	0
	Mt. St. Anne Plot	1900	E	0
	Norberts Cutblock	1700	E	12 to 26
	Sam's Plot	1770	N	10
Sam's Run	1910	SE	23 to 28	

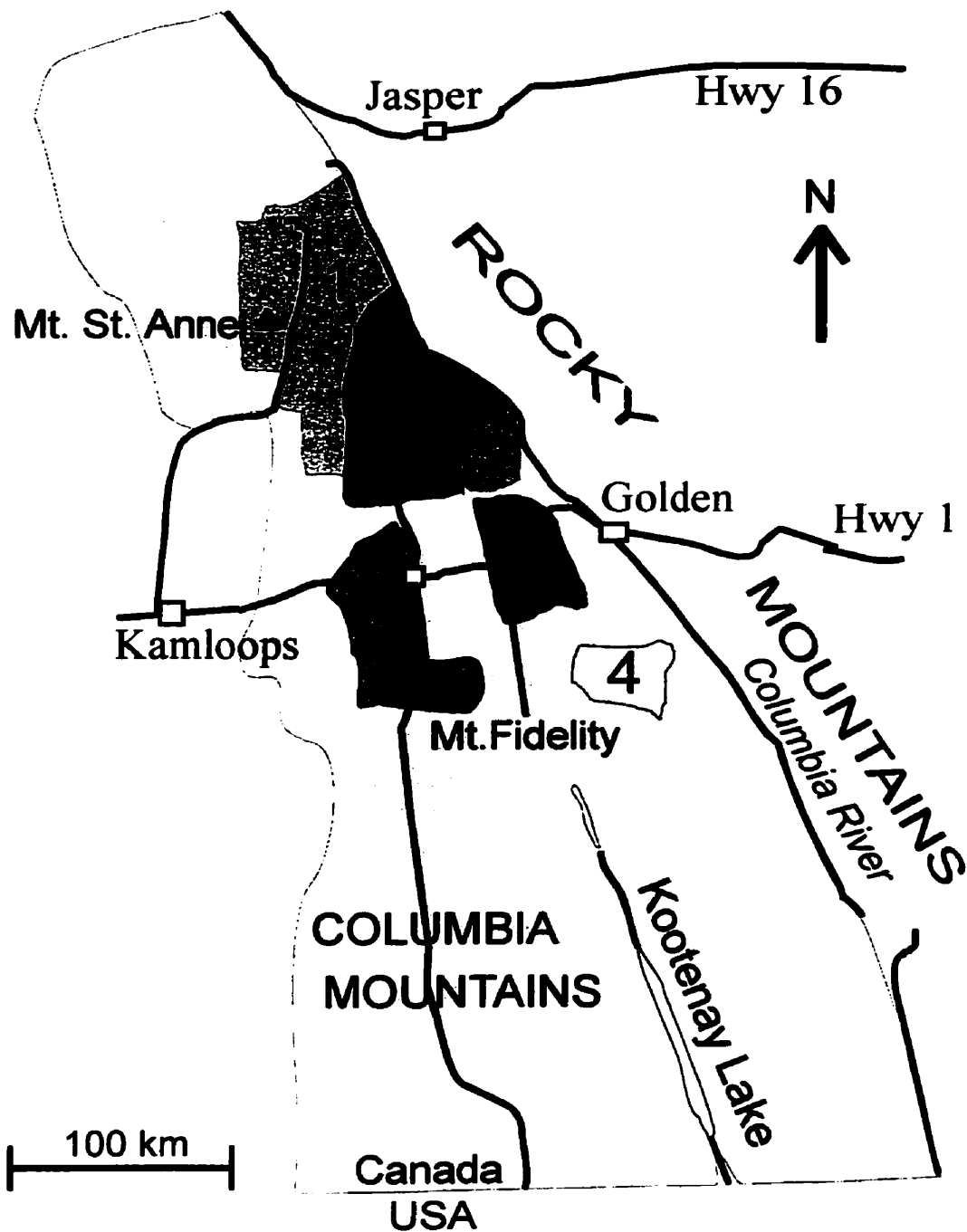


**Figure 3.1:** Study areas in the Columbia Mountains: 1) Mike Wiegele Helicopter Skiing, 2) Canadian Mountain Holidays Adamants, Gothics, Monashees, and Revelstoke, 3) Glacier National Park, 4) Canadian Mountain Holidays Bobbie Burns. Mt. St. Anne and Mt. Fidelity study plots shown. Other study sites located within areas 1,3,4 (Table 3.1). Skier-triggered avalanche activity data for Mt. Fidelity region gathered from areas 2 and 3. Skier-triggered avalanche activity data for Mt. St. Anne region gathered from area 1.

## **3.2 Sites for snowpack observations**

### **3.2.1 Study plots and slopes**

The changes in snowpack properties, including buried surface hoar layers, measured for this project were observed at fixed study locations. These locations were selected, in consultation with the appropriate co-operating organisation, to be: generally safe from the threat of avalanches, relatively sheltered from wind effects, uniform in terrain and snowpack, and representative of the snowpack in the surrounding avalanche starting zones. Flat study sites are referred to as study plots; sloping sites are referred to as study slopes. Study sites were visited on a fixed schedule, ideally with no more than eight days between visits.

### **3.2.2 Study sites with automated meteorological stations**

Two study sites for this project were located adjacent to automated meteorological stations: Mt. Fidelity in the Selkirk range and Mt. St. Anne in the Cariboo range, both in the Columbia Mountains of western Canada. The automatic weather data includes the daily snowfall at each site, which may be used to calculate the daily load increments on a buried surface hoar layer. Furthermore, both sites are located in or adjacent to areas for which skier-triggered avalanche activity in the surrounding region was reported.

The Mt. Fidelity study site (Figure 3.1) is located at 1905 m a.s.l., 900 m above the Trans-Canada Highway in Rogers Pass, British Columbia, near the west end of Glacier National Park.

Mt. Fidelity is used by Glacier National Park's Avalanche Control Section for avalanche forecasting, and automated measurements from this site were provided by this group. The Fidelity study slopes varied between approximately 15 and 30 degrees inclination, on a predominantly east-facing ridge, and were the sites of weak layer strength change measurements collected by University of Calgary researchers over the winters 1998-1999, 1999-2000, 2000-2001. Skier-triggered avalanche activity for this region was recorded by University of Calgary staff in Glacier National Park, and by four neighbouring helicopter skiing operations located within approximately 100 km of the study site (Figure 3.1).

The Mt. St. Anne study station is located at 1900 m a.s.l., northwest of the town of Blue River, British Columbia. The study site is operated by Mike Wiegele Helicopter Skiing, and University of Calgary research technicians made measurements over the winters 1993-2001 at this site.

### **3.2.3 Airbox study sites**

Several study sites for this project are called "Airbox" sites (Table 3.1). Snowpack data were recorded above boxes placed on the ground during the summer and subsequently buried in the snowpack (Airboxes). These boxes created an artificially thin area of the snowpack (depth < 1 m) for a separate study (Jamieson and Johnston, 1999). Shear strength data from these sites were not found to differ significantly from nearby study sites, thus allowing the snowpack data from these sites to be used in this study.

### **3.3 Equipment**

#### **3.3.1 Manual snow study equipment**

A collapsible snow shovel is used to dig snow pits and, together with a snow saw, to perform the compression test (Canadian Avalanche Association, 1995).

A collapsible avalanche probe, typically around 3 m in length, is used to measure height of snowpack and ascertain uniformity of snow cover in a study site.

A snow crystal screen with grids of 1, 2, and 3mm on a side and a mm ruled edge is used in conjunction with a hand lens (loupe) to identify and measure the average size of disaggregated snow crystals (Figure 3.2).

A folding ruler is used to locate layers, measure height of snowpack and thickness of layers, and place thermometers in the snow profile (Figures 3.2 and 1.7).

A digital thermometer (accurate to 0.2°C) is used to measure a snow temperature profile every 0.1 m from the snow surface. Additional temperature measurements were often taken in the middle of the surface hoar layer and at 0.05 m above and below this location.

Two different stainless steel shear frames, 100 and 250 cm<sup>2</sup> in size, were used for the strength measurements of surface hoar layers (Figure 1.8). They are slightly tapered from the front (where a string is attached for use of a force gauge) to the back, to reduce friction between the snow and the sides of the frame. The frames are sharpened at the bottom to enable placement in the snow above the weak layer with less force, and thereby reduce the chances of disturbing the weak layer.



**Figure 3.2:** A folding ruler in use in the snow pit wall, with an observer using a crystal screen and magnifier to examine snow crystals. ASARC photo.



**Figure 3.3:** A ring flash and macro lens being used for snow pit wall microphotography. ASARC photo.

Three different force gauges, with capacities of 3, 10, and 30 kg are used in conjunction with a shear frame to measure the shear strength of a surface hoar layer (Figure 1.8). The gauge used depends on the expected strength of the layer to be tested. Between 10% and 100% of the gauges' capacity, they are rated to be accurate to within 1% of the capacity. A switch on the gauge selects recording of current force or maximum force.

A force gauge and core sampling tube and bag are used in one method of measuring the slab weight per unit area. A density sampling tube and digital scale are used in another.

A camera with a macro lens and ring flash is used to take pictures of disaggregated (separated from the buried surface hoar layers) and in-situ (snow pit wall) snow crystals (Figure 3.3).

### **3.3.2 Automated meteorological equipment**

Automated precipitation gauges were located adjacent to the Mt. St. Anne and Mt. Fidelity study sites. These record precipitation as equivalent mm of water and are used to record new loading on a buried surface hoar layer each day for the preceding 24 hour period.

## **3.4 Measurement procedures**

### **3.4.1 Snowpack properties**

On each measurement day, the buried surface hoar layer(s) were identified in a snow pit wall with a profile of snowpack layers, compression test, rutschblock test, or shovel test (Canadian Avalanche Association, 1995).

A snow profile was observed (Figure 1.7), including properties of the surface hoar layers (maximum and minimum grain size, layer thickness, temperature, temperature gradient, shear strength) and of the overlying slab (load, slab thickness), and the height of the snowpack.

The shear strength of each layer is the average obtained from a set of approximately 12 shear frame tests (Figure 1.8). The snow overlying the buried surface hoar layer was removed, leaving 40-45 mm of undisturbed snow above the weak layer. A shear frame was carefully inserted into the snow such that the frame bottom was 2-5 mm above the weak layer (Perla and Beck, 1983). A thin blade was passed around the shear frame to ensure surrounding snow was not bonding to the shear frame, cutting to but not through the weak layer. A force gauge was hooked to a cord attached to the shear frame and pulled smoothly and rapidly ( $< 1$  s to failure). This results in a brittle, planar failure of the weak layer just below the bottom of the frame, with non-planar fractures identified by a descriptor (see Geldsetzer et al., 1999). Details of the shear frame test can be found in Jamieson and Johnston (2001). Shear strength is the maximum reading on the force gauge divided by the area of the frame, and adjusted for size effects (Sommerfeld, 1980; Föhn, 1987).

The maximum and minimum extent of the characteristic surface hoar crystals in a buried layer were observed. This was done according to industry guidelines (Canadian Avalanche Association, 1995), manually separating the crystals from the snowpack and observing them with a low magnification (8X) hand lens on a crystal screen with 1, 2, 3, and 10 mm grids.

The thickness of a buried surface hoar layer was measured by placing a millimetre scale against the vertical snow pit wall and recording the layer thickness to the nearest millimetre in approximately three locations on the snow pit wall. The results were averaged by the observer to obtain the thickness of the weak layer.

The load due to the snow slab overlying a buried surface hoar layer ( $\sigma$ ) was measured in two ways. The first method involves taking a vertical core sample of the slab by inserting a tube vertically through the snowpack layers above the surface hoar layer. Several such cores were often taken to reduce measurement error. In this first method,

$$\sigma = mg/\text{Area} \quad (1)$$

where  $m$  is the average mass of the core samples,  $g$  is the acceleration due to gravity, and Area is the cross-sectional area of the sample tube (28 cm<sup>2</sup>). The second method is to calculate the load from the thickness and measured densities of the snowpack layers above the buried surface hoar layer,

$$\sigma = g(\rho_1 h_1 + \rho_2 h_2 + \dots), \quad (2)$$

where  $\rho_i$  and  $h_i$  are the density and thickness of the  $i_{\text{th}}$  layer. For layers which were too thin (less than 40 mm) to measure with the small (100 cm<sup>3</sup>) density sampling tube, the density was estimated from hand hardness and grain type as described by Geldsetzer and Jamieson (2000). These two methods of load measurement are used to minimise the sampling error from each method (Jamieson and Johnston, 1999), and values from both methods were averaged to obtain the load.

Manual measurements of snowpack temperatures and temperature gradient across the buried surface hoar layers were taken on each observation day with digital

display thermometers with a resolution of 0.2°C. The temperature gradient across a buried surface hoar layer was calculated from the temperatures 50 mm above and below the suspected failure plane. Weak layer temperatures and temperature gradients were monitored continuously with thermistors for a number of the weak layers in this study, and showed excellent correspondence with manual measurements.

The height of the snowpack was measured in one of two ways. If the snow profile was excavated to ground level, the height of snowpack was measured with the folding ruler on the pit wall. If the snow profile was not excavated to ground level, a collapsible snow probe with graduated (cm) markings was inserted into the snowpack until it touched ground, and the height of snowpack was recorded from the probe scale.

### **3.4.2 Photographic techniques**

Approximately every 8 to 14 days, buried surface hoar layers were photographed by two different methods: in-situ as they are found naturally in the snowpack, and as crystals disaggregated from each layer (e.g. Davis et al., 1996; Jamieson and Schweizer, 2000). The in-situ photos were made by inserting a black screen approximately 10-20 mm behind the weak layer, parallel to the pit wall to provide background contrast. Disturbed or fractured crystals in front of the screen were carefully removed, leaving only surface hoar crystals in their natural buried state to be photographed with a macro lens and ring flash (Figure 3.3). Some crystals were then carefully disaggregated from the pit wall, without breaking them into smaller pieces, and placed on a 10 mm grid to be photographed with a macro lens and ring flash. A ring flash was used to enable hand-held photos to be taken without a tripod.

### **3.5 Avalanche activity**

Observed avalanche activity was recorded according to industry guidelines (Canadian Avalanche Association, 1995), including the type of release (slab or loose snow), size based on destructive potential (size range 1 to 4, including half-sizes), type of trigger (natural, explosive, skier, cornice fall, etc.), liquid water content (dry, moist, wet), aspect, elevation, location, and date and time of occurrence.

## **4. PREDICTING SHEAR STRENGTH OF BURIED SURFACE HOAR LAYERS**

### **4.1 Introduction**

#### **4.1.1 Goals of a shear strength prediction model**

The objective of this chapter was to develop a model that could be used operationally to predict the shear strength of buried surface hoar layers in the Columbia Mountains. Ideally, an observer may perform standard snowpack and weather observations (Canadian Avalanche Association, 1995) in a study plot in the Columbia Mountains, and then use the model to forecast the strength change until the next snowpack observation day. The predicted strength, if accurate, may then be assimilated with other forecasting variables and methods to aid the forecaster in making decisions.

Three different techniques were used to develop three models to predict the shear strength of buried surface hoar layers in the Columbia Mountains. These are denoted the Shear Strength—Power Law, -Interval, and -Lagged Load models. The development of each model is discussed in Sections 4.2, 4.3, and 4.4, respectively. Model accuracy and testing is discussed in Section 4.5, and the results of this chapter are summarised in Section 4.6.

#### **4.1.2 Snowpack and shear strength measurement variables**

In order to develop the most accurate yet practical models, a large number of variables based on easily measured snowpack properties were considered (Table 4.1).

Shear strength of the buried surface hoar  $\Sigma$  is referred to as the response (dependent) variable, while the other snowpack variables are referred to as predictor (independent) variables.

Depending on the modelling technique, different variables can be used. Once a model based on a number of these variables has shown promise for predicting the shear strength of buried surface hoar layers in the Columbia Mountains, the physical interpretation may be addressed. A new model can then be constructed, using only variables that are easily measured by an avalanche forecaster or technician and/or have conceptually straightforward physical meaning. It is proposed that this second model iteration will be more preferable for operational use, provided that it provides accuracy similar to the original model. This concept of model refinement will be applied in this chapter.

**Table 4.1:** Snowpack variables and units.

<b>Variable</b>	<b>Description (units)</b>
$\Sigma$	Shear strength of weak layer (kPa)
$\sigma$	Vertical load (force per unit area) due to snow overlying weak layer (kPa)
H	Thickness of snow slab overlying weak layer, measured vertically (cm)
HS	Total height of snowpack (cm)
Thick	Thickness of weak layer (cm)
Twl	Temperature of weak layer ( $^{\circ}\text{C}$ )
TG	Magnitude of temperature gradient across weak layer ( $^{\circ}\text{C m}^{-1}$ )
Emin	Minimum grain size in weak layer (mm)
Emax	Maximum grain size in weak layer (mm)
(Emax-Emin)	Difference between max. and min. grain size in weak layer (mm)
(TG/Twl)	Average temperature gradient across weak layer divided by average weak layer temperature ( $\text{m}^{-1}$ )

#### 4.1.3 Shear strength of buried surface hoar layers in the Columbia Mountains

The data set of buried surface hoar layers in this study includes 514 strength measurements on 92 time series of buried surface hoar in the Columbia Mountains, from the years 1992 to 2001 (Table 4.2). Each time series is a sequence of measurements of a particular layer at a particular study site over time (10-100 days). Most layers in this study involved sector plate forms of surface hoar (Section 2.2.1). The author was involved in data collection for time series during the winters 1999-2000 and 2000-2001.

The time series of strength measurements of a buried surface hoar layer is shown in Figure 4.1. As is typical of buried layers of surface hoar in the Columbia Mountains, this layer showed rapid strength gain during the first 20 to 30 days after burial. Most skier-triggered slab avalanches on these layers typically occur over this same time period (e.g. Chalmers and Jamieson, in press). Subsequent strength gain was much more gradual.

The object of this study is the prediction of strength changes of buried surface hoar layers, with the intent of aiding the forecasting of skier-triggered slab avalanches. Thus, the analysis will focus on the first 30 days following the burial of a surface hoar layer.

Decreases in shear strength of a surface hoar layer may be measured (Figure 4.1). Variations in shear strength may arise due to natural variability of the layer in the study site. In the Columbia Mountains, surface hoar layers are often too deep in the snowpack for strength decreases to be due to external (meteorological) forcing. Shear strength decreases are often observed later in the winter months as snowpack temperatures warm to around  $-1^{\circ}\text{C}$ , but are not associated with increased avalanche activity on the surface hoar layer.

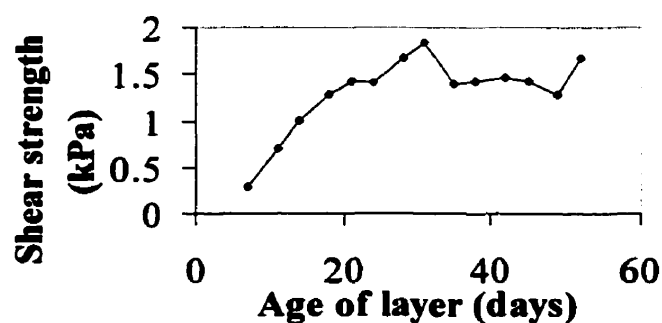


**Figure 4.1:** Shear strength of the surface hoar layer buried 20-January-2001 in the Mt. St. Anne study plot.

**Table 4.2:** Time series of strength of surface hoar layers 1992-2001.

<b>Burial date</b>	<b>Location</b>	<b>N</b>	<b>Burial date</b>	<b>Location</b>	<b>N</b>
05-Dec-92	Tower Study Slope	2	17-Feb-96	Mt. St. Anne Study Plot	6
15-Nov-93	Mt. St. Anne Study Plot	5	17-Jan-97	Vermont Study Plot	15
04-Dec-93	Mt. St. Anne Study Plot	7	17-Jan-97	Vermont Airbox	15
18-Dec-93	Sam's Study Plot	5	17-Jan-97	Pygmy Run	8
29-Dec-93	Mt. St. Anne Study Plot	7	17-Jan-97	North Moose Log Cut	13
29-Dec-93	Sam's Study Plot	5	17-Jan-97	Mt. St. Anne Study Plot	13
21-Jan-94	Mt. St. Anne Study Plot	2	17-Jan-97	Mt. St. Anne Airbox	10
05-Feb-94	Sam's Run	2	17-Jan-97	Elk Study Plot	4
05-Feb-94	Sam's Study Plot	2	17-Jan-97	Elk Study Slope	4
05-Feb-94	Mt. St. Anne Study Plot	7	10-Feb-97	Norberts Cutblock	2
05-Feb-94	Tower Study Slope	2	10-Feb-97	Mt. St. Anne Study Plot	9
15-Dec-94	Vermont Study Plot	9	10-Feb-97	Mt. St. Anne Airbox	8
15-Dec-94	Elk Study Plot	6	10-Feb-97	Mt. St. Anne Cutblock	7
07-Jan-95	Vermont Study Plot	8	11-Feb-97	Vermont Study Plot	8
07-Jan-95	Mt. St. Anne Study Plot	9	11-Feb-97	Vermont Airbox	8
07-Jan-95	Mt. St. Anne Airbox	8	11-Feb-97	Pygmy Run	7
07-Jan-95	Mt. St. Anne Landing	2	11-Feb-97	North Moose Log Cut	8
14-Feb-95	Mt. St. Anne Study Plot	5	01-Mar-97	North Moose Log Cut	2
28-Dec-95	Mt. St. Anne Study Plot	10	01-Mar-97	Pygmy Run	2
28-Dec-95	Mt. St. Anne Airbox	4	01-Mar-97	Vermont Airbox	2
28-Dec-95	Mt. St. Anne Cutblock	8	01-Mar-97	Vermont Study Plot	2
01-Jan-96	Mt. St. Anne Airbox	3	08-Dec-97	Mt. St. Anne Cutblock	6
01-Jan-96	Mt. St. Anne Study Plot	4	08-Dec-97	Mt. St. Anne Study Plot	7
04-Feb-96	Mt. St. Anne Study Plot	3	26-Dec-97	Middle Moose Study Plot	14

**Table 4.2 (continued) : Time series of strength of surface hoar layers 1992-2001.**

<b>Burial date</b>	<b>Location</b>	<b>N</b>	<b>Burial date</b>	<b>Location</b>	<b>N</b>
26-Dec-97	Vermont Study Plot	7	30-Dec-99	Cheops Study Plot	12
02-Feb-98	Mt. St. Anne Study Plot	3	30-Dec-99	Fidelity Study Slope	15
03-Feb-98	Middle Moose Study Plot	7	30-Dec-99	Mt. St. Anne Study Plot	13
03-Feb-98	Pygmy Run	2	31-Jan-00	Cheops Study Plot	9
03-Feb-98	Vermont Study Plot	6	31-Jan-00	Fidelity Study Slope	10
13-Feb-98	Mt. St. Anne Study Plot	9	31-Jan-00	Mt. St. Anne Study Plot	12
13-Feb-98	Mt. St. Anne Airbox	11	31-Jan-00	Mt. St. Anne Airbox	10
17-Feb-98	Middle Moose Study Plot	3	05-Feb-00	Cheops Study Plot	7
17-Feb-98	Vermont Study Plot	2	21-Feb-00	Cheops Study Plot	6
25-Feb-98	Mt. St. Anne Cutblock	2	21-Feb-00	Fidelity Study Slope	6
25-Feb-98	Mt. St. Anne Study Plot	7	21-Feb-00	Mt. St. Anne Cutblock	6
25-Feb-98	Mt. St. Anne Airbox	7	17-Nov-00	Fidelity Study Slope	3
25-Feb-98	Mt. St. Anne Cutblock	2	24-Nov-00	Fidelity Study Slope	6
28-Feb-98	Middle Moose Study Plot	3	07-Dec-00	Mt. St. Anne Study Plot	8
28-Feb-98	Vermont Airbox	3	13-Jan-01	Fidelity Study Slope	17
28-Feb-98	Vermont Study Plot	3	20-Jan-01	Mt. St. Anne Study Plot	14
03-Jan-99	Fidelity Study Slope	4	28-Jan-01	Fidelity Study Slope	15
03-Jan-99	Cheops Study Plot	4	23-Feb-01	Mt. St. Anne Study Plot	4
24-Jan-99	Cheops Study Plot	2	23-Feb-01	Fidelity Study Slope	8
24-Jan-99	Fidelity Study Slope	3			
24-Jan-99	Cheops Study Plot	7			
16-Feb-99	Fidelity Study Slope	8			
16-Feb-99	Cheops Study Plot	10			
12-Mar-99	Fidelity Study Slope	2			

## 4.2 Shear strength – Power Law model

### 4.2.1 Introduction

Following burial by snowfall, a surface hoar layer in the Columbia Mountains typically increases in strength rapidly for 20 to 30 days, then slows in rate of strength gain (as in Figure 4.1). This appears to indicate power law relationship between shear strength and time. In dimensionless parameters, this relationship may be expressed as:

$$\Sigma/\Sigma_1 = (t/t_1)^A , \quad (4.1)$$

where  $\Sigma$  is shear strength,  $\Sigma_1$  is a constant representing shear strength on the first day after the layer is buried (day 1) – also called initial shear strength,  $t$  is time (in days),  $t_1$  is 1 (day 1), and  $A$  is the exponential shear strength growth constant of the particular surface hoar layer.

The objective of the analysis in this section was to find values of  $\Sigma_1$  and  $A$  for surface hoar layers in the Columbia Mountains, and thus describe the shear strength of these layers over time by Equation 4.1.

The data were examined for serial correlations with the Durbin-Watson test (Mendenhall and Sincich, 1996, p. 430), with overall inconclusive results. Nonetheless, there may be serial correlations present in some of the data, which would cause model significance p-values to be overestimated. Using a similar dataset and analysis, Johnson (2000, p. 55) noted that, “statistical analysis of the serial correlations is difficult because of the small time series and irregular time intervals.” Henceforth, some overestimation of significance p-values may be assumed.

### 4.2.2 Dataset

In an effort to more closely model gains in shear strength over the period of time in which surface hoar layers are commonly prone to skier triggering, the data set for this analysis included only time series for which strength was measured at least 4 times within the first 30 days after burial. These layers are listed in Table 4.3. Two layers were used for model testing but not for model formulation. Listed in italics in Table 4.3, these layers were selected for model testing because good records of skier-triggered avalanches were available.

### 4.2.3 Parameter fitting for individual time series

A least-squares regression was performed on each time series in Table 4.3, in order to fit the parameters  $\Sigma_1$  and  $A$  from Equation 4.1. An important assumption for the validity of least-squares regression analysis is a random scatter of the residuals (the difference between measured and predicted  $\Sigma$  on a measurement day) of regression (Mendenhall and Sincich, 1996, pp. 394-404), indicating constant variance of residuals over the range of the response variable. This assumption was not validated by regression on the untransformed Equation 4.1, which may be inferred from the residuals shown in Figure 4.2 (selected at random from the time series of Table 4.3). A logarithmic transformation of Equation 4.1 was used to stabilise the variance of residuals and provide a linear regression:

$$\ln(\Sigma / \Sigma_1) = \ln[(t/t_1)^A]$$

or

$$\ln(\Sigma) = \ln(\Sigma_1) + A \ln(t/t_1) . \tag{4.2}$$

**Table 4.3:** Surface hoar time series with 4 or more measurements during the first 30 days of burial. Fitted parameters  $\Sigma_1$  and  $A$  as well as  $R^2$  for fit to Equation 4.2 shown. Series with significant fit ( $p \leq 0.05$ ) in bold. Series in italics reserved for model testing.

Location	Burial date	$R^2$	$\Sigma_1$	$A$
<b>Mt. St. Anne Study Plot</b>	<b>04-Dec-93</b>	<b>0.998</b>	<b>0.157</b>	<b>0.887</b>
<b>*Mt. St. Anne Study Plot</b>	<b>29-Dec-93</b>	<b>0.991</b>	<b>0.148</b>	<b>0.812</b>
<b>Sam's Study Plot</b>	<b>29-Dec-93</b>	<b>0.991</b>	<b>0.351</b>	<b>0.795</b>
<b>Mt. St. Anne Study Plot</b>	<b>05-Feb-94</b>	<b>0.979</b>	<b>0.007</b>	<b>1.800</b>
<b>Elk Study Plot</b>	<b>15-Dec-94</b>	<b>0.735</b>	<b>0.012</b>	<b>1.455</b>
Vermont Study Plot	07-Jan-95	-0.185	0.713	-0.608
<b>Mt. St. Anne Study Plot</b>	<b>07-Jan-95</b>	<b>0.962</b>	<b>0.068</b>	<b>1.110</b>
<b>Mt. St. Anne Airbox</b>	<b>07-Jan-95</b>	<b>0.937</b>	<b>0.107</b>	<b>0.830</b>
<b>Mt. St. Anne Study Plot</b>	<b>14-Feb-95</b>	<b>0.943</b>	<b>0.245</b>	<b>0.736</b>
<b>Mt. St. Anne Study Plot</b>	<b>28-Dec-95</b>	<b>0.961</b>	<b>0.076</b>	<b>1.058</b>
<b>Mt. St. Anne Airbox</b>	<b>28-Dec-95</b>	<b>0.912</b>	<b>0.104</b>	<b>0.914</b>
<b>Mt. St. Anne Study Plot</b>	<b>01-Jan-96</b>	<b>0.955</b>	<b>0.196</b>	<b>0.878</b>
Mt. St. Anne Study Plot	17-Feb-96	0.684	0.476	0.525
<b>Vermont Study Plot</b>	<b>17-Jan-97</b>	<b>0.822</b>	<b>0.160</b>	<b>0.586</b>
<b>Vermont Airbox</b>	<b>17-Jan-97</b>	<b>0.770</b>	<b>0.135</b>	<b>0.637</b>
<b>Pygmy Run</b>	<b>17-Jan-97</b>	<b>0.836</b>	<b>0.423</b>	<b>0.414</b>
North Moose Log Cut	17-Jan-97	0.682	0.028	1.178
<b>*Mt. St. Anne Study Plot</b>	<b>17-Jan-97</b>	<b>0.878</b>	<b>0.342</b>	<b>0.617</b>
Mt. St. Anne Airbox	17-Jan-97	0.625	0.578	0.300
Elk Study Slope	17-Jan-97	0.672	0.098	0.870
<b><i>Mt. St. Anne Study Plot</i></b>	<b><i>10-Feb-97</i></b>	<b><i>0.934</i></b>	<b><i>0.031</i></b>	<b><i>1.409</i></b>
<b>Mt. St. Anne Airbox</b>	<b>10-Feb-97</b>	<b>0.861</b>	<b>0.071</b>	<b>0.967</b>
Mt. St. Anne Cutblock	10-Feb-97	0.381	0.258	0.465
<b>Vermont Study Plot</b>	<b>11-Feb-97</b>	<b>0.942</b>	<b>0.019</b>	<b>1.145</b>
<b>Vermont Airbox</b>	<b>11-Feb-97</b>	<b>0.819</b>	<b>0.008</b>	<b>1.380</b>
<b>Pygmy Run</b>	<b>11-Feb-97</b>	<b>0.633</b>	<b>0.059</b>	<b>0.958</b>
North Moose Log Cut	11-Feb-97	0.340	0.070	0.659

**Table 4.3 (continued):** Surface hoar time series with 4 or more measurements during the first 30 days of burial. Fitted parameters  $\Sigma_1$  and  $A$  as well as  $R^2$  for fit to Equation 4.2 shown. Series with significant fit ( $p \leq 0.05$ ) in bold. Series in italics reserved for model testing.

Location	Burial date	$R^2$	$\Sigma_1$	$A$
Middle Moose Study Plot	26-Dec-97	0.769	0.229	0.668
Vermont Study Plot	26-Dec-97	0.539	0.294	0.568
<b>*Middle Moose Study Plot</b>	<b>03-Feb-98</b>	<b>0.979</b>	<b>0.021</b>	<b>1.069</b>
<b>Mt. St. Anne Study Plot</b>	<b>13-Feb-98</b>	<b>0.831</b>	<b>0.433</b>	<b>0.505</b>
<b>Mt. St. Anne Airbox</b>	<b>13-Feb-98</b>	<b>0.861</b>	<b>0.435</b>	<b>0.428</b>
<b>Mt. St. Anne Study Plot</b>	<b>25-Feb-98</b>	<b>0.934</b>	<b>0.093</b>	<b>0.951</b>
<b>Mt. St. Anne Airbox</b>	<b>25-Feb-98</b>	<b>0.991</b>	<b>0.066</b>	<b>1.064</b>
Fidelity Study Slope	03-Jan-99	0.921	0.262	0.923
<b>Cheops Study Plot</b>	<b>03-Jan-99</b>	<b>0.917</b>	<b>0.090</b>	<b>1.146</b>
Cheops Study Plot	24-Jan-99	0.742	0.128	1.113
<b>Fidelity Study Slope</b>	<b>16-Feb-99</b>	<b>0.922</b>	<b>0.024</b>	<b>1.504</b>
<b>Cheops Study Plot</b>	<b>16-Feb-99</b>	<b>0.957</b>	<b>0.077</b>	<b>1.116</b>
<b>*Fidelity Study Slope</b>	<b>30-Dec-99</b>	<b>0.950</b>	<b>0.022</b>	<b>1.535</b>
<i>Mt. St. Anne Study Plot</i>	<i>30-Dec-99</i>	<i>0.907</i>	<i>0.092</i>	<i>0.969</i>
Cheops Study Plot	31-Jan-00	0.510	0.361	0.469
<b>Fidelity Study Slope</b>	<b>31-Jan-00</b>	<b>0.938</b>	<b>0.088</b>	<b>0.989</b>
<b>Mt. St. Anne Study Plot</b>	<b>31-Jan-00</b>	<b>0.963</b>	<b>0.200</b>	<b>0.598</b>
<b>Mt. St. Anne Airbox</b>	<b>31-Jan-00</b>	<b>0.790</b>	<b>0.381</b>	<b>0.314</b>
<b>Cheops Study Plot</b>	<b>21-Feb-00</b>	<b>0.934</b>	<b>0.108</b>	<b>0.918</b>
Fidelity Study Slope	21-Feb-00	0.580	0.088	0.919
<b>Mt. St. Anne Cutblock</b>	<b>21-Feb-00</b>	<b>0.976</b>	<b>0.077</b>	<b>1.065</b>
<b>Fidelity Study Slope</b>	<b>24-Nov-00</b>	<b>0.901</b>	<b>0.222</b>	<b>0.586</b>
<b>Fidelity Study Slope</b>	<b>13-Jan-01</b>	<b>0.766</b>	<b>0.046</b>	<b>0.886</b>
<b>Mt. St. Anne Study Plot</b>	<b>20-Jan-01</b>	<b>0.914</b>	<b>0.033</b>	<b>1.226</b>
<b>*Fidelity Study Slope</b>	<b>28-Jan-01</b>	<b>0.906</b>	<b>0.216</b>	<b>0.652</b>
<b>Mt. St. Anne Study Plot</b>	<b>23-Feb-01</b>	<b>0.977</b>	<b>0.053</b>	<b>1.140</b>
<b>Fidelity Study Slope</b>	<b>23-Feb-01</b>	<b>0.969</b>	<b>0.124</b>	<b>0.804</b>

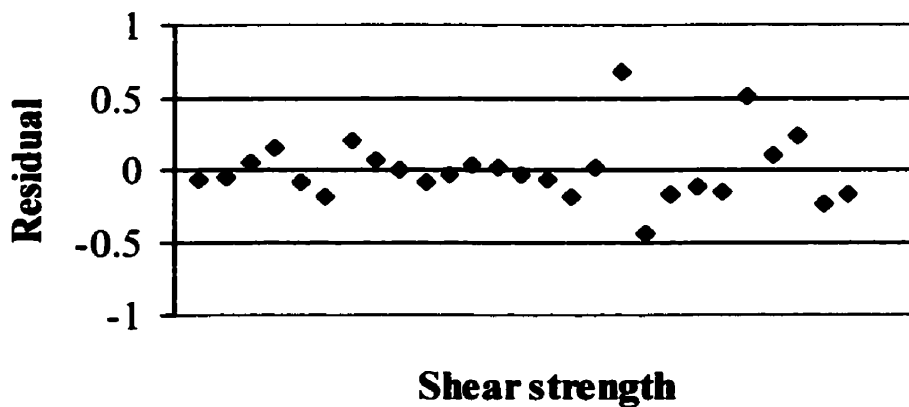


**Figure 4.2:** Residuals of regression on untransformed Equation 4.1. Five series from Table 4.3 (marked with \*) selected at random.

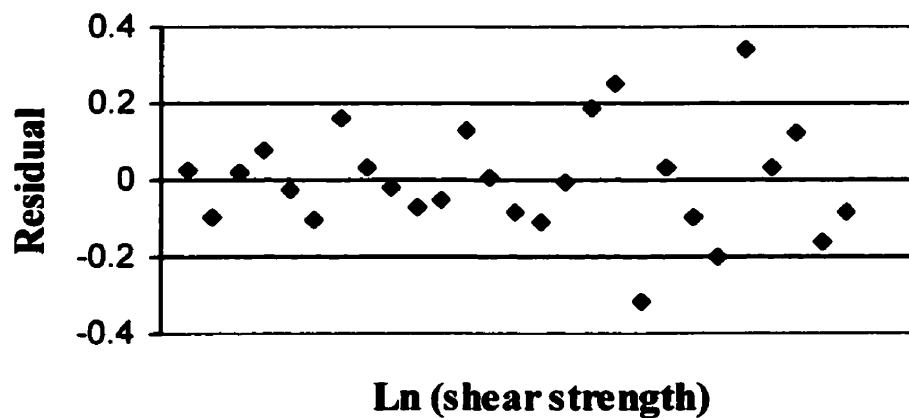


**Figure 4.3:** Residuals of regression on transformed Equation 4.2. Same series used as in Figure 4.2.

An analysis of the residuals of regression for Equation 4.2 (Figure 4.3) shows a more random scatter about zero, and reduced dependence on the response variable.

The results of the fit of each layer to Equation 4.2 are listed in Table 4.3. Those series whose fitted parameters  $\Sigma_1$  and  $A$  were both significant at a 95% probability level ( $p \leq 0.05$ ) are shown in bold; these were used for further analysis (total 41 series). As can be seen in Table 4.3, the  $R^2$  values of regression are mostly  $\approx 0.9$ , indicating a good fit of the model to the data (Mendenhall and Sincich, 1996, pp. 127-137).

#### 4.2.4 Description of parameter values

The descriptive statistics for the fitted parameters  $\Sigma_1$  and  $A$  are listed in Table 4.4. For the Columbia Mountains, the mean value of  $\Sigma_1$  is 0.137 kPa, which may be interpreted as the mean shear strength of buried surface hoar layers on the first day of burial. The mean value for  $A$  is 0.949, which indicates that, in the Columbia Mountains, the shear strength of buried surface hoar layers generally increases almost linearly with time for the first 30 days after burial. The distributions of  $\Sigma_1$  and  $A$  are shown in Figures 4.4 and 4.5, respectively.

**Table 4.4** : Descriptive statistics for  $\Sigma_1$  and  $A$ .

<b>Variable</b>	<b>Valid N</b>	<b>Mean</b>	<b>Median</b>	<b>Min.</b>	<b>Max.</b>	<b>Std. dev.</b>
$\Sigma_1$	41	0.137	0.092	0.007	0.435	0.125
$A$	41	0.948	0.951	0.314	1.8	0.328

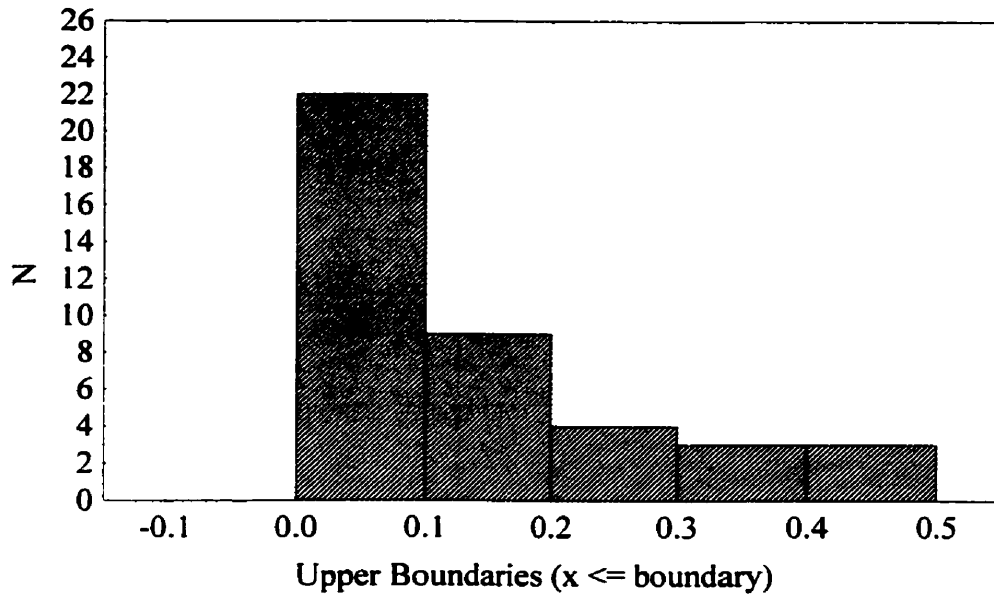


**Figure 4.4 :** Distribution of  $\Sigma_1$  values for time series from Table 4.3.

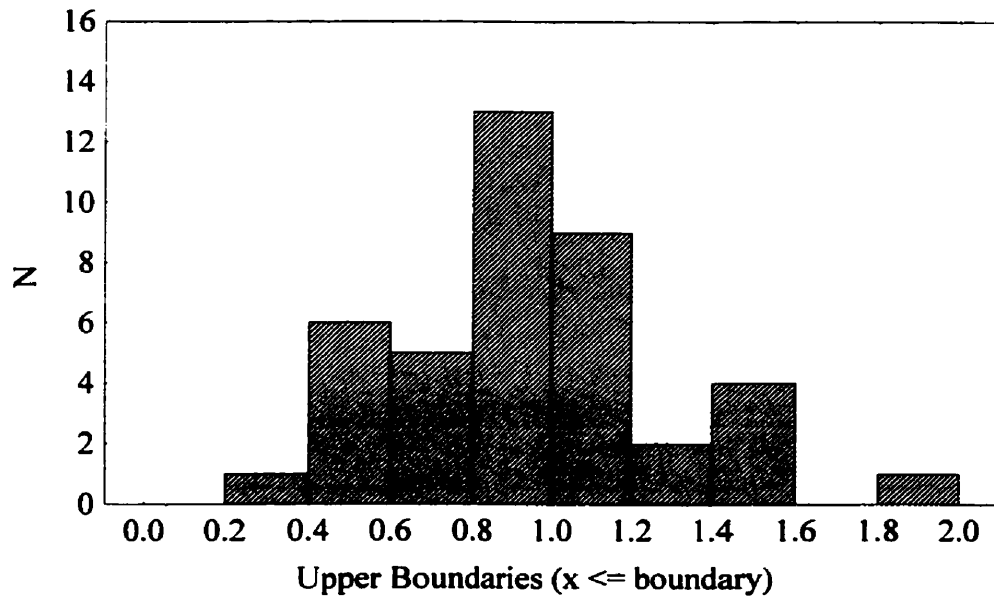


**Figure 4.5 :** Distribution of  $A$  values from Table 4.3.

#### 4.2.5 Snowpack factors influencing model parameters

In order to determine which factors in the snowpack may influence the values of  $\Sigma_1$  and  $A$  in the Columbia Mountains, variables based on snowpack observations from the surface hoar series were correlated with  $\Sigma_1$  and  $A$ , using Spearman rank correlations. Spearman statistics were used to establish relationships amongst variables that may not be normally distributed. Spearman rank R values of magnitude 1 indicate a perfect correlation. The closer a value is in magnitude to 1 indicates a better correlation, 0 indicates a weak correlation. Positive (+) values imply an increasing relationship between variables, negative (-) values a decreasing relationship (Statistica, 1999).

The form of the snowpack (predictor) variables (Table 4.1) used in the shear strength-time model and their physical meanings are listed in Table 4.5. Some of these variables were based directly on snowpack measurements, others were combinations of these variables. Initial values are from the first day on which a particular layer was measured, which is not necessarily the first day of burial. Series values are derived from the interval between the first and last days of measurement (on or before day 30). Values of  $\sigma_1$ , or load overlying the weak layer on the first day of burial, were obtained by a regression of load  $\sigma$  against time.

**Table 4.5:** General forms of snowpack variables for Shear Strength-Power Law model.

Form of variable	Description
$VAR_1$	Value on first day of burial (from regression)
$VAR_0$	Value on first measurement day
$VAR_{series\ avg}$	Average value over measured series
$\Delta VAR_{series}$	Change in value over measured series
$(\Delta VAR/\Delta t)_{series}$	Rate of change in value over measured series ( <i>VAR UNITS d<sup>-1</sup></i> )

**Table 4.6:** Spearman rank correlations of  $\Sigma_1$  and  $A$  with snowpack variables. Significant correlations ( $p < 0.05$ ) highlighted.

Correlation $\Sigma_1$ and variable	Spearman R	p-level	Correlation $A$ and variable	Spearman R	p-level
$\sigma_1$	<b>0.630</b>	<b>&lt;0.001</b>	$\sigma_1$	<b>-0.543</b>	<b>0.001</b>
$\sigma_0$	0.198	0.226	$\sigma_0$	-0.047	0.776
$\sigma_{\text{series avg}}$	<b>0.331</b>	<b>0.040</b>	$\sigma_{\text{series avg}}$	-0.070	0.671
$\Delta\sigma_{\text{series}}$	0.225	0.169	$\Delta\sigma_{\text{series}}$	-0.065	0.692
$\Delta\sigma_{\text{series}}$	0.133	0.420	$\Delta\sigma_{\text{series}}$	0.069	0.678
$H_0$	0.210	0.183	$H_0$	-0.089	0.574
$H_{\text{series avg}}$	0.207	0.188	$H_{\text{series avg}}$	0.007	0.963
$\Delta H_{\text{series}}$	0.042	0.793	$\Delta H_{\text{series}}$	0.076	0.635
$(\Delta H/\Delta t)_{\text{series}}$	-0.063	0.694	$(\Delta H/\Delta t)_{\text{series}}$	0.183	0.246
$HS_0$	0.007	0.966	$HS_0$	0.182	0.250
$HS_{\text{series avg}}$	-0.015	0.926	$HS_{\text{series avg}}$	0.214	0.174
$\Delta HS_{\text{series}}$	0.080	0.615	$\Delta HS_{\text{series}}$	-0.020	0.900
$(\Delta HS/\Delta t)_{\text{series}}$	0.009	0.956	$(\Delta HS/\Delta t)_{\text{series}}$	0.067	0.672
Thick <sub>0</sub>	-0.024	0.900	Thick <sub>0</sub>	-0.088	0.638
Thick <sub>0</sub>	-0.161	0.388	Thick <sub>0</sub>	0.028	0.882
$\Delta\text{Thick}_{\text{series}}$	-0.285	0.120	$\Delta\text{Thick}_{\text{series}}$	0.293	0.110
$(\Delta\text{Thick}/\Delta t)_{\text{series}}$	-0.243	0.188	$(\Delta\text{Thick}/\Delta t)_{\text{series}}$	0.261	0.156
$\text{Twl}_0$	0.049	0.760	$\text{Twl}_0$	-0.091	0.567
$\text{Twl}_{\text{series avg}}$	0.092	0.564	$\text{Twl}_{\text{series avg}}$	-0.142	0.371
$\Delta\text{Twl}_{\text{series}}$	0.129	0.416	$\Delta\text{Twl}_{\text{series}}$	-0.081	0.611
$(\Delta\text{Twl}/\Delta t)_{\text{series}}$	0.052	0.745	$(\Delta\text{Twl}/\Delta t)_{\text{series}}$	0.018	0.910
$\text{TG}_0$	-0.185	0.242	$\text{TG}_0$	0.069	0.662

**Table 4.6 (continued):** Spearman rank correlations of  $\Sigma_1$  and  $A$  with snowpack variables. Significant correlations ( $p < 0.05$ ) highlighted.

Correlation $\Sigma_1$ and variable	Spearman R	p-level	Correlation $A$ and variable	Spearman R	p-level
TG <sub>series avg</sub>	-0.108	0.494	TG <sub>series avg</sub>	-0.007	0.965
$\Delta$ TG <sub>series</sub>	0.206	0.192	$\Delta$ TG <sub>series</sub>	-0.105	0.507
$(\Delta$ TG/ $\Delta$ t) <sub>series</sub>	0.259	0.097	$(\Delta$ TG/ $\Delta$ t) <sub>series</sub>	-0.152	0.335
Emin <sub>o</sub>	-0.018	0.910	Emin <sub>o</sub>	-0.031	0.845
Emin <sub>series avg</sub>	0.000	0.998	Emin <sub>series avg</sub>	-0.063	0.697
$\Delta$ Emin <sub>series</sub>	-0.130	0.422	$\Delta$ Emin <sub>series</sub>	0.146	0.368
$(\Delta$ Emin/ $\Delta$ t) <sub>series</sub>	-0.131	0.422	$(\Delta$ Emin/ $\Delta$ t) <sub>series</sub>	0.143	0.378
Emax <sub>o</sub>	-0.215	0.222	Emax <sub>o</sub>	0.110	0.534
Emax <sub>series avg</sub>	-0.149	0.440	Emax <sub>series avg</sub>	-0.001	0.994
$\Delta$ Emax <sub>series</sub>	-0.013	0.948	$\Delta$ Emax <sub>series</sub>	-0.050	0.797
$(\Delta$ Emax/ $\Delta$ t) <sub>series</sub>	0.010	0.959	$(\Delta$ Emax/ $\Delta$ t) <sub>series</sub>	-0.076	0.694
(Emax-Emin) <sub>o</sub>	-0.203	0.249	(Emax-Emin) <sub>o</sub>	0.083	0.641
(Emax-Emin) <sub>series avg</sub>	-0.192	0.319	(Emax-Emin) <sub>series avg</sub>	0.008	0.967
$\Delta$ (Emax-Emin) <sub>series</sub>	-0.133	0.491	$\Delta$ (Emax-Emin) <sub>series</sub>	0.025	0.897
$[\Delta$ (Emax-Emin)/ $\Delta$ t] <sub>series</sub>	-0.090	0.643	$[\Delta$ (Emax-Emin)/ $\Delta$ t] <sub>series</sub>	-0.012	0.949
(TG/Tw) <sub>o</sub>	0.198	0.208	(TG/Tw) <sub>o</sub>	-0.052	0.745
(TG/Tw) <sub>series avg</sub>	0.087	0.582	(TG/Tw) <sub>series avg</sub>	0.060	0.707

The results of the Spearman rank correlations of  $\Sigma_1$  and  $A$  with snowpack variables are shown in Table 4.6, with significant values ( $p < 0.05$ ) highlighted. The initial shear strength  $\Sigma_1$  showed a significant positive correlation only with  $\sigma_1$  and  $\sigma_{\text{series avg}}$ . The exponential growth constant  $A$  showed a significant negative correlation with  $\sigma_1$ .

Because they both correlate with  $\sigma_1$ , the cross-correlation between  $\Sigma_1$  and  $A$  was examined. The Spearman R value of this correlation is -0.921 and is highly significant ( $p < 0.01$ ). Additionally,  $\sigma_1$  and  $\sigma_{\text{series avg}}$  are significantly cross-correlated, with a Spearman R value of 0.358. Because  $\sigma_{\text{series avg}}$  is a variable that requires knowledge of series changes in advance, it is of little use for forecasting purposes, and is not used in the rest of this section.

The results of this Spearman rank analysis showed important correlations of  $\Sigma_1$  and  $A$  with the load on a buried surface hoar layer on the first day of burial  $\sigma_1$ . More initial load on a layer means that it tends to be stronger initially, but slower to subsequently gain strength. Because load variables were the only significant correlations, the results imply that load plays a very important role in the strength and strength change of buried surface hoar layers.

Since  $\Sigma_1$  and  $A$  correlated with initial load  $\sigma_1$ , these parameters were expressed as a function of initial load on a buried surface hoar layer, via simple least-squares regression. The results of this regression are shown in Tables 4.7 and 4.8.

**Table 4.7:** Regression of  $\Sigma_1$  with  $\sigma_1$ .

Adjusted R <sup>2</sup> = .172 p<.007	Coeff. B	St. Err. of B
Intercept	0.0787	0.0309
$\sigma_1$	0.501	0.174

**Table 4.8:** Regression of  $A$  with  $\sigma_1$ .

Adjusted R <sup>2</sup> = .058 p<.085	Coeff. B	St. Err. of B
Intercept	1.03797	0.08557
$\sigma_1$	-0.8539	0.48154

Table 4.7 shows that the regression of  $\Sigma_1$  against  $\sigma_1$  is significant at the 95% level ( $p < 0.007$ ). Table 4.8 shows that the regression of  $A$  against  $\sigma_1$  is not significant at the 95% level ( $p < 0.085$ ). Thus, only  $\Sigma_1$  may be expressed as a function of  $\sigma_1$ , from the calculated B parameters of Table 4.7:

$$\Sigma_1^* = 0.0787 \text{ kPa} + 0.501 \cdot \sigma_1 \quad (4.3)$$

#### 4.2.6 Results

With the completion of the analysis of  $\Sigma_1$  and  $A$ , Equation 4.1 may now be expressed as a model for the shear strength of buried surface hoar layers in the Columbia mountains:

$$\Sigma^* = \Sigma_1^* \cdot (t/t_1)^A \quad (4.4)$$

where  $\Sigma^*$  is the forecast shear strength on day  $t$ ,  $\Sigma_1^* = 0.0787 \text{ kPa} + 0.501 \cdot \sigma_1$  (Equation 4.3), and  $A = A_{\text{avg}} = 0.948$  (from Table 4.4). The load on the first day of burial  $\sigma_1$  may be estimated from automated precipitation gauge or manual measurements near the study site.

The Shear Strength-Power Law model clearly shows the importance of load overlying a layer of buried surface hoar to the shear strength of the layer. This idea is developed further in the Shear Strength—Lagged Load model of Section 4.4. The fit of the Shear Strength-Power Law model to the data will be examined in Section 4.5.

### 4.3 Shear Strength – Interval model

#### 4.3.1 Introduction

The objective of the Shear Strength - Interval model is to develop an empirical formula to predict the current strength of a buried surface hoar layer, and forecast the forthcoming change in strength. This model is based on a set on snowpack observations taken on any given day within the first 30 days that the layer is buried in the snowpack. The model may be broken into two components: estimating shear strength of the buried surface hoar layer on the day when the snowpack observations are made, then estimating the strength change between the measurement day and an arbitrarily selected day up to eight days in the future. In an operational situation, the next day would be the day on which a new set of snowpack observations is made (and the model is re-initialised).

This model may be portrayed mathematically as a combination of two empirical functions:

$$\Sigma_j^* = \Sigma_i^* + (\Delta t_{ij}) \cdot (\Delta \Sigma / \Delta t)_{ij}^* , \quad (4.5)$$

where  $\Sigma_i^*$  and  $(\Delta \Sigma / \Delta t)_{ij}^*$  are functions of snowpack observations on day i, or abbreviated as:

$$\Sigma_i^* = \Sigma_i^*(\text{snowpack observations } i) \quad (4.6)$$

$$(\Delta \Sigma / \Delta t)_{ij}^* = (\Delta \Sigma / \Delta t)_{ij}^*(\text{snowpack observations } i) . \quad (4.7)$$

In Equations 4.5, 4.6 and 4.7,  $\Sigma_i^*$  is the estimated shear strength on day i (kPa),  $(\Delta t_{ij})$  is the time interval between day i and day j ( $t_j - t_i$ ), where  $1 < j \leq (i + 8)$ ,  $(\Delta \Sigma / \Delta t)_{ij}^*$  is the model estimated rate of change in shear strength ( $\text{kPa d}^{-1}$ ) between day i and day j, and  $\Sigma_j^*$  is the forecast shear strength on day j.

### 4.3.2 Dataset

The dataset for this model consisted of 84 time series of measurements of buried surface hoar layers (Table 4.9). In an effort to better model the strength changes of these layers over realistic intervals between operational study plot measurements, intervals larger than 8 days were rejected. Furthermore, in order to model strength changes over the time frame in which buried surface hoar layers are prone to cause skier-triggered slab avalanches, only measurements within the first 30 days of burial were included. This created a dataset of 361 strength measurements, or 278 measurement intervals.

For purposes of model testing and application, two time series were removed from the dataset prior to developing the model. These are the same layers removed in Section 4.2 and are highlighted in Table 4.9.

### 4.3.3 Distribution of measured data

Descriptive statistics on the measured shear strength data  $\Sigma_i$  (shear strength at the start of a measurement interval) and  $(\Delta\Sigma/\Delta t)_{ij}$  (rate of change in shear strength over a measurement interval) are shown in Table 4.10. The distributions of  $(\Delta\Sigma/\Delta t)_{ij}$  and  $\Sigma_i$  are plotted in Figures 4.6 and 4.7, respectively.

**Table 4.10:** Descriptive statistics for  $\Sigma_i$  and  $(\Delta\Sigma/\Delta t)_{ij}$ .

Variable	Valid N	Mean	Median	Min.	Max.	Std.Dev.
$\Sigma_i$	278	1.05	0.93	0.05	4.79	0.70
$(\Delta\Sigma/\Delta t)_{ij}$	278	6.70E-02	6.68E-02	-3.19E-01	4.26E-01	8.89E-02

**Table 4.9:** Surface hoar layers used in Shear Strength-Interval model. Highlighted layers excluded from model construction .

Location	Burial date	N
Mt. St. Anne Study Plot	15-Nov-93	3
Mt. St. Anne Study Plot	04-Dec-93	4
Sam's Study Plot	18-Dec-93	2
Mt. St. Anne Study Plot	29-Dec-93	4
Sam's Study Plot	29-Dec-93	2
Sam's Study Plot	29-Dec-93	2
Mt. St. Anne Study Plot	21-Jan-94	2
Sam's Run	05-Feb-94	2
Sam's Study Plot	05-Feb-94	2
Mt. St. Anne Study Plot	05-Feb-94	4
Tower Study Slope	05-Feb-94	2
Vermont Study Plot	15-Dec-94	3
Elk Study Plot	15-Dec-94	5
Vermont Study Plot	07-Jan-95	7
Mt. St. Anne Study Plot	07-Jan-95	7
Mt. St. Anne Airbox	07-Jan-95	7
Mt. St. Anne Landing	07-Jan-95	2
Mt. St. Anne Study Plot	14-Feb-95	2
Mt. St. Anne Study Plot	14-Feb-95	3
Mt. St. Anne Study Plot	28-Dec-95	3
Mt. St. Anne Airbox	28-Dec-95	3
Mt. St. Anne Airbox	01-Jan-96	2
Mt. St. Anne Study Plot	01-Jan-96	3
Mt. St. Anne Study Plot	04-Feb-96	2

Location	Burial date	N
Mt. St. Anne Study Plot	17-Feb-96	4
Vermont Study Plot	17-Jan-97	8
Vermont Airbox	17-Jan-97	8
Pygmy Run	17-Jan-97	5
North Moose Log Cut	17-Jan-97	5
Mt. St. Anne Study Plot	17-Jan-97	7
MSA RP Airbox	17-Jan-97	5
Elk Study Plot	17-Jan-97	3
Elk Study Slope	17-Jan-97	4
<b>Mt. St. Anne Study Plot</b>	<b>10-Feb-97</b>	<b>6</b>
Mt. St. Anne Airbox	10-Feb-97	6
Mt. St. Anne Cutblock	10-Feb-97	5
Vermont Study Plot	11-Feb-97	7
Vermont Airbox	11-Feb-97	7
Pygmy Run	11-Feb-97	6
North Moose Log Cut	11-Feb-97	7
North Moose Log Cut	01-Mar-97	2
Pygmy Run	01-Mar-97	2

**Table 4.9 (continued):** Surface hoar layers used in Shear Strength-Interval model.  
 Highlighted layers excluded from model construction .

<b>Location</b>	<b>Burial date</b>	<b>N</b>	<b>Location</b>	<b>Burial date</b>	<b>N</b>
Vermont Airbox	01-Mar-97	2	Fidelity Study Slope	12-Mar-99	2
Vermont Study Plot	01-Mar-97	2	Cheops Study Plot	30-Dec-99	3
Middle Moose Study Plot	26-Dec-97	5	Fidelity Study Slope	30-Dec-99	5
Vermont Study Plot	26-Dec-97	6	<b>Mt. St. Anne Study Plot</b>	<b>30-Dec-99</b>	<b>5</b>
Middle Moose Study Plot	03-Feb-98	2	Cheops Study Plot	31-Jan-00	5
Pygmy Run	03-Feb-98	2	Fidelity Study Slope	31-Jan-00	6
Mt. St. Anne Study Plot	13-Feb-98	6	Mt. St. Anne Study Plot	31-Jan-00	8
Mt. St. Anne Airbox	13-Feb-98	7	Mt. St. Anne Airbox	31-Jan-00	8
Middle Moose Study Plot	17-Feb-98	3	Cheops Study Plot	05-Feb-00	3
Vermont Study Plot	17-Feb-98	2	Cheops Study Plot	21-Feb-00	5
Mt. St. Anne Cutblock	25-Feb-98	2	Fidelity Study Slope	21-Feb-00	4
Mt. St. Anne Study Plot	25-Feb-98	5	Mt. St. Anne Cutblock	21-Feb-00	6
Mt. St. Anne Airbox	25-Feb-98	5	Fidelity Study Slope	17-Nov-00	3
Mt. St. Anne Cutblock	25-Feb-98	2	Fidelity Study Slope	24-Nov-00	5
Middle Moose Study Plot	28-Feb-98	3	Fidelity Study Slope	13-Jan-01	6
Vermont Airbox	28-Feb-98	3	Mt. St. Anne Study Plot	20-Jan-01	7
Vermont Study Plot	28-Feb-98	3	Fidelity Study Slope	28-Jan-01	8
Fidelity Study Slope	03-Jan-99	3	Mt. St. Anne Study Plot	23-Feb-01	4
Cheops Study Plot	03-Jan-99	4	Fidelity Study Slope	23-Feb-01	7
Fidelity Study Slope	24-Jan-99	2			
Cheops Study Plot	24-Jan-99	4			
Fidelity Study Slope	16-Feb-99	6			
Cheops Study Plot	16-Feb-99	7			

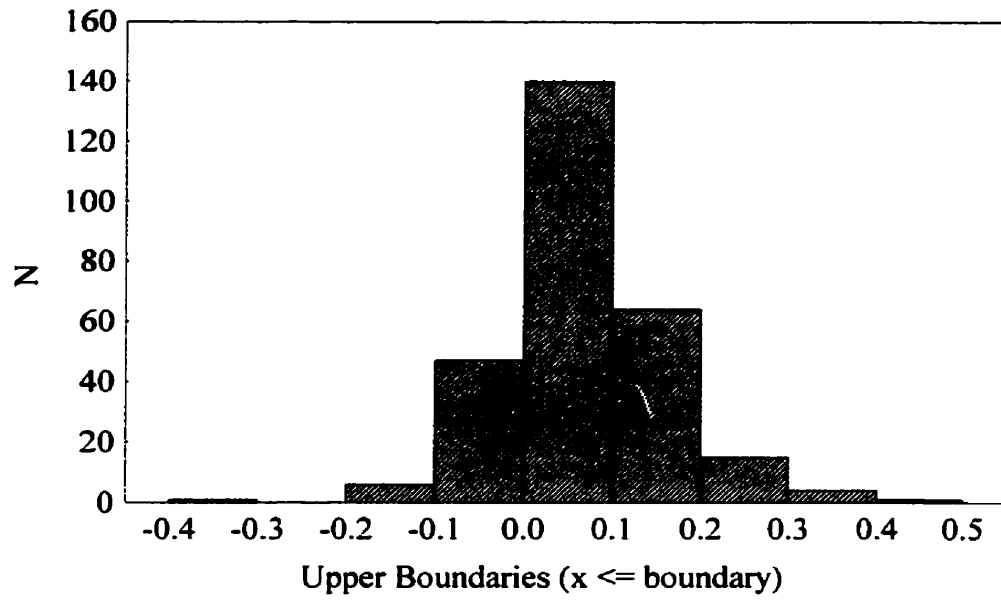


**Figure 4.6 :** Distribution of  $(\Delta\Sigma/\Delta t)_{ij}$ .

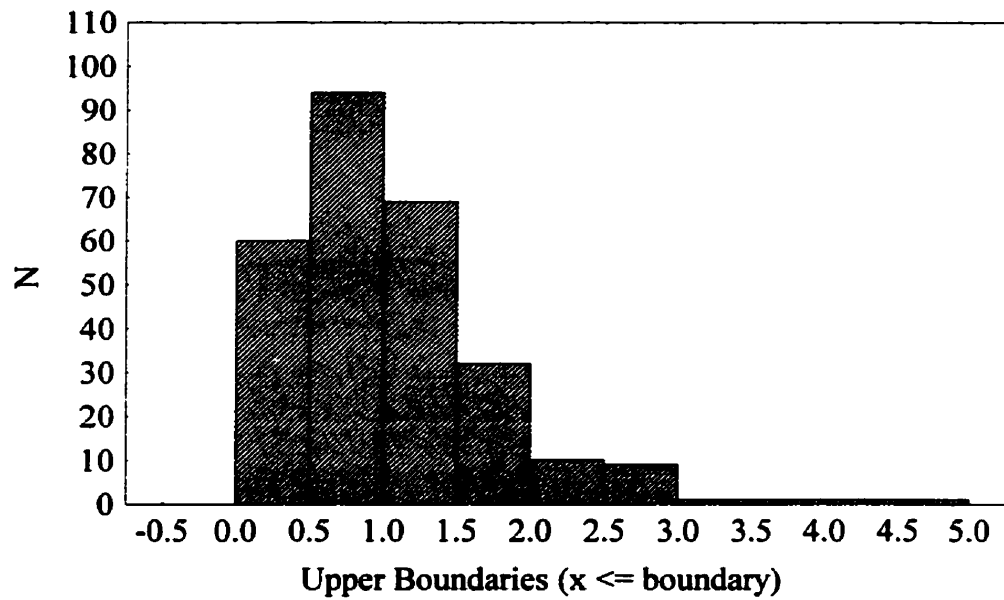


**Figure 4.7 :** Distribution of  $\Sigma_i$ .

#### 4.3.4 Snowpack variables

The form of the snowpack variables used in the development of the Shear Strength – Interval model are shown in Table 4.11.

**Table 4.11:** General forms of snowpack variables for Shear Strength-Interval model.

<b>Form of variable</b>	<b>Description</b>
$VAR_i$	Value at start of measurement
$VAR_{avg\ ij}$	Average value over measured interval
$\Delta VAR_{ij}$	Change in value over measured interval
$(\Delta VAR/\Delta t)_{ij}$	Rate of change in value over measured interval ( $VAR\ UNITS\ d^{-1}$ )

In the interests of optimising model construction, predictor variables that do not have a significant correlation with the response variables  $(\Delta\Sigma/\Delta t)_{ij}$  and  $\Sigma_i$  were eliminated from the list of input variables. This was done with Spearman rank correlations, as shown in Table 4.12. Significant correlations ( $p < 0.05$ ) are highlighted; the corresponding variables are used in subsequent analysis.

Closely following the example of Jamieson and Johnston (1999), the possible associations between the significant independent predictor variables and the response variables of the shear strength – interval model and physical snowpack processes may be addressed (see Chapter 2). This largely based on the sign of the coefficients of each predictor variable (Table 4.12); a “+” sign indicates an increasing relationship, a “-” sign indicates a decreasing relationship.

Age of the weak layer ( $t$ ). Older layers are stronger but slower to gain strength, as illustrated in Figure 4.1.

Load on the weak layer ( $\sigma$ ). More load is associated with surface hoar layers that are stronger and gain strength faster. This is probably due to increased thinning of the weak layer, which implies more bonding and greater strength (see Chapter 2).

**Table 4.12: Spearman rank correlations between response and predictor variables in Shear Strength—Interval model.**

Correlation with $(\Delta\Sigma/\Delta t)_{ij}$	Spearman R	p-level
$t_i$	<b>-2.50E-01</b>	<b>&lt; 0.001</b>
$\Sigma_i$	<b>-1.73E-01</b>	<b>0.004</b>
$\sigma_i$	3.60E-02	0.556
$\sigma_{avg\ ij}$	<b>1.26E-01</b>	<b>0.040</b>
$\Delta\sigma_{ij}$	<b>2.11E-01</b>	<b>0.001</b>
$(\Delta\sigma/\Delta t)_{ij}$	<b>2.11E-01</b>	<b>0.001</b>
$H_i$	1.11E-01	0.065
$H_{avg\ ij}$	<b>1.82E-01</b>	<b>0.002</b>
$\Delta H_{ij}$	<b>1.44E-01</b>	<b>0.016</b>
$(\Delta H/\Delta t)_{ij}$	<b>1.32E-01</b>	<b>0.028</b>
$HS_i$	<b>2.42E-01</b>	<b>&lt; 0.001</b>
$HS_{avg\ ij}$	<b>2.50E-01</b>	<b>&lt; 0.001</b>
$\Delta HS_{ij}$	8.04E-02	0.181
$(\Delta HS/\Delta t)_{ij}$	7.99E-02	0.184
<b>Thick<sub>i</sub></b>	<b>-1.34E-01</b>	<b>0.044</b>
<b>Thick<sub>avg\ ij</sub></b>	<b>-1.56E-01</b>	<b>0.020</b>
$\Delta Thick_{ij}$	3.42E-02	0.610
$(\Delta Thick/\Delta t)_{ij}$	2.67E-02	0.690
$Twl_i$	7.58E-02	0.209
$Twl_{avg\ ij}$	6.90E-02	0.254
$\Delta Twl_{ij}$	-3.34E-02	0.581
$(\Delta Twl/\Delta t)_{ij}$	-4.79E-02	0.429
<b>TG<sub>i</sub></b>	<b>-2.79E-01</b>	<b>&lt; 0.001</b>

Correlation with $\Sigma_i$	Spearman R	p-level
$t_i$	<b>6.60E-01</b>	<b>&lt; 0.001</b>
$\sigma_i$	<b>8.08E-01</b>	<b>&lt; 0.001</b>
$\sigma_{avg\ ij}$	<b>7.45E-01</b>	<b>&lt; 0.001</b>
$\Delta\sigma_{ij}$	-1.48E-03	0.981
$(\Delta\sigma/\Delta t)_{ij}$	-4.75E-02	0.442
$H_i$	<b>6.86E-01</b>	<b>&lt; 0.001</b>
$H_{avg\ ij}$	<b>6.11E-01</b>	<b>&lt; 0.001</b>
$\Delta H_{ij}$	<b>-1.74E-01</b>	<b>0.004</b>
$(\Delta H/\Delta t)_{ij}$	<b>-1.83E-01</b>	<b>0.002</b>
$HS_i$	<b>3.03E-01</b>	<b>&lt; 0.001</b>
$HS_{avg\ ij}$	<b>2.88E-01</b>	<b>&lt; 0.001</b>
$\Delta HS_{ij}$	-8.86E-02	0.141
$(\Delta HS/\Delta t)_{ij}$	-9.48E-02	0.115
<b>Thick<sub>i</sub></b>	<b>-3.47E-01</b>	<b>&lt; 0.001</b>
<b>Thick<sub>avg\ ij</sub></b>	<b>-4.01E-01</b>	<b>&lt; 0.001</b>
$\Delta Thick_{ij}$	1.29E-02	0.847
$(\Delta Thick/\Delta t)_{ij}$	1.93E-02	0.773
$Twl_i$	<b>1.23E-01</b>	<b>0.041</b>
$Twl_{avg\ ij}$	<b>1.69E-01</b>	<b>0.005</b>
$\Delta Twl_{ij}$	-4.96E-02	0.413
$(\Delta Twl/\Delta t)_{ij}$	-6.57E-02	0.277
<b>TG<sub>i</sub></b>	<b>-1.57E-01</b>	<b>0.009</b>
<b>TG<sub>avg\ ij</sub></b>	<b>-2.29E-01</b>	<b>&lt; 0.001</b>

**Table 4.12 (continued):** Spearman rank correlations between response and predictor variables in Shear strength—Interval model.

<b>Correlation with <math>(\Delta\Sigma/\Delta t)_{ij}</math></b>	<b>Spearman R</b>	<b>p-level</b>	<b>Correlation with <math>\Sigma_i</math></b>	<b>Spearman R</b>	<b>p-level</b>
<b>TG<sub>avg ij</sub></b>	<b>-2.58E-01</b>	<b>&lt; 0.001</b>	<b><math>\Delta TG_{ij}</math></b>	2.56E-02	0.671
<b><math>\Delta TG_{ij}</math></b>	<b>1.63E-01</b>	<b>0.007</b>	<b><math>(\Delta TG/\Delta t)_{ij}</math></b>	2.69E-02	0.655
<b><math>(\Delta TG/\Delta t)_{ij}</math></b>	<b>1.66E-01</b>	<b>0.005</b>	<b>E<sub>min i</sub></b>	<b>-2.72E-01</b>	<b>&lt; 0.001</b>
<b>E<sub>min i</sub></b>	5.95E-03	0.922	<b>E<sub>min avg ij</sub></b>	<b>-2.85E-01</b>	<b>&lt; 0.001</b>
<b>E<sub>min avg ij</sub></b>	-3.57E-02	0.558	<b><math>\Delta E_{min ij}</math></b>	-3.94E-03	0.948
<b><math>\Delta E_{min ij}</math></b>	-3.23E-02	0.595	<b><math>(\Delta E_{min}/\Delta t)_{ij}</math></b>	-4.02E-03	0.947
<b><math>(\Delta E_{min}/\Delta t)_{ij}</math></b>	-2.50E-02	0.681	<b>E<sub>max i</sub></b>	<b>-3.88E-01</b>	<b>&lt; 0.001</b>
<b>E<sub>max i</sub></b>	-8.59E-03	0.896	<b>E<sub>max avg ij</sub></b>	<b>-3.81E-01</b>	<b>&lt; 0.001</b>
<b>E<sub>max avg ij</sub></b>	-8.46E-02	0.219	<b><math>\Delta E_{max ij}</math></b>	1.93E-02	0.780
<b><math>\Delta E_{max ij}</math></b>	6.23E-02	0.366	<b><math>(\Delta E_{max}/\Delta t)_{ij}</math></b>	3.05E-02	0.658
<b><math>(\Delta E_{max}/\Delta t)_{ij}</math></b>	6.72E-02	0.329	<b><math>(E_{max}-E_{min})_i</math></b>	<b>-3.86E-01</b>	<b>&lt; 0.001</b>
<b><math>(E_{max}-E_{min})_i</math></b>	-3.68E-02	0.575	<b><math>(E_{max}-E_{min})_{avg ij}</math></b>	<b>-4.25E-01</b>	<b>&lt; 0.001</b>
<b><math>(E_{max}-E_{min})_{avg ij}</math></b>	-8.89E-02	0.196	<b><math>\Delta(E_{max}-E_{min})_{ij}</math></b>	1.84E-02	0.789
<b><math>\Delta(E_{max}-E_{min})_{ij}</math></b>	6.82E-02	0.322	<b><math>(\Delta(E_{max}-E_{min})/\Delta t)_{ij}</math></b>	2.82E-02	0.682
<b><math>(\Delta(E_{max}-E_{min})/\Delta t)_{ij}</math></b>	6.49E-02	0.346	<b><math>(TG/Twl)_i</math></b>	<b>1.45E-01</b>	<b>0.016</b>
<b><math>(TG/Twl)_i</math></b>	<b>2.71E-01</b>	<b>&lt; 0.001</b>	<b><math>(TG/Twl)_{avg ij}</math></b>	<b>2.02E-01</b>	<b>0.001</b>
<b><math>(TG/Twl)_{avg ij}</math></b>	<b>2.39E-01</b>	<b>&lt; 0.001</b>			

**Thickness of slab overlying the weak layer (H).** Thicker slabs are associated with greater strength and faster rates of strength gain. Also associated with more load ( $\sigma$ ) overlying the weak layer, and lower magnitudes of temperature gradients (TG) across the weak layer, which may be due to rounding metamorphism and increased bonding and strength gain (Colbeck, 1987).

**Layer thickness (Thick).** Thicker layers of buried surface hoar are associated with lower strength and are slower to gain strength. This is possibly due to a larger “umbrella effect” and therefore fewer bonds between surface hoar crystals and at the base of the surface hoar layer (see Chapter 2).

**Weak layer temperature (T<sub>wl</sub>).** Warmer (sub-zero) temperatures are associated with stronger layers of buried surface hoar. This is possibly due to increased rounding metamorphism at warmer temperatures, manifested in buried surface hoar layers as increased rounding and clustering of grains (see Chapter 2). In the Columbia Mountains, colder surface hoar layers occur in shallower snowpacks (HS).

**Magnitude of temperature gradient across the buried surface hoar layer (TG).** Larger magnitude temperature gradient is associated with lower strength and slower rates of strength gain. This is possibly due to slower bonding associated with a high-TG regime of metamorphism (Colbeck, 1987).

**Snowpack depth (HS).** Greater snowpack depth is associated with stronger surface hoar layers and larger rates of strength gain. Deeper snowpacks are also associated with larger loads ( $\sigma$ ), thicker slabs (H), and likely smaller magnitude temperature gradients (TG) across buried weak layers.

Characteristic grain size of the surface hoar layer ( $E_{min}$ ,  $E_{max}$ ). Layers of larger crystals are associated with lower shear strength and slower strength gain. Larger grains are also associated with thicker layers (Thick) of buried surface hoar (see above).

Weak layer temperature gradient (TG) divided by weak layer temperature (T<sub>wl</sub>). Higher values are associated with slower rates of strength gain, and also with thinner snowpacks (HS), thinner slabs (H), and larger temperature gradients (TG).

#### **4.3.5 Initial regression**

In order to examine which measurable snowpack factors correlated with shear strength, a stepwise, multiple least-squares regression was first performed on the response variable  $(\Delta\Sigma/\Delta t)_{ij}$ , rate of strength change over measurement interval, using the predictor variables selected in Section 4.3.4. Strength at the start of the interval  $\Sigma_i$  was included in the list of predictor variables. Stepwise regression was deemed suitable for this analysis because it has a tendency to choose important predictor variables from a long list of input variables (Mendenhall and Sincich, 1996, p. 242). This assisted in further paring down the list of variables to be used in the model.

The results of this regression on  $(\Delta\Sigma/\Delta t)_{ij}$  are shown in Table 4.13. Variables were included in each step if their computed F-statistic was greater than 1. For details of this technique, please see Statistica (1999). The variables selected by stepwise regression on  $(\Delta\Sigma/\Delta t)_{ij}$  were  $HS_{avg\ ij}$ ,  $\Sigma_i$ ,  $\sigma_{avg\ ij}$ ,  $Thick_{avg\ ij}$ ,  $TG_i$ ,  $(TG/T_{wl})_i$ ,  $t_i$ , and  $H_i$ .

**Table 4.13** : Results of initial multiple stepwise least-squares regression on  $(\Delta\Sigma/\Delta t)_{ij}$ .

<b>Adjusted R<sup>2</sup>= 0.318 p&lt;.00001</b>	<b>Coefficient B</b>	<b>St. Err. of B</b>
Intercept	1.13E-01	2.46E-02
HS <sub>avg ij</sub>	2.46E-04	7.08E-05
Σ <sub>i</sub>	-9.35E-02	1.39E-02
σ <sub>avg ij</sub>	1.24E-01	3.17E-02
Thick <sub>avg ij</sub>	-6.90E-02	1.29E-02
TG <sub>i</sub>	-4.77E-01	1.22E-02
(TG/Twl) <sub>i</sub>	-1.45	5.07E-01
t <sub>i</sub>	-1.39E-03	9.69E-04
H <sub>i</sub>	-5.14E-04	5.07E-04

**Table 4.14** : Results of initial multiple stepwise least-squares regression on Σ<sub>i</sub>.

<b>Adjusted R<sup>2</sup>= 0.739 p&lt;0.0001</b>	<b>Coefficient B</b>	<b>St. Err. of B</b>
Intercept	3.31E-01	1.37E-01
σ <sub>i</sub>	1.40E+00	1.54E-01
Thick <sub>i</sub>	-3.67E-01	6.28E-02
t <sub>i</sub>	1.69E-02	4.87E-03
H <sub>i</sub>	-8.62E-03	2.68E-03
HS <sub>avg ij</sub>	9.96E-04	3.56E-04
E <sub>min i</sub>	2.54E-02	1.38E-02
Twl <sub>avg ij</sub>	2.93E-02	1.62E-02

A stepwise regression was also performed on  $\Sigma_i$ . This permitted the development of an empirical formula for predicting  $\Sigma_i$  as a function of snowpack variables. This formula may be substituted for  $\Sigma_i$  in the formula yielded by the stepwise regression on  $(\Delta\Sigma/\Delta t)_{ij}$  (see Section 4.3.1). The results of this regression are shown in Table 4.14. The variables selected by stepwise regression on  $\Sigma_i$  were  $\sigma_i$ ,  $\text{Thick}_i$ ,  $t_i$ ,  $H_i$ ,  $\text{HS}_{\text{avg } ij}$ ,  $E_{\text{min } i}$ , and  $\text{Twl}_{\text{avg } ij}$ .

#### 4.3.6 Refinement via outlier analysis

A residual of regression is the difference between measured and predicted values of the dependent variable for the same values of predictor variables. The residuals of the analyses of Section 4.3.5 are shown in Figure 4.8 for  $(\Delta\Sigma/\Delta t)_{ij}$  and in Figure 4.9 for  $\Sigma_i$ . These are shown as standard residuals; the x-axis values correspond to the number of standard deviations from 0. Figures 4.8 and 4.9 show what appears to be, as a first approximation, a normal distribution of the residuals about 0. According to Mendenhall and Sincich (1996, p. 414), it is common practice to consider residual values greater than 3 standard deviations from 0 to be statistical outliers. Such outliers are often removed from the model dataset in order to improve model fit, as was the case here. The outliers from the regression analyses of Section 4.3.5 are shown in Table 4.15.

**Table 4.15** : Outliers of initial regression on  $(\Delta\Sigma/\Delta t)_{ij}$  and  $\Sigma_i$ .

$(\Delta\Sigma/\Delta t)_{ij}$			$\Sigma_i$		
Date	Location	Burial date	Date	Location	Burial date
06-Feb-99	Cheops	24-Jan-99	18-Feb-94	MSA RP	05-Feb-94
09-Mar-99	Cheops	16-Feb-99	13-Feb-99	Cheops	24-Jan-99
15-Mar-99	Cheops	16-Feb-99	09-Mar-99	Cheops	09-Mar-99
			14-Jan-00	Cheops	30-Dec-99

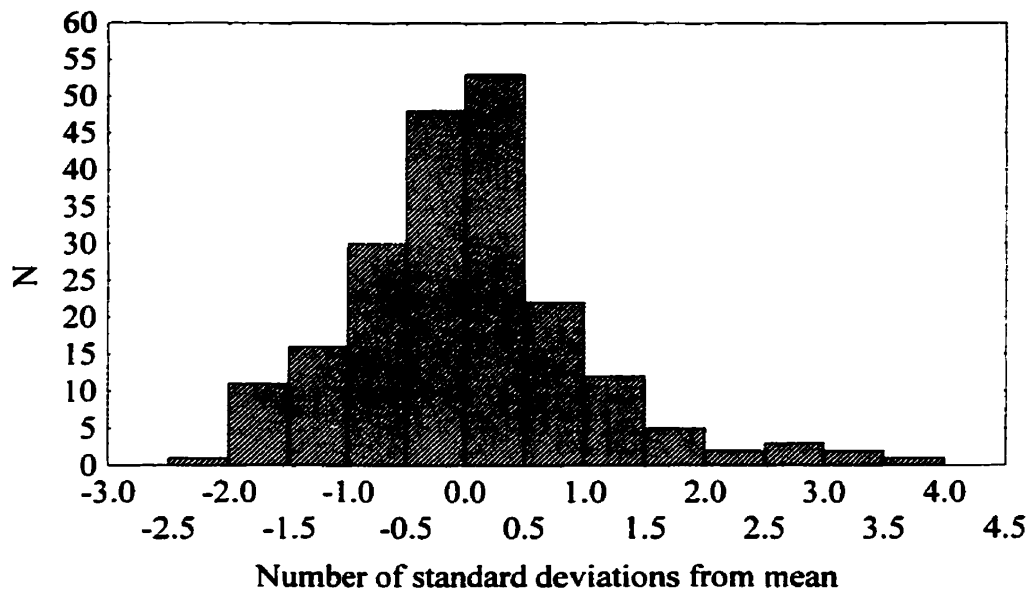


**Figure 4.8 :** Distribution of residuals of initial regression on  $(\Delta\Sigma/\Delta t)_{ij}$ .

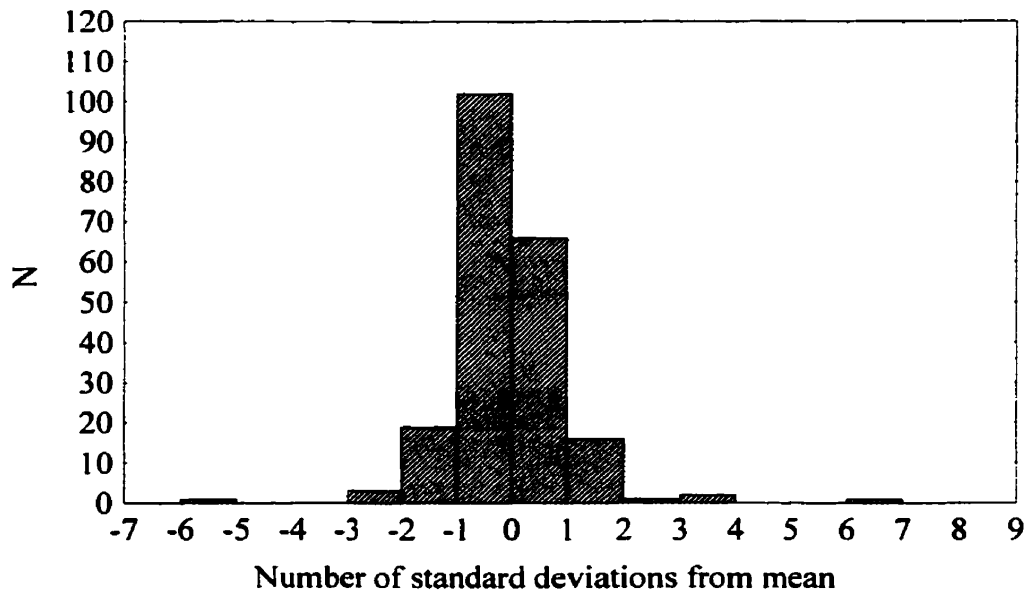


**Figure 4.9 :** Distribution of residuals of initial regression on  $\Sigma_i$ .

It is important to examine the data from these measurement days in order to understand why the regression analysis provides a poor fit to these points.

The 18-Feb-94 data shows the surface hoar in the 05-Feb-94 weak layer (Table 4.15) to be 30 mm in size; this is an unusually large size of surface hoar grains disaggregated from a buried weak layer, which may account for the poor model fit. This layer was also monitored at the Sam's Run, Sam's Plot, and Tower study sites. All of these sites show unusually large surface hoar in this layer, which is the only layer in the entire study for which surface hoar crystals of this size were observed. The 05-Feb-94 layer may thus be considered somewhat of a physical anomaly and is removed from the dataset in subsequent analysis.

Five of the seven statistical outliers shown in Table 4.15 were from the Cheops study site during the winter of 1998-1999. This indicates that there was some common factor that made the regression fit poorly for these layers. The data from all surface hoar layers monitored at the Cheops and Fidelity study sites over that winter indicate several reasons to believe these layers constitute poor data for model construction. The maximum layer thickness measured in any of the Rogers Pass study sites that winter was 3.5 mm; all of these layers were less than half of the mean layer thickness (7.0 mm) of the entire dataset. The maximum grain size measured in these layers was 5 mm; all of these layers had grains considerably smaller than the average maximum grain size (7.5 mm) of the entire dataset. The surface hoar in these layers was often found to be mixed with other grain types, which is rarely seen in the rest of the dataset. Field notes show that these layers were difficult to locate in the snowpack because they were extremely thin.

Microphotographic records of these layers (example shown in Figure 4.10) show surface hoar that was poorly developed, small, and often hard to distinguish from the stellar crystals on which it formed. This becomes evident when the crystals from these layers are compared to a more typical surface hoar layer (Figure 4.11). Based on this evidence, all of the surface hoar layers from the winter 1998-1999 at the Cheops and Fidelity study sites were removed from the dataset in an effort to improve the regression fit.

The final outlier, measured on 14-Jan-00 at the Cheops study site on the 30-Dec-99 weak layer was removed from the dataset. No physical argument for the removal of this entire layer may be found, so the other measurements on this layer were left intact.

#### **4.3.7 Refinement via variable selection**

As stated at the beginning of this chapter, in order for a model to be operationally useful, the input variables must be easily measured by a forecaster or technician and/or have conceptually straightforward physical meaning. Variables such as  $HS_{avg\ ij}$ ,  $Thick_{avg\ ij}$ ,  $\sigma_{avg\ ij}$ , and  $Twl_{avg\ ij}$  are thus of questionable usefulness, since they require advanced knowledge of snowpack characteristics several days in the future in order to calculate their values. An alternative approach with useful variables is to perform a regression similar to that in Section 4.3.5, except using only snowpack variables that are measurable at the start of the prediction interval, at time  $t_i$ , as input variables. If the results are comparable to those yielded by the first regression analysis, the second analysis is preferable for operational use.

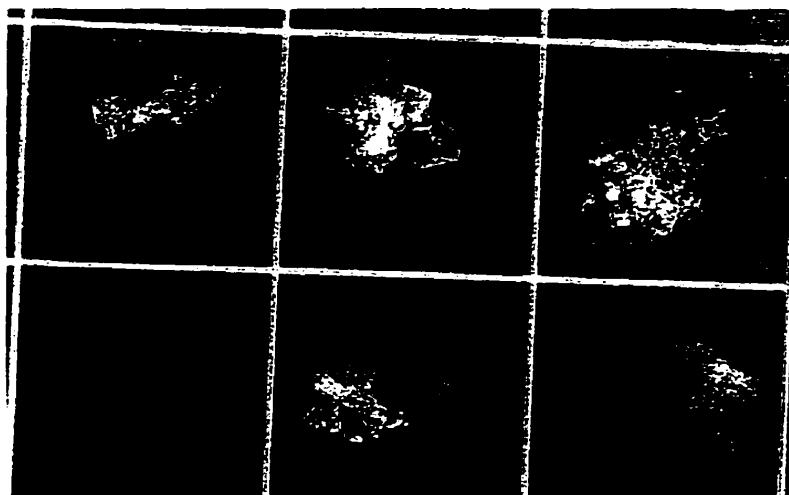


**Figure 4.10:** Surface hoar crystals disaggregated from layer buried 23-January-1999 at the Cheops study site. 10 mm grid. ASARC photo.

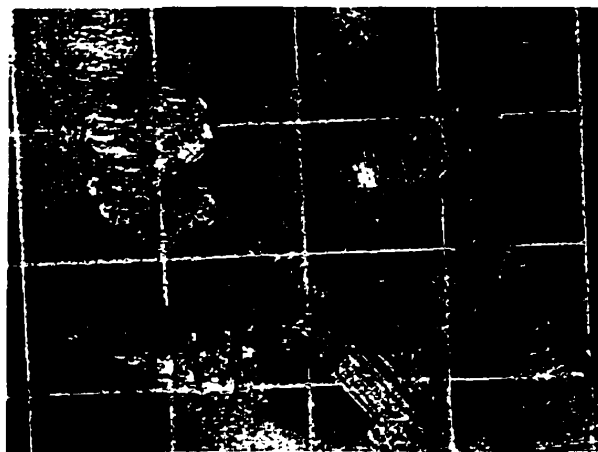


**Figure 4.11:** Surface hoar crystals disaggregated from layer buried 30-December-1999 at the Fidelity study site. 10 mm grid. ASARC photo.

To examine the merit of substituting snowpack variables measured at the start of an interval for less operationally useful interval averages, the correlation between these variables was measured with Spearman rank statistics. The results (Table 4.16) show that the substitution of initial values for interval values of the variables was quite reasonable, as the correlation tended to be very high ( $R \approx 0.9$ ) for the set of over 200 data points. Thus, variables at time  $t_i$  were substituted for interval average variables from the regression analysis of Section 4.3.5 in subsequent analysis.

**Table 4.16** : Cross correlations between predictor variables, initial regression.

<b>Cross correlation</b>	<b>Spearman R</b>	<b>p-level</b>
$\sigma_i$ & $\sigma_{avg\ ij}$	0.937	< 0.001
$HS_i$ & $HS_{avg\ ij}$	0.976	< 0.001
$Thick_i$ & $Thick_{avg\ ij}$	0.948	< 0.001
$Twl_i$ & $Twl_{avg\ ij}$	0.880	< 0.001

#### 4.3.8 Simplified regression

The regression analysis from Section 4.3.5 was performed again, using the dataset modified in Section 4.3.6, and only predictor variables measured at time  $t_i$ , as discussed in Section 4.3.7. The results of this regression are shown in Tables 4.17 and 4.18 for  $(\Delta\Sigma/\Delta t)_{ij}$  and  $(\Sigma_i)$ , respectively.

#### 4.3.9 Comparison of initial and simplified regression analysis

The regression analyses of Sections 4.3.5 and 4.3.8 are compared, based on the output in Tables 4.13 and 4.17 for  $(\Delta\Sigma/\Delta t)_{ij}$  and Tables 4.14 and 4.18 for  $\Sigma_i$ . Mendenhall and Sincich (1996, p.199) recommend the (F test) p-values as a test of overall model adequacy.

**Table 4.17** : Results of simplified multiple stepwise regression on  $(\Delta\Sigma/\Delta t)_{ij}$  .

<b>Adjusted R<sup>2</sup>= 0.317 p&lt;.00001</b>	<b>Coefficient B</b>	<b>St. Err. of B</b>
Intercept	0.119	2.2E-02
t <sub>i</sub>	-0.000547	8.7E-04
Σ <sub>i</sub>	-0.124	1.6E-02
σ <sub>i</sub>	0.107	3.1E-02
H <sub>i</sub>	0.000131	4.8E-04
HS <sub>i</sub>	0.000176	6.7E-05
Thick <sub>i</sub>	-0.0473	1.1E-02
TG <sub>i</sub>	-0.378	1.1E-01
(TG/Twl) <sub>i</sub>	-0.827	4.5E-01

**Table 4.18** : Results of simplified multiple stepwise regression on Σ<sub>i</sub> .

<b>Adjusted R<sup>2</sup>= 0.742 p&lt;0.0001</b>	<b>Coefficient B</b>	<b>St. Err. of B</b>
Intercept	0.336	9.8E-02
t <sub>i</sub>	0.0139	3.7E-03
σ <sub>i</sub>	1.18	1.2E-01
H <sub>i</sub>	-0.00625	2.2E-03
HS <sub>i</sub>	0.000804	2.9E-04
Thick <sub>i</sub>	-0.287	4.8E-02
Twl <sub>i</sub>	0.0187	1.1E-02
Emin <sub>i</sub>	0.0204	1.0E-02

A significance level of 99% or better ( $p$  value  $< 0.01$ ) indicates that the model is useful for predicting the response variable. The output results of regression indicate that both the initial and simplified regression results for both response variables  $\Sigma_i$  and  $(\Delta\Sigma/\Delta t)_{ij}$  are significant.

In ranking the initial and simplified regression results, the Adjusted  $R^2$  (adj.  $R^2$ ) value is of interest, since it accounts for both the number of data points and the number of fitted parameters. Like  $R^2$ , the closer the value of this coefficient is to 1, the better the model fits the data (Mendenhall and Sincich, 1996, pp. 191-193). For the regressions on  $(\Delta\Sigma/\Delta t)_{ij}$ , Tables 4.13 and 4.17 show that the initial regression had a slightly better fit (initial adj.  $R^2 = 0.318$ , simplified adj.  $R^2 = 0.317$ ). For the regressions on  $\Sigma_i$ , Tables 4.14 and 4.18 show that the simplified regression had a slightly better fit (initial adj.  $R^2 = 0.739$ , simplified adj.  $R^2 = 0.742$ ). Considering the model objectives previously discussed, the simplified regression is clearly the preferable choice. These regression results are used in all subsequent analysis in this section.

#### **4.3.10 Residual analysis**

Before constructing a model from the results of the simplified regression of Section 4.3.8, the residuals of regression were analysed to determine the validity of this technique for modelling the strength of buried surface hoar layers. According to Mendenhall and Sincich (1996, pp. 115, 175), the two assumptions to be tested are constant variance and normal distribution of residuals.

The assumption of constant variance was tested by examining a plot of residual values for random scatter about zero. These plots, shown in Figures 4.12 for  $(\Delta\Sigma/\Delta t)_{ij}$  and 4.13 for  $\Sigma_i$ , show random scatter of the residuals and indicate that the assumption of constant variance was satisfied.

To assess the normality of residuals, the distribution was plotted in Figures 4.14 for  $(\Delta\Sigma/\Delta t)_{ij}$  and 4.15 for  $\Sigma_i$ , along with the expected normal distribution and the results of the Kolmogorov-Smirnov (K-S) and Lilliefors tests of normality. The K-S tests if a sample fits a given normal distribution, whereas the Lilliefors test allows for the fitting of parameters (Statsoft, 1994, p. 1379). Although the Lilliefors test may be considered preferable for this study, both tests, as well as the bell shape of the residuals, will be considered in evaluating the normality of the residuals. From Figures 4.14 and 4.15, it can be seen that the hypothesis of normality was not rejected for the K-S test and was rejected for the Lilliefors test at the 95% significance level. Visually, the fit to the normal distribution seems quite reasonable for both. According to Mathsoft (1997, pp. 41-43) the results of regression are robust enough for such a distribution of residuals.

Since the two key assumptions for multiple least squares regression analysis were satisfied, it was concluded that the technique of least squares multiple regression was a valid one for this model.

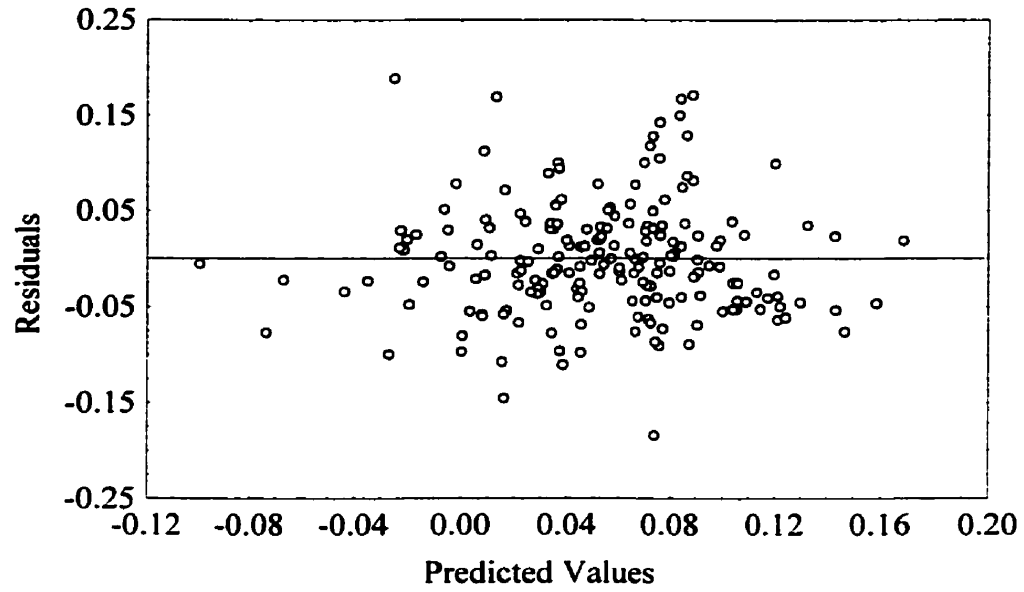


**Figure 4.12 :** Scatter of residuals of simplified regression on  $(\Delta\Sigma/\Delta t)_{ij}$ .

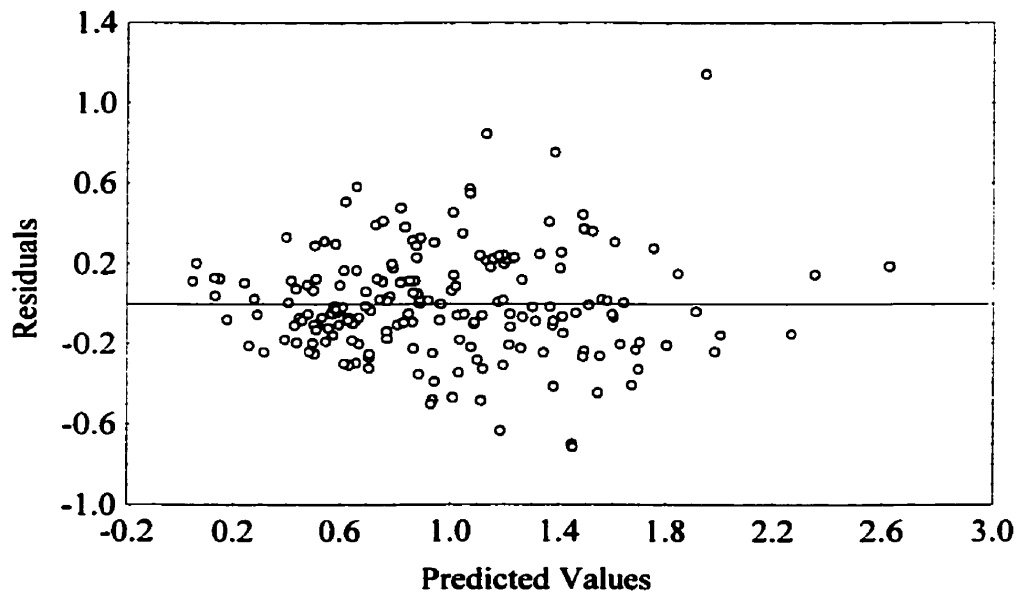


**Figure 4.13:** Scatter of residuals of simplified regression on  $\Sigma_i$ .

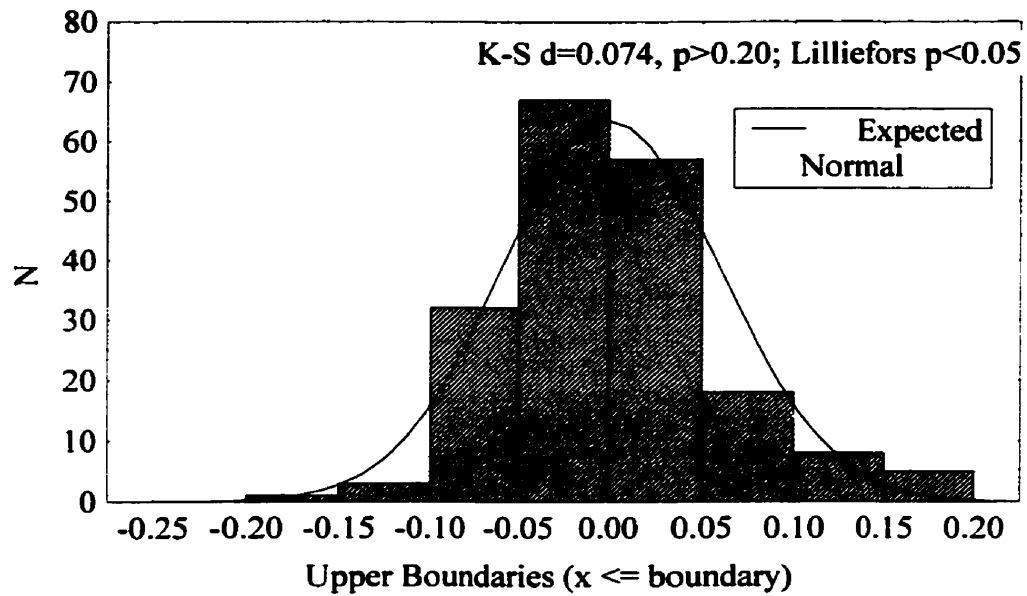


**Figure 4.14** : Distribution of residuals of simplified regression on  $(\Delta\Sigma/\Delta t)_{ij}$ . Results of tests for normality shown.

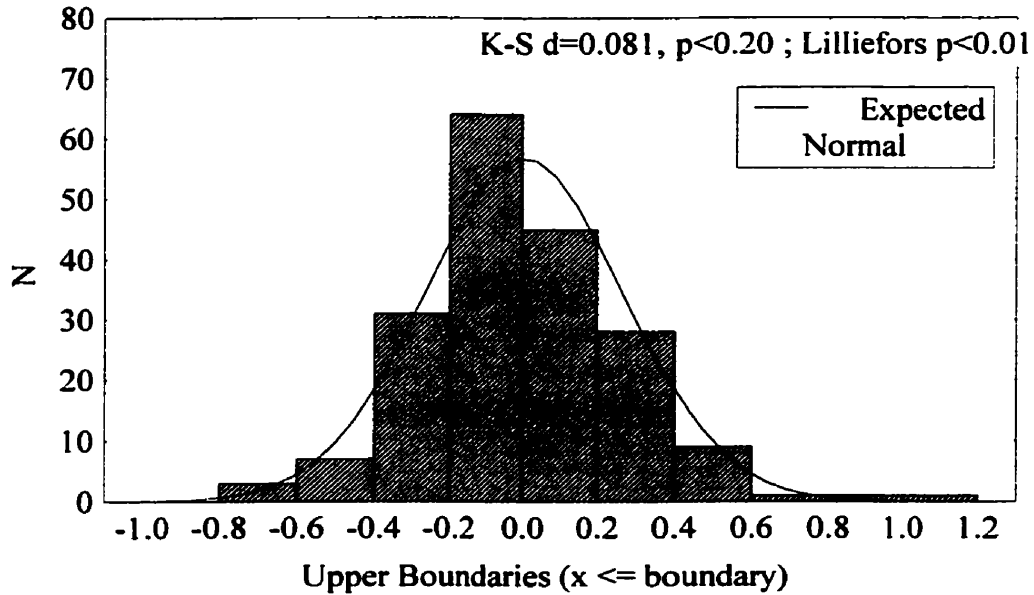


**Figure 4.15** : Distribution of residuals of simplified regression on  $\Sigma_i$ . Results of tests for normality shown.

### 4.3.11 Model formula

From Section 4.3.1, the proposed model for predicting the shear strength of buried surface hoar layers over short time intervals was:

$$\Sigma_j^* = \Sigma_i^* + (\Delta t_{ij}) \cdot (\Delta \Sigma / \Delta t)_{ij}^* , \quad (4.5)$$

$$\text{where } \Sigma_i^* = \Sigma_i^*(\text{snowpack observations } i) \quad (4.6)$$

$$\text{and } (\Delta \Sigma / \Delta t)_{ij}^* = (\Delta \Sigma / \Delta t)_{ij}^*(\text{snowpack observations } i) . \quad (4.7)$$

With the selection of regression results made in the previous section, deriving empirical formulae for  $(\Delta \Sigma / \Delta t)_{ij}^*$  and  $\Sigma_i^*$  was a simple matter. These formulae are linear functions of the variables of regression and their standardised coefficients of regression, B (Mendenhall and Sincich, 1996, p. 353), which are shown in Tables 4.17 and 4.18. Thus, the formulae are:

$$\begin{aligned} \Sigma_i^* = & 0.336 \text{ kPa} + (0.0139 \text{ kPa d}^{-1} \cdot t_i) + (1.18 \cdot \sigma_i) - (0.00625 \text{ kPa cm}^{-1} \cdot H_i) \\ & + (0.000804 \text{ kPa cm}^{-1} \cdot HS_i) - (0.287 \text{ kPa cm}^{-1} \cdot Thick_i) + (0.0187 \text{ kPa } ^\circ\text{C}^{-1} \cdot Twl_i) \\ & + (0.0204 \text{ kPa mm}^{-1} \cdot Emin_i). \end{aligned} \quad (4.8)$$

$$\begin{aligned} (\Delta \Sigma / \Delta t)_{ij}^* = & 0.119 \text{ kPa} - (0.000547 \text{ kPa d}^{-1} \cdot t_i) - (0.124 \cdot \Sigma_i) + (0.107 \cdot \sigma_i) \\ & + (0.000131 \text{ kPa cm}^{-1} \cdot H_i) + (0.000176 \text{ kPa cm}^{-1} \cdot HS_i) \\ & - (0.0473 \text{ kPa cm}^{-1} \cdot Thick_i) - (0.378 \text{ kPa m } ^\circ\text{C}^{-1} \cdot TG_i) \\ & - [0.827 \text{ kPa m}^{-1} \cdot (TG/Twl_i)]. \end{aligned} \quad (4.9)$$

Finally, predicting the strength of a buried surface hoar layer on day  $j$  after a layer is buried, is possible from a set of snowpack observations at time  $i$  days ( $1 < j \leq i+8$ ).

## **4.4 Shear Strength – Lagged Load model**

### **4.4.1 Introduction**

The results of Sections 4.2 and 4.3 show that the load overlying a buried surface hoar layer plays an important role in the shear strength of the layer; shear strength was correlated with load variables in both the Power Law and Interval models (Tables 4.6 and 4.12). Johnson (2000) found that load was the most important factor influencing the shear strength of persistent weak layers of faceted crystals. Jamieson and others (2000), in a case study of slab avalanche activity on a persistent weak layer of faceted crystals, found that the loading of 3 or more days before an avalanche cycle was correlated with slab avalanche activity. Such results indicate that a closer examination of the relationship between load and shear strength for persistent weak layers is warranted.

An examination of the effects of load may also be argued on a physical basis. It is proposed that, for a buried surface hoar layer, two different physical regimes of layer strengthening are in effect. During periods of snowfall and for a few days after, increased load overlying a buried surface hoar layer causes the layer to thin (compress) and strengthen (see Chapter 2). Later in this load response period, these mechanisms are not as significant, and a surface hoar layer is expected to be slower to gain strength. The surface hoar layer will be more subject to temperature-gradient driven metamorphism at such times, which has not been shown to be associated with rapid strength gain of surface hoar layers in the Columbia Mountains (see Chapter 2). As an example of this mixed-regime behaviour, the shear strength and daily load on a buried surface hoar layer is shown in Figure 4.16. It can be seen that the example layer is indeed slower to gain shear strength over periods in which there is little or no snowfall.

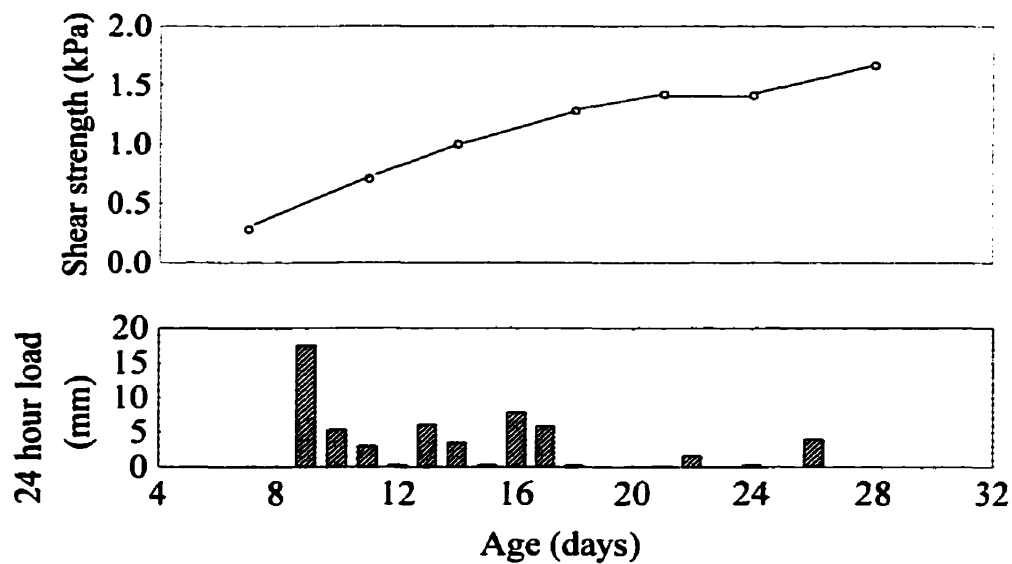


**Figure 4.16 :** Shear strength and daily load on the layer of surface hoar buried 20-January-2001 at the Mt. St. Anne Study Plot .

In this section, a model is developed that relates daily load on a surface hoar layer (the new precipitation over the previous 24 hours, recorded by an automated precipitation gauge adjacent to the study site) to the shear strength of the layer. The goals of this model were to determine the delayed or lagged effect of load on shear strength, and then to use the model to predict the shear strength of a buried surface hoar layer, based on daily load only.

#### 4.4.2 Dataset

The model of this section requires daily precipitation (load) readings. The instrumentation required to collect this data was available only at the Mt. St. Anne and Mt. Fidelity study sites, so only buried surface hoar layers at these locations were used for this analysis. Time series removed from the dataset of Section 4.3.6 for physical reasons were also excluded from this section.

**Table 4.19:** Surface hoar series for the Lagged Load model .

<b>Location</b>	<b>Date of burial</b>	<b>Location</b>	<b>Date of burial</b>
Mt. St. Anne (MSA) Study Plot	15-Nov-93	Fidelity Study Slope	30-Dec-99
MSA Study Plot	04-Dec-93	<b>MSA Study Plot</b>	<b>30-Dec-99</b>
MSA Study Plot	29-Dec-93	Fidelity Study Slope	31-Jan-00
MSA Study Plot	21-Jan-94	MSA Study Plot	31-Jan-00
MSA Study Plot	07-Jan-95	Fidelity Study Slope	21-Feb-00
MSA Study Plot	14-Feb-95	Fidelity Study Slope	24-Nov-00
MSA Study Plot	28-Dec-95	Fidelity Study Slope	13-Jan-01
MSA Study Plot	17-Feb-96	MSA Study Plot	20-Jan-01
MSA Study Plot	17-Jan-97	Fidelity Study Slope	28-Jan-01
<b>MSA Study Plot</b>	<b>10-Feb-97</b>	Fidelity Study Slope	23-Feb-01
MSA Study Plot	13-Feb-98	MSA Study Plot	23-Feb-01
MSA Study Plot	25-Feb-98		

The layers used in this section are listed in Table 4.19. Layers not included in formulating the model for purposes of model testing (as in Sections 4.2 and 4.3) are highlighted.

#### 4.4.3 Formulation and construction

The Shear Strength – Lagged Load model was developed to establish a simple linear relationship between the shear strength on a given day and the load on each of the previous days. The model is of the form

$$\Sigma_i^* = \Sigma_{i-k} + c_1\sigma_{i-1} + c_2\sigma_{i-2} + c_3\sigma_{i-3} + \dots + c_k\sigma_{i-k} \quad (4.10)$$

Where  $k$  is the number of “lagged” days included in the model,  $\sigma_{i-1} \dots \sigma_{i-k}$  are the new (24 hour) loads measured on each of the 1 to  $k$  previous days,  $\Sigma_i^*$  is the predicted shear strength on day  $i$ , and  $\Sigma_{i-k}$  is the measured shear strength on  $k$  days previous. The coefficients  $c_1 \dots c_k$  are fitted via a numerical technique that seeks values of  $c_1 \dots c_k$  such that the sum of squares of errors between measured and predicted shear strength on snow-pack observation days is minimised.

This technique uses Generalized Reduced Gradient nonlinear optimisation code, which has been used in other circumstances to fit models to data (for more information, see Frontsys, 2001).

In order to determine the effective time delay of load on a buried surface hoar layer, the model was fitted for values of  $k = 1, 2, 3, \dots, 8$ . The values of the coefficients  $c_1 \dots c_k$  indicate the relative importance of lag effect of load on each of the  $k$  days examined. The same number of observations are used for each value of  $k$ , such that the total sum of squares of residuals is a measure of which model in this section has the best fit to the data. The models created are thus of the form  $\Sigma_i^* = \Sigma_{i-1} + c_1 \sigma_{i-1}$ ,  $\Sigma_i^* = \Sigma_{i-2} + c_1 \sigma_{i-1} + c_2 \sigma_{i-2}$ , etc.

Once the important lag terms have been determined, the model is used to predict the shear strength of buried surface hoar layers.

#### 4.4.4 Determining lag effects

The coefficients determined by the Shear Strength-Lagged Load model construction for lag terms of 1 to 8 days are shown in Table 4.20. The sum of the squares of the residuals for the 61 days on which predicted strength and measured strength were available is also shown.

The six-term model has the lowest sum of squares of errors, which is a direct indicator of the fit of the model to the observed shear strength data. This implies that load on a buried surface hoar layer on each of the previous six days are important predictors of layer's shear strength.

**Table 4.20 : Results of fitting Lagged Load model.**

<b>No. of lag terms</b>	<b>Fitted coefficients</b>		<b>Sum of squares of residuals</b>
1	c1	0.0138	18.79
2	c1 c2	0.0153 0.0126	18.82
3	c1 c2 c3	0.0099 0.0104 0.0202	19.18
4	c1 c2 c3 c4	0.0135 0.0070 0.0135 0.0201	19.14
5	c1 c2 c3 c4 c5	0.0029 0.0153 0.0124 0.0154 0.0203	20.59
6	c1 c2 c3 c4 c5 c6	0.0203 0.0000 0.0158 0.0003 0.0206 0.0232	17.49
7	c1 c2 c3 c4 c5 c6 c7	0.0118 0.0126 0.0119 0.0000 0.0166 0.0134 0.0322	17.80
8	c1 c2 c3 c4 c5 c6 c7 c8	0.0193 0.0117 0.0257 0.0073 0.0056 0.0128 0.0222 0.0115	18.98

The fitted coefficients of the eight lag models showed considerable fluctuations in value, depending on the number of terms in the model. Thus, the load on a particular previous day did not stand out as most important to the shear strength of a buried surface hoar layer. Furthermore, the coefficients of load two and four days previous in the six-term model were near zero in value, yet the coefficients of one and six days previous were close in magnitude, which shows no clear dominant lag effect.

The results of the lagged load model show that the load on several previous days has an influence on the change in shear strength of a buried surface hoar layer, but do not allow the influence of various lag terms to be determined.

#### **4.4.5 Model formula**

The six-term lagged load model provided the best fit to the data used to construct it, and is given by:

$$\Sigma_i^* = \Sigma_{i-6} + 0.0203 \cdot \sigma_{i-1} + 0.0158 \cdot \sigma_{i-3} + 0.000319 \cdot \sigma_{i-4} + 0.0206 \cdot \sigma_{i-5} + 0.0232 \cdot \sigma_{i-6} \quad (4.11)$$

## **4.5 Model testing**

### **4.5.1 Introduction**

In this section, the models developed in Sections 4.2, 4.3 and 4.4 of this chapter are tested for their fit to the data used to construct the models. The predictive capabilities of these models are also tested for several buried surface hoar time series that were not used to build the models. From these results, the model best suited for predicting changes in the shear strength of buried surface hoar layer is selected.

As previously discussed, the goal of this study is to develop a model to predict the shear strength of buried surface hoar layers that is suitable for operational avalanche forecasting. In order to fulfil this goal, the model must be based on simple weather and snowpack observations and must not require shear frame measurements. The Shear Strength - Power Law model of Section 4.2 predicts the shear strength over the first 30 days, based on load on the layer on the first day of burial. This model may be initialised with load obtained from automated precipitation gauge data adjacent to the study site. The Shear Strength – Interval model developed in Section 4.3 predicts the shear strength at the start of a time interval and the change in shear strength over the interval based on simple snowpack observations, and is thus suitable for operational use. The Shear Strength - Lagged Load model developed in Section 4.4 predicts the change in shear strength of buried surface hoar layers based on initial shear strength and measured daily load on the layer. In order for this model to be operationally useful, it must use a predicted initial shear strength and not a measured one. Bearing this in mind, the estimate of initial shear strength developed in Section 4.3 is used to initialise the Lagged Load model in the following sections.

#### 4.5.2 Fit to model-building dataset

In order to test which model best fits the model-building dataset, the models were compared over a common set of data points. This required both a complete set of snowpack observations and a set of daily load values from adjacent weather stations. Both of these criteria were fulfilled for surface hoar time series at the Mt. St. Anne and Mt. Fidelity study sites from the winter 1995-1996 onwards (subset of Table 4.2). This amounted to 81 observation days. In order to test the predictive power of the models, the predicted shear strength values at the end of each measurement interval were then computed and compared to the measured shear strengths (Figures 4.17, 4.18, 4.19). The sum of the squares of residuals and the adjusted  $R^2$  statistic (Section 4.3.9) for each model over these data points was calculated.

The results of the tests of model fit are shown in Table 4.21. Figure 4.20 shows some example time series, selected at random. The adjusted  $R^2$  statistic gives the fraction of variability in the data that is explained by each model (Mendenhall and Sincich, 1996, pp. 191-193). The Power Law model explains 50% of the variability in the data, the Interval model 72%, and the Lagged Load model 41%. The Interval model has the lowest value of the sum of squares of residuals and the lowest adjusted  $R^2$  value (Table 4.21), and therefore provides the best fit to the model-building dataset.

**Table 4.21** : Results of testing fit of model to model-building data.

<b>Model</b>	<b>Sum of squares of residuals over test of fit data</b>	<b>Adjusted <math>R^2</math> sample statistic</b>
Power Law	35.0	0.50
Interval	5.33	0.72
Lagged Load	7.92	0.41

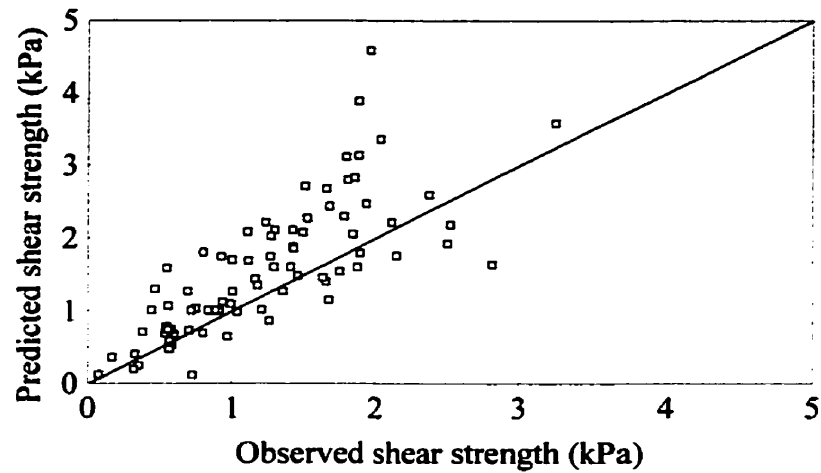


**Figure 4.17** : Observed vs. predicted shear strength, Power Law model. Line of 1:1 correspondence shown.

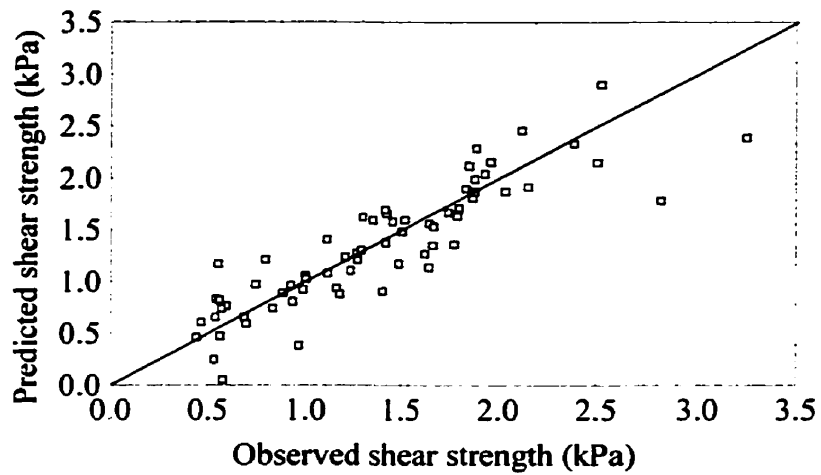


**Figure 4.18** : Observed vs. predicted shear strength, Interval model.

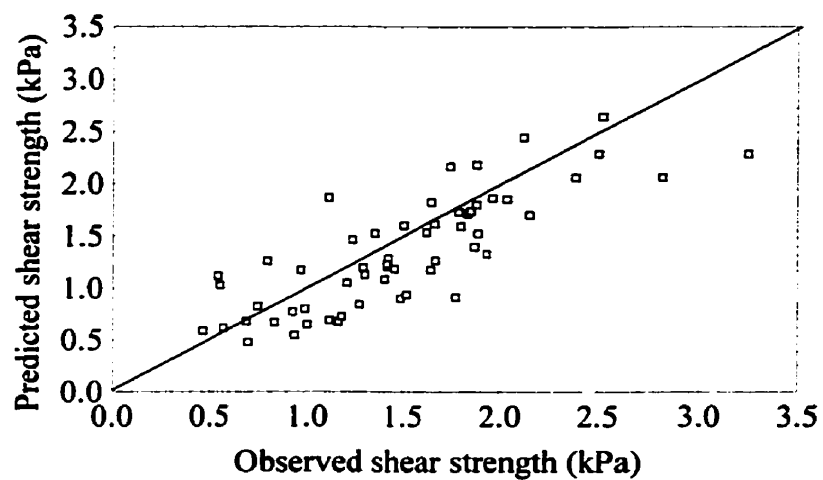


**Figure 4.19** : Observed vs. predicted shear strength, Lagged Load model.

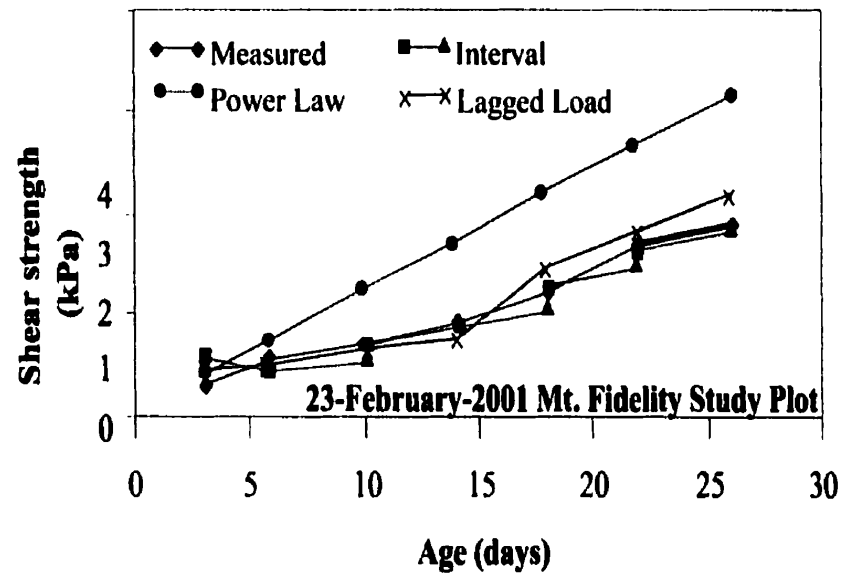
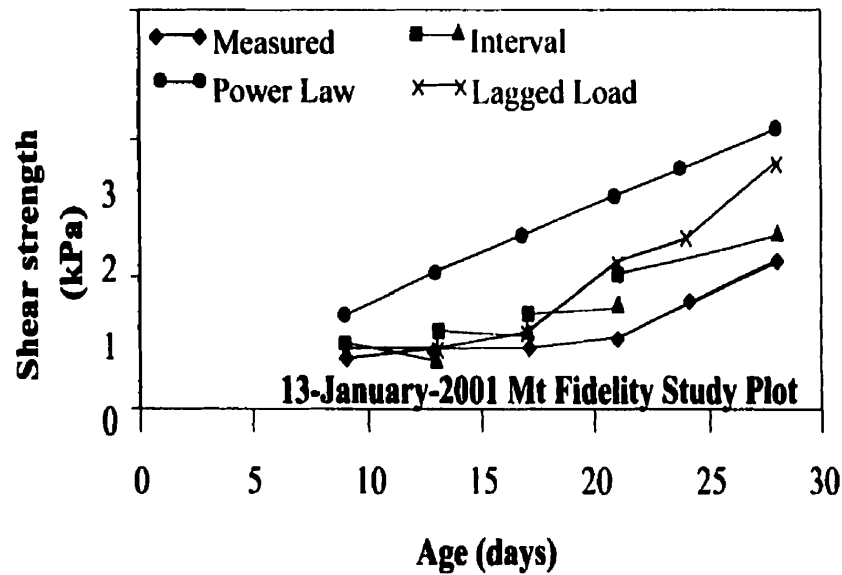
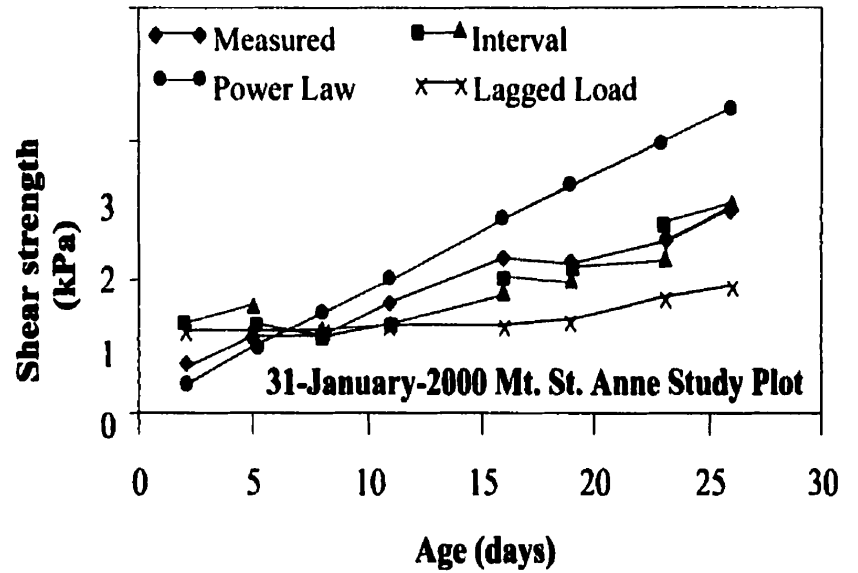
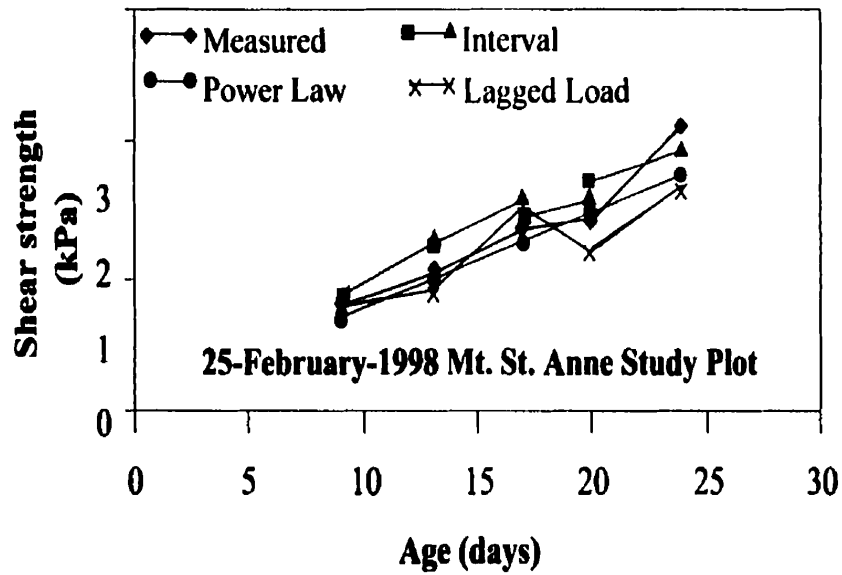


**Figure 4.20:** Testing model fit to model-building data. Examples shown selected at random.

### 4.5.3 Test layers

Two time series of buried surface hoar, buried 10-February-1997 and 30-December-1999 at the Mt. St. Anne Study Plot (Appendix), were withheld from the datasets used to construct the models in Chapter 4. In this section, the models are applied to the 11 data points of these layers in order to assess their predictive capabilities. The sum of squares of residuals between model forecast and measured values are compared in order to assess which model is the best for predicting the shear strength of buried surface hoar layers in the Columbia Mountains. The results of comparison are shown in Table 4.22 and Figure 4.21.

In applying the models to these test layers, the Interval model again shows the best fit to the measured data.

**Table 4.22 : Results of model forecasting for test layers.**

<b>Model</b>	<b>Sum of squares of errors over test layer data</b>
Power Law	2.34
Interval	1.04
Lagged Load	4.09

### 4.5.4 Selecting the best model

Since the Interval model provides the best fit to both the data used in model construction and to the measured shear strength of the test layers, it is concluded that this is the best model to be used in further applications. In terms of ease of operational use, both the Power Law and Lagged Load models are of less cost, as they require no and one set of snowpack observations, respectively. However, it must be noted that weekly study plot observations are part of many operational avalanche forecasting operations, in which case the superior Interval model may be used at little additional cost.

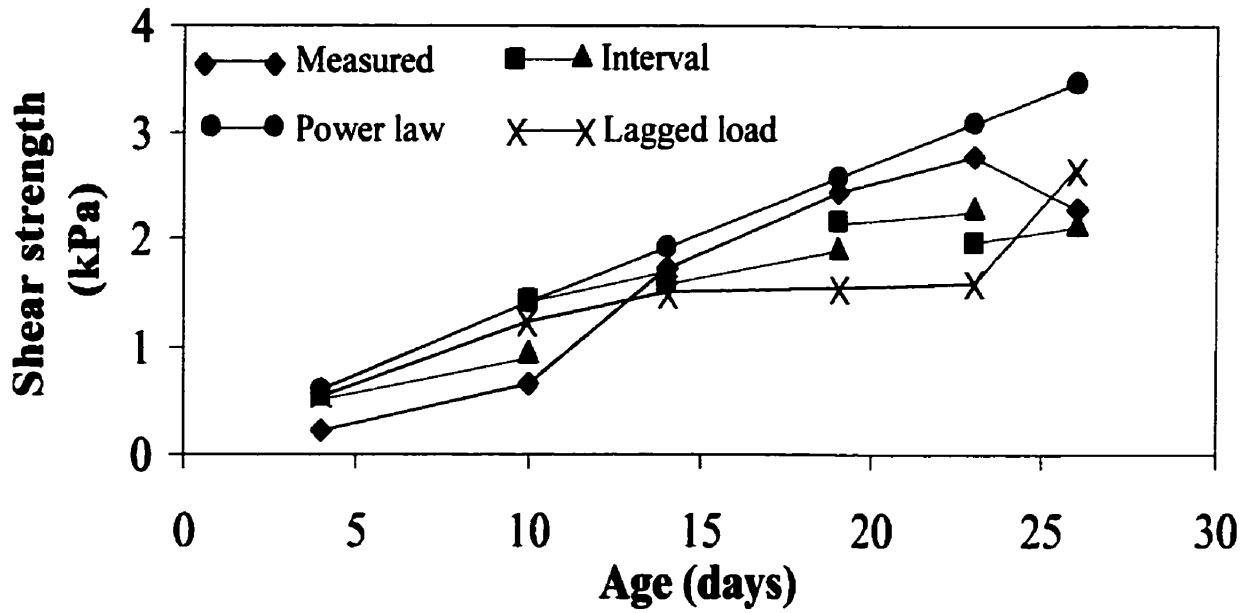


**Figure 4.21a:** Testing model forecast shear strength for 10-February-1997 test series at Mt. St Anne Study Plot.

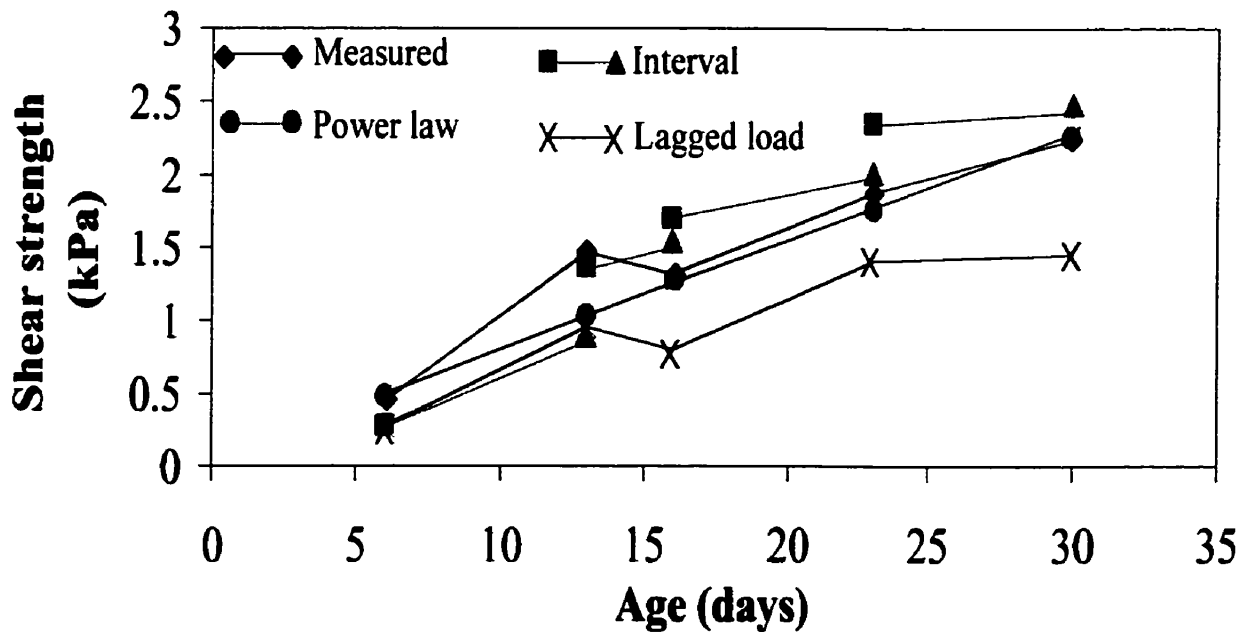


**Figure 4.21b:** Testing model forecast shear strength for 30-December-1999 test series at Mt. St. Anne Study Plot.

## **4.6 Summary**

In this chapter, three models were developed to forecast the shear strength of buried surface hoar layers. The data used to construct these models were for layers that had been buried in the Columbia Mountains for less than 30 days, with constituent surface hoar crystals between 5 and 30 mm in observed size, typically of sector plate form.

The Shear-Strength Power Law model forecasts the shear strength of buried surface hoar layers, based on the load (vertical force per unit area) overlying the layer on the first day in which it was buried in the snowpack.

The Shear-Strength Interval model forecasts the change in strength of a buried surface hoar layer over a period of time up to 8 days following the day on which a set of snowpack observations of the layer is taken. The required snowpack observations are all part of standard industry guidelines (Canadian Avalanche Association, 1995), except for measuring the thickness of the buried surface hoar layer to the nearest millimetre.

The Shear Strength-Lagged Load model forecasts the strength of a buried surface hoar layer based on the daily additional load (precipitation) on the layer over 6 days previous to the forecast day.

The three models were tested for their fit to the model-building dataset and for their true predictive abilities on two buried surface hoar layers not included in the model-building dataset. The Power Law model explains 50% of the variability in the measured data, the Interval model 72%, and the Lagged Load model 41%. Additionally, the Shear Strength-Interval model provides the most accurate forecast shear strength on the test layers; it is the best of the three.

For the two test series in Section 4.5.3, the Shear Strength-Interval model is used to forecast shear strength at the end of an interval (9 data points) to within an average of 18% of the measured values, where

$$\% \text{ error} = \text{magnitude of } [(\Sigma_{\text{measured}} - \Sigma_{\text{forecast}}) / \Sigma_{\text{measured}}] \cdot 100\%. \quad (4.12)$$

The accuracy of the model may be better established with further test series.

The next chapter examines the utility of the Shear Strength-Interval model for operational avalanche forecasting.

## **5. FORECASTING SKIER-TRIGGERED AVALANCHES**

### **5.1 Introduction**

A recent study by Chalmers and Jamieson (in press) showed that study plot measurements of a buried surface hoar layer may potentially be used to extrapolate the stability of the layer for skier-triggered slab avalanches in a large surrounding region (up to 100 km in radius)(see Chapter 2). Shear strength of the layer is one such study plot measurement, but a stability index  $Sk_{38}$  that is the ratio of shear strength to shear stress on the weak layer provides a better physical interpretation of stability.

Jamieson and Johnston (1998) showed that, for tests on a specific avalanche slope,  $Sk_{38} < 1$  indicated unstable conditions (skier-triggered avalanches expected),  $Sk_{38} > 1.5$  indicated stable conditions (skier-triggered avalanches unlikely), while  $1 \leq Sk_{38} \leq 1.5$  indicated transitional conditions between stable and unstable (skier-triggered avalanches possible). In examining the usefulness of extrapolating  $Sk_{38}$  to skier-triggered avalanche activity in the surrounding region for several layers of buried surface hoar, Chalmers and Jamieson (in press) found that these threshold values appeared to be the same.

The objective of this chapter is twofold. First, the usefulness of an  $Sk_{38}$  extrapolated from study plot measurements will be determined by relating daily values of  $Sk_{38}$  to avalanche activity. Second, the potential for the model results of Chapter 4 to be used to forecast regional skier-triggered avalanche activity will be examined.

## 5.2 Dataset

The study plot observations of buried surface hoar layers from the Mt. St. Anne and Mt. Fidelity study sites may be correlated with skier-triggered avalanche activity data from helicopter skiing operations in the surrounding regions. Mt. St. Anne is centrally located in a large helicopter skiing operation, approximately 5000 km<sup>2</sup> in area (Figure 3.1). Mt. Fidelity is situated within approximately 100 km of four helicopter skiing operations of similar snowpack conditions (Figure 3.1).

The twelve surface hoar time series used in this chapter are listed in Table 5.1. All of these series have a record of skier-triggered avalanche activity. All but two of these series were used to construct the Shear Strength-Interval model of Chapter 4; the measured and predicted values of shear strength of six of these series are used to estimate  $Sk_{38}$ , while the others have insufficient observational snowpack data and are used to produce measured  $Sk_{38}$  only. The two series not used to construct the model are used to test predicted  $Sk_{38}$  with avalanche activity.

**Table 5.1:** Surface hoar time series used in forecasting application.

Location	Burial date	Skier-triggered activity records	$Sk_{38}$	Used to build or test model
Mt. St. Anne	29-Dec-93	yes	measured	build
Mt. St. Anne	05-Feb-94	yes	measured	build
Mt. St. Anne	07-Jan-95	yes	measured	build
Mt. St. Anne	28-Dec-95	yes	measured	build
Mt. St. Anne	10-Feb-97	yes	measured, forecast	test
Mt. Fidelity	30-Dec-99	yes	measured, forecast	build
Mt. St. Anne	30-Dec-99	yes	measured, forecast	test
Mt. Fidelity	21-Feb-00	yes	measured, forecast	build
Mt. St. Anne	20-Jan-01	yes	measured, forecast	build
Mt. Fidelity	28-Jan-01	yes	measured, forecast	build
Mt. St. Anne	23-Feb-01	yes	measured, forecast	build
Mt. Fidelity	23-Feb-01	yes	measured, forecast	build

### 5.3 Extrapolated skier stability index

The values of the skier stability index (measured and/or modelled) and skier-triggered avalanche activity over the first 30 days of layer burial are plotted in Figure 5.1.

From these data, the number of days with and without skier-triggered avalanches for these time series are tabulated for the days when  $Sk_{38}$  indicated unstable ( $Sk_{38} < 1$ ) and stable ( $Sk_{38} > 1.5$ ) conditions (Table 5.2).

**Table 5.2:** Form of contingency table for testing  $Sk_{38}$ .

	# Days with avalanches	# Days without avalanches
<b><math>Sk_{38} &lt; 1</math></b>		
<b><math>Sk_{38} &gt; 1.5</math></b>		

Four of these contingency tables were constructed: (1) model-building layers with measured  $Sk_{38}$ , (2) model-building layers with modelled (forecast)  $Sk_{38}$ , (3) model-testing layers with measured  $Sk_{38}$ , and (4) and model-testing layers with modelled (forecast)  $Sk_{38}$ . The Chi-square test of independence was performed on each of these tables (Stephens, 1998, pp. 253-256). Chi-square values with significant p-levels ( $p < 0.1$ ) indicate that days with avalanche activity depend on the value of  $Sk_{38}$ . The contingency tables and the results of the Chi-square test are shown in Table 5.3.

Table 5.3a shows that measured  $Sk_{38}$  was a highly significant predictor of regional skier-triggered avalanche activity ( $p < 10^{-4}$ ) (89% of avalanche days outside of the transitional period occurred while  $Sk_{38} < 1$ ). Table 5.3b shows that the model-fitted  $Sk_{38}$  is also a highly significant predictor of skier-triggered avalanche activity ( $p < 10^{-4}$ ) (93% of avalanche days outside of the transitional period occurred while  $Sk_{38} < 1$ ). This implies that the fit of the model to the measured data is operationally useful.

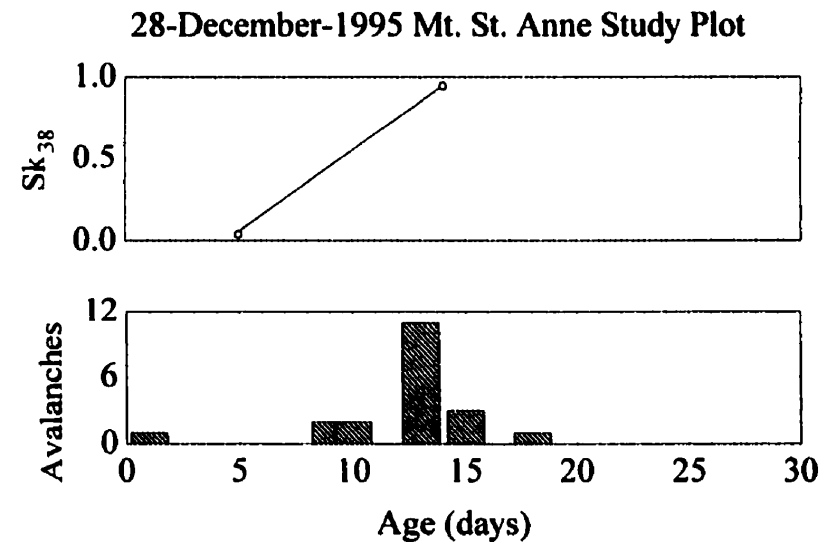
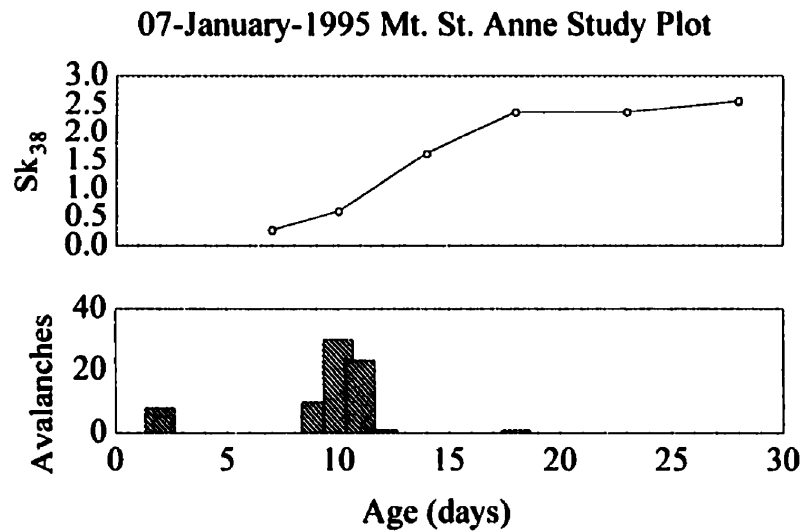
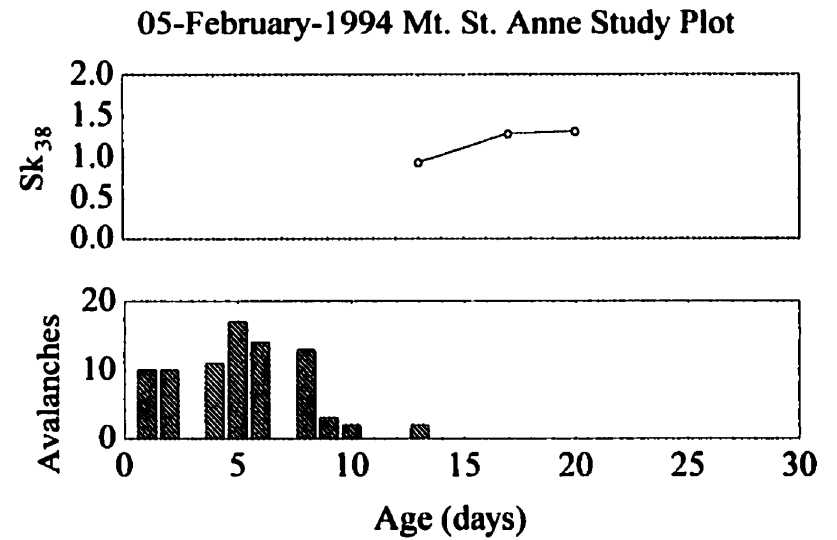
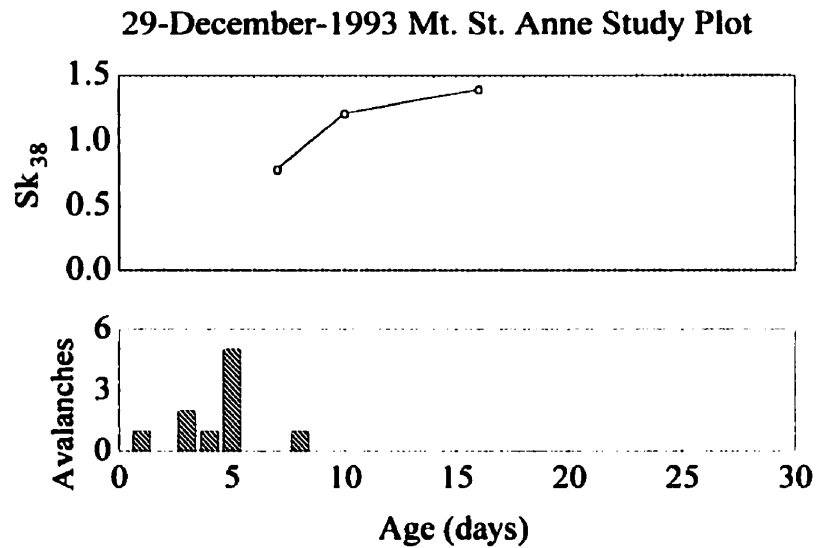


**Figure 5.1a:** Skier stability index  $Sk_{38}$  and associated skier-triggered avalanche activity for surface hoar time series from Table 5.1.

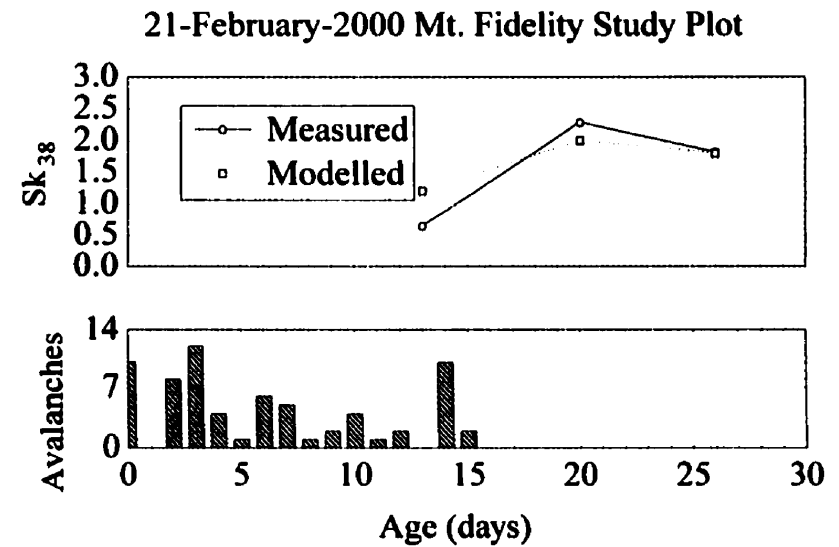
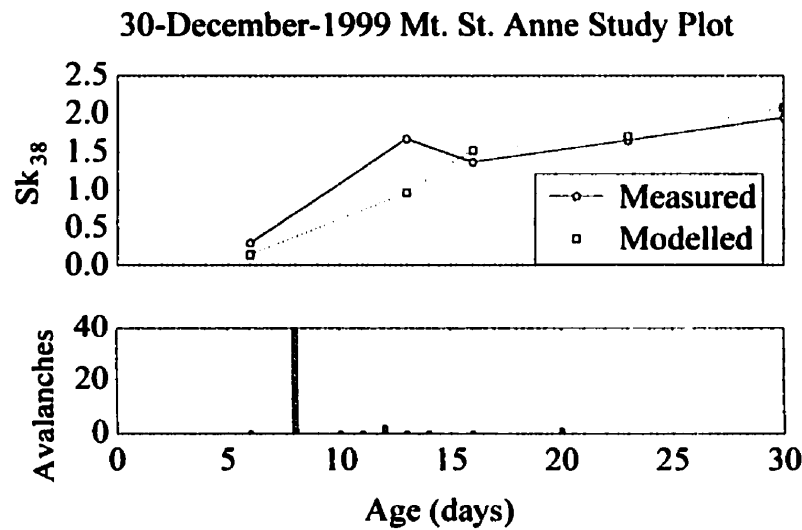
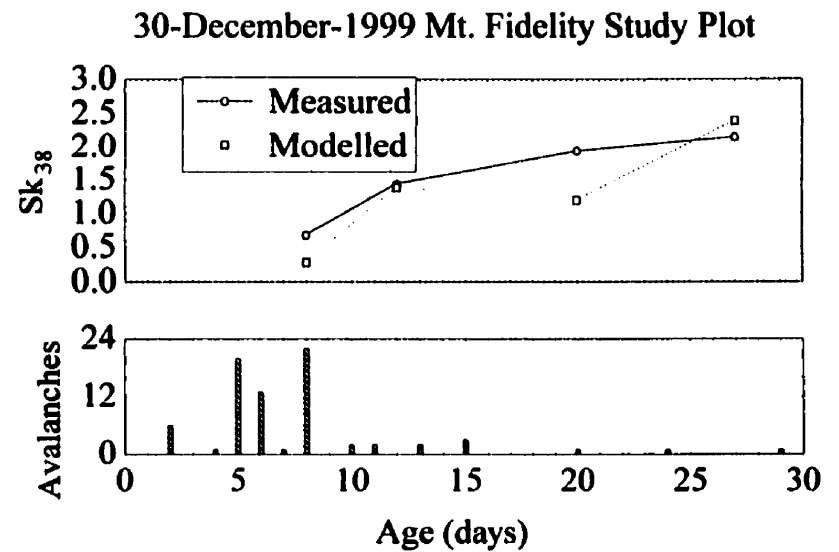
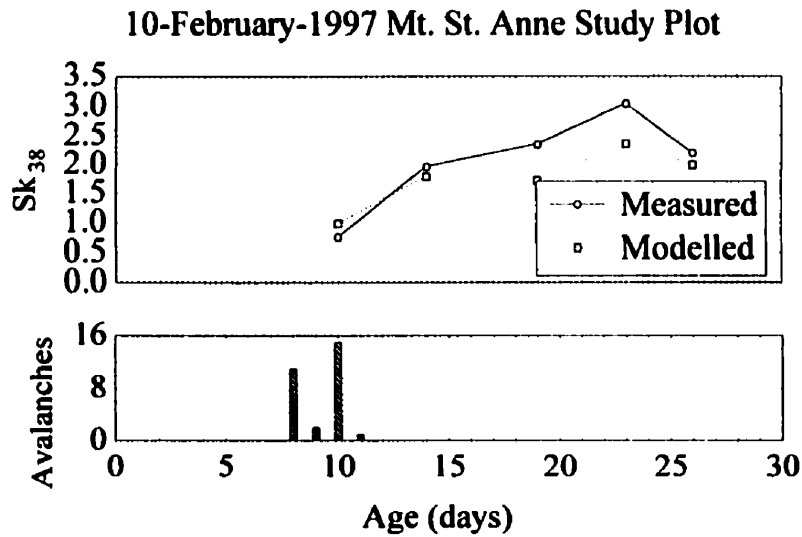
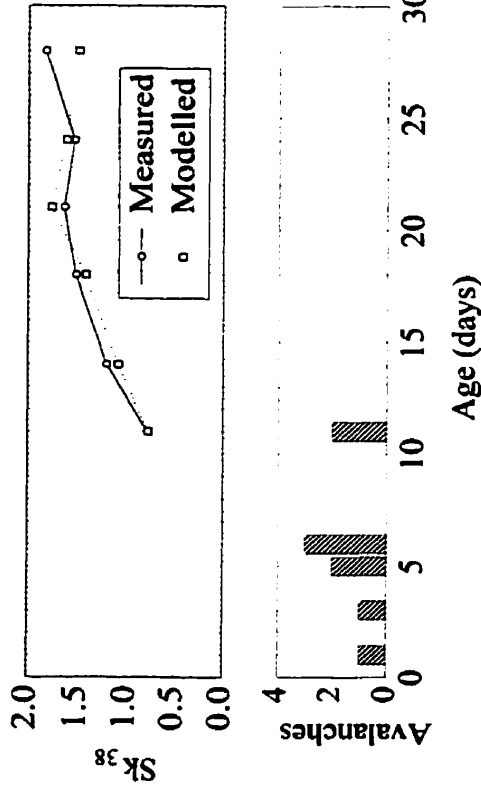
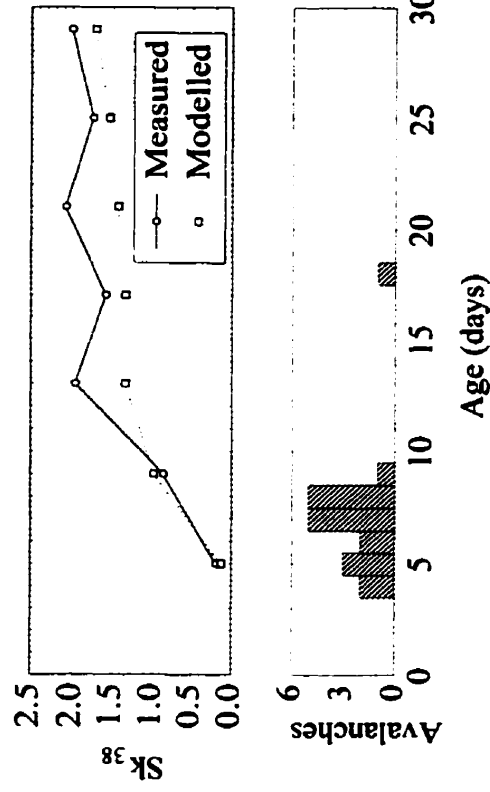


**Figure 5.1b:** Skier stability index  $Sk_{38}$  and associated skier-triggered avalanche activity for surface hoar time series from Table 5.1.

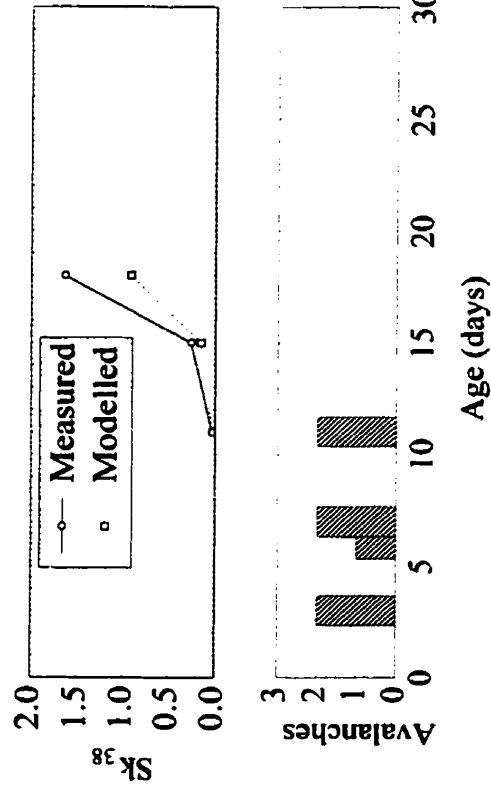
20-January-2001 Mt. St. Anne Study Plot



28-January-2001 Mt. Fidelity Study Plot



23-February-2001 Mt. St. Anne Study Plot



23-February-2001 Mt. Fidelity Study Plot

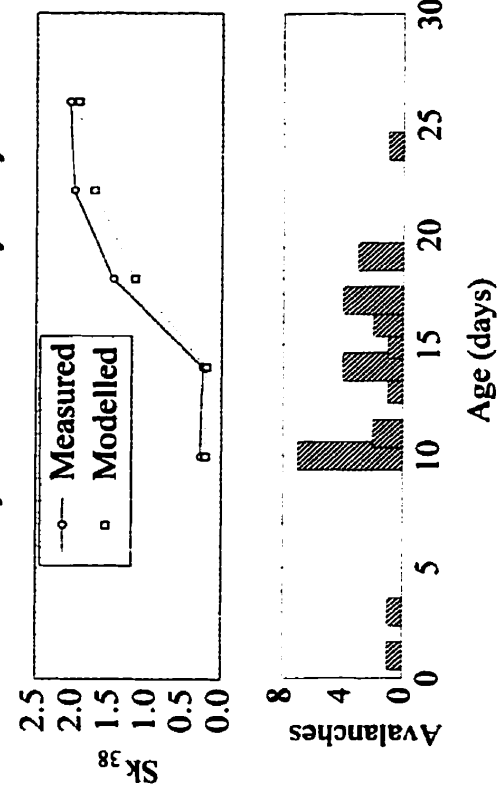


Figure 5.1c: Skier stability index  $SK_{38}$  and associated skier-triggered avalanche activity for surface hoar time series from Table 5.1.

**Table 5.3: Master contingency table and results of testing Sk<sub>38</sub>.**

	Model building layers			Model testing layers		
<b>Measured</b>	<b>5.3a</b>			<b>5.3c</b>		
	$p < 10^{-4}$	# Aval. days	# Non-aval. days	$p = 0.15$	# Aval. days	# Non-aval. days
	Sk38 < 1	64	62	Sk38 < 1	5	14
	Sk38 > 1.5	8	108	Sk38 > 1.5	3	26
<b>Forecast</b>	<b>5.3b</b>			<b>5.3d</b>		
	$p < 10^{-4}$	# Aval. days	# Non-aval. days	$p = 0.004$	# Aval. days	# Non-aval. days
	Sk38 < 1	40	36	Sk38 < 1	7	14
	Sk38 > 1.5	3	53	Sk38 > 1.5	1	29

For the surface hoar layers not used to formulate the model, Table 5.3c shows that measured  $Sk_{38}$  was not a significant predictor of regional skier-triggered avalanche activity on these layers ( $p = 0.15$ ), but Table 5.3d shows that the model forecast  $Sk_{38}$  was such a predictor ( $p = 0.004$ ). The results of Tables 5.3c and 5.3d are influenced by the small number of data available for the Chi-square test; the test statistic adjusted for small sample size (Statistica, 1999) showed that the results of Table 5.3d are of borderline significance ( $p = 0.1$ ). For the measured  $Sk_{38}$  on these two layers; 63% of avalanche days outside of the transitional period were when  $Sk_{38} < 1$ . For the forecast  $Sk_{38}$ , 88% of avalanche days outside of the transitional period were when  $Sk_{38} < 1$ . Also, approximately twice as many non-avalanche days occur when  $Sk_{38}$  predicts stability ( $> 1.5$ ), compared to when it predicts instability ( $< 1$ ). Even for these small datasets,  $Sk_{38}$  shows predictive merit.

#### **5.4 Extrapolated model skier stability index**

The results of this chapter indicate that the skier stability index  $Sk_{38}$  is a good predictor of the regional skier-triggered avalanche activity on layers of buried surface hoar in the Columbia mountains. Skier-triggered avalanches in the region are likely when  $Sk_{38} < 1$  and highly unlikely when  $Sk_{38} > 1.5$ . The shear strength-interval model fit to the data implies that it may be used to accurately forecast  $Sk_{38}$  and regional skier-triggered avalanche activity up to 8 days in the future, based on study plot snowpack observations only. The results of testing the model on two layers of buried surface hoar further show that it may be used as a forecasting tool, but more testing data are required to improve the statistical argument.

## **6. CONCLUSIONS**

### **6.1 Conclusions**

Surface hoar layers buried in the Columbia Mountains of western Canada present a serious hazard to both recreational and professional backcountry users. During the first 30 days in which these layers are buried in the snowpack, they show important increases in shear strength and most skier-triggering of slab avalanches occurs.

The Shear Strength-Power Law model shows that the load overlying a layer of buried surface hoar on the first day of burial plays an important role to the initial shear strength of the layer.

The Shear Strength-Interval model establishes a number of variables as predictors of the shear strength of a buried surface hoar layer. These include age of the layer, load, slab thickness, height of snowpack, layer thickness, weak layer temperature, minimum constituent grain size, and temperature gradient across the layer.

The Shear Strength-Lagged Load model examines the delayed effect of load on the shear strength of a buried surface hoar layer. This model suggests that the load up to six days previously influences the shear strength of a buried surface hoar layer.

Testing the fit of the models to the model-building dataset shows that the Shear Strength-Interval model provides the best fit; the Power Law model explains 50% of the variability in the data, the Interval model 72%, and the Lagged Load model 41%. Testing the models on two test series shows that the Shear Strength-Interval model is the most accurate, to within an average of 18% of measured shear strength.

It is established that the skier stability index  $Sk_{38}$ , based on measurements in a centrally located study plot, is a good predictor of regional skier-triggered avalanche activity on layers of buried surface hoar in the Columbia Mountains. The Shear Strength-Interval model may be used to forecast  $Sk_{38}$  and regional skier-triggered avalanche activity up to 8 days in advance, but more data are required to verify the robustness of this model.

The Shear Strength-Interval model shows potential for operational use as an avalanche forecasting tool in the Columbia Mountains. It was developed using data from the first 30 days after burial and for layers of surface hoar with sector plate crystals between 5 and 30 mm in measured size. This model requires standard snowpack observation techniques, and additional measurements of surface hoar layer thickness to the nearest millimetre. This model is limited to use as a forecasting tool only, as extrapolating study plot stability indices over a large region will not indicate stability specific to avalanche start zones where terrain or weather yield snowpack conditions atypical of the forecast area.

## **6.2 Suggestions for further research**

Time series snowpack and avalanche occurrence observations for more layers of buried surface hoar in the Columbia Mountains are required to further establish the accuracy of the shear strength prediction model and to statistically establish its reliability as an avalanche forecasting tool.

In order to determine if the shear strength prediction model may be applied to snowpack climates outside of the Columbia Mountains, time series observations of surface hoar layers in other regions are required. Such data would also serve to better isolate the influence of specific snowpack properties on the shear strength of buried surface hoar layers.

This study provides important connections between snowpack properties, buried surface hoar layers, and skier-triggered avalanches on these layers, but these connections are empirical and statistical in nature only. Much more research is required in order to examine the physical mechanisms that link micromechanical and textural properties of surface hoar layers to the shear strength of these layers.

## REFERENCES

- Akitaya, E., 1974. Studies on depth hoar. *Contributions from the Institute of Low Temperature Science*, Series A, 26, 1-67.
- Breyfogle, S.R., 1986. Growth characteristics of hoarfrost with respect to avalanche occurrence. *Proceedings of the International Snow Science Workshop at Lake Tahoe*, October, 1986. ISSW Workshop Committee, Homewood, Ca., 216-222.
- Canadian Avalanche Association, 1995. *Observation Guidelines and Recording Standards for Weather, Snowpack and Avalanches*. Canadian Avalanche Association, Revelstoke, BC.
- Chalmers, T.S. and Jamieson, J.B., 2001. Extrapolating the skier stability of buried surface hoar layers from study plot measurements. In press for *Cold Regions Science and Technology*.
- Colbeck, S.C., 1987. A review of the metamorphism and classification of the seasonal snow cover. *Avalanche Formation, Movement and Effects*, B. Salm and H. Gubler, ed. International Association of Hydrological Sciences, Publication No. 162, 3-33.
- Colbeck, S.C., 1988. On the micrometeorology of surface hoar growth on snow in mountainous areas. *Boundary Layer Meteorology* 44, 1-12.
- Colbeck, S.C., 1991. The layered character of snow covers. *Reviews of Geophysics* 29 (1), 81-86.
- Davis, R.E., Jamieson, J.B., Hughes, J., and Johnston, C.D., 1996. Observations on buried surface hoar – Persistent failure planes for slab avalanches in British Columbia, Canada. *Proceedings of the International Snow Science Workshop at Banff*, October, 1996. Canadian Avalanche Association, Revelstoke, BC, 81-85.
- Davis, R.E., Jamieson, J.B., and Johnston, C.D., 1998. Observations on buried surface hoar layers in British Columbia, Canada: Section analysis of layer evolution. *Proceedings of the International Snow Science Workshop at Sunriver*, September, 1998. Stevens Pass Ski Area, PO Box 98, Skykomish, Wa., 86-92.
- Fierz, C. and Gauer, P., 1998. Snow cover evolution in complex alpine terrain: Measurements and modelling including snow drift effects. *Proceedings of the International Snow Science Workshop at Sunriver*, September, 1998. Stevens Pass Ski Area, PO Box 98, Skykomish, Wa., 284-289.
- Föhn, P., 1987. The stability index and various triggering mechanisms. In *Avalanche formation, movement, and effects*, B. Salm and H. Gubler, ed. International Association of Hydrological Sciences, Publication No. 162, 195-207.

Föhn, P., 1992. Characteristics of weak snow layers or interfaces. *Proceedings of the International Snow Science Workshop at Breckenridge*, October, 1992. Colorado Avalanche Information Centre, Denver, Co. 160-170.

Föhn, P. and Camponovo, C., 1996. Improvements by measuring shear strength of weak layers. *Proceedings of the International Snow Science Workshop at Banff*, October, 1996. Canadian Avalanche Association, Revelstoke, B.C., 158-162.

Frontsys, 2001. Generalized Reduced Gradient. On the world wide web at: [www.optimalmethods.com](http://www.optimalmethods.com).

Geldsetzer, T., Jamieson, J.B., and Johnston, C.D., 1997. Visible changes in buried surface hoar over time. *Avalanche News* 52, 16-17.

Geldsetzer, T., Jamieson, J.B., Johnston, C.D., Johnson, B. and Johnson, G., 1999. Applied Snow and Avalanche Research Group Field Work Manual: Winter 1999-2000. Dept. of Civil Engineering, University of Calgary.

Geldsetzer, T. and Jamieson, J.B., 2000. Estimating dry snow density from grain form and hand hardness. *Proceedings of the International Snow Science Workshop at Big Sky*, October, 2000. American Avalanche Association, PO Box 1032, Bozeman, MT 59771, 121-127.

Hachikubo, A. and Akitaya, E., 1998. Daytime preservation of surface hoar crystals. *Annals of Glaciology* 26, 22-26.

Jamieson, J.B. and Geldsetzer, T., 1996. *Avalanche Accidents in Canada Volume 4: 1984-1996*. Canadian Avalanche Association, Revelstoke, B.C.

Jamieson, J.B. and Geldsetzer, T., 1999. Patterns in unexpected skier-triggered avalanches. *Avalanche News* 58, 7-17.

Jamieson, J.B., Geldsetzer, T. and Stethem, C., 2000. Case study of a deep slab instability and associated dry slab avalanches. *Proceedings of the International Snow Science Workshop at Big Sky*, October, 2000. American Avalanche Association, PO Box 1032, Bozeman, MT 59771, 101-108.

Jamieson, J.B. and Johnston, C.D., 1992. Snowpack characteristics associated with avalanche accidents. *Canadian Geotechnical Journal* 29, 862-866.

Jamieson, J.B. and Johnston, C.D., 1993. Shear frame stability parameters for large-scale avalanche forecasting. *Annals of Glaciology* 18, 268-273.

Jamieson, J.B. and Johnston, C.D., 1994. Monitoring a shear frame stability index and skier-triggered slab avalanches involving persistent snowpack weaknesses. *Proceedings of the International Snow Science Workshop 1994*. International Snow Science Workshop Committee, PO Box 49, Snowbird, Utah 84092, pp. 14-21.

- Jamieson, J.B. and Johnston, C.D., 1997. Mechanisms for strength changes of buried surface hoar layers. *Avalanche News* 53, 7-11.
- Jamieson, J.B. and Johnston, C.D., 1998. Refinements to the stability index for skier-triggered dry-slab avalanches. *Annals of Glaciology* 26, 296-302.
- Jamieson, J.B. and Johnston, C.D., 1999. Snowpack factors associated with strength change of buried surface hoar layers. *Cold Regions Science and Technology* 30, 19-34.
- Jamieson, J.B. and Johnston, C.D., 2001. Evaluation of the shear frame test for weak snowpack layers. *Annals of Glaciology* 32.
- Jamieson, J.B. and Schweizer, J., 2000. Texture and strength changes of buried surface hoar layers with implications for dry snow-slab avalanche release. *Journal of Glaciology* 46 (152), 151-160.
- Jamieson, J.B., 1995. *Avalanche prediction for persistent snow slabs*. PhD Thesis, Dept. of Civil Engineering, University of Calgary.
- Johnson, G., 2000. *Observations of faceted crystals in alpine snowpacks*. MSc Thesis, Dept. of Civil Engineering, University of Calgary.
- Kobayashi, T., 1961. The growth of snow crystals at low supersaturations. *Phil. Mag.* 6, 1363-1370.
- Lachapelle, E.R., 1980. The fundamental processes in conventional avalanche forecasting. *Journal of Glaciology* 26 (94), 75-84.
- Lang, R.M., Leo, B.R. and Brown, R.L., 1984. Observations on the growth process and strength characteristics for surface hoar. *Proceedings of the International Snow Science Workshop at Aspen*, October, 1984. Mountain Rescue-Aspen Inc., Aspen, CO., 188-195.
- Mathsoft, 1997. *S-Plus 4 Guide to Statistics*. Mathsoft, Inc., Seattle, WA.
- McClung, D.M. and Schaerer, P., 1993. *The Avalanche Handbook*. The Mountaineers, Seattle, WA.
- McClung, D.M., 1987. Mechanics of snow slab failure from a geotechnical perspective. *Avalanche Formation, Movement and Effects*, B. Salm and H. Gubler, ed. International Association of Hydrological Sciences, Publication No. 162, 475-507.
- Mendenhall, W. and Sincich, T., 1996. *A second course in statistics: Regression analysis*, 5<sup>th</sup> ed. Prentice-Hall, Inc. Upper Saddle River, NJ.

Meteo France, 1996. *CROCUS 2.2 user's guide*. Centre d'études de la neige, 1441 rue de la piscine, 38406 St Martin d'Herès CEDEX, France.

Mingo, L., 1996. *Assessment of the snow-cover numerical model CROCUS – Application to avalanches and hydrology*. MSc Thesis, Dept. of Civil Engineering, University of British Columbia.

Perla, R.I., 1982. Preparation of section planes in snow specimens. *Journal of Glaciology*, 28 (98): 199-204.

Perla, R.I. and Beck, T.M.H., 1983. Experience with shear frames. *Journal of Glaciology*, 29 (103): 485-491.

Roch, A., 1966. Les variations de la résistance de la neige. *Proceedings of the International Symposium on Scientific Aspects of Snow and Ice Avalanches*. Gentbrugge, Belgium, IAHS Publication, pp. 182-195.

Schleiss, V.G. and Schleiss, W.E., 1970. Avalanche hazard evaluation and forecast Rogers Pass, Glacier National Park. National Research Council of Canada, Technical Memorandum 98, 115-121.

Schweizer, J., Skjonsberg, D. and McMahon, B., 1996. Experience with stability evaluation for a surface hoar layer during winter 1995-1996 at Rogers Pass, British Columbia, Canada. *Proceedings of the International Snow Science Workshop at Banff*, October, 1996. Canadian Avalanche Association, Revelstoke, B.C., 126-128.

Schweizer, J., Jamieson, J.B., and Skjonsberg, D., 1998. Avalanche forecasting for transportation corridor and backcountry in Glacier National Park. *Proceedings of 25 Years of Snow Avalanche Research* (Voss, May 1998), edited by Erik Hestnes, Norwegian Geotechnical Institute, Publication 203, 238-244.

Schweizer, J. and Jamieson, J.B., 2001. Snow cover properties for skier-triggered avalanches. In press for *Cold Regions Science and Technology*.

Shapiro, L.H., Johnson, J.B., Sturm, M. and Blaisedell, G.L., 1997. Snow mechanics: Review of the state of knowledge and applications. US Army CRREL Report 97-3.

Sommerfeld, R.A., 1980. Statistical models of snow strength. *Journal of Glaciology* 26 (94), 217-223.

Statistica, 1999. Electronic manual. Statsoft, Tulsa, OK.

Statsoft, 1994. *Statistica Volume I: General Conventions and Statistics*. Statsoft, Tulsa, OK.

Stephens, L., 1998. *Beginning Statistics*. McGraw – Hill, New York, NY.

**APPENDIX**

**Mt. St. Anne Plot** Surface hoar layer buried 10-February-1997

Date	Age (days)	HS (cm)	24 hr load (mm)	Slab load (kPa)	H (cm)	Emin (mm)	Emax (mm)	TG (deg C/m)	T w l (deg C)	Thick (cm)	Measured shear strength (kPa)	Model predicted shear strength			
												Lagged Load (kPa)	Power Law (kPa)	Interval (start) (kPa)	Interval (end) (kPa)
14-Feb-97	4	289	20	0.26	30	3	9	1.6	-6.7	0.5	0.22	0.53	0.59	0.53	
15-Feb-97	5		12									0.65			
16-Feb-97	6		4									0.76			
17-Feb-97	7		6.4									0.88			
18-Feb-97	8		5.6									1.00			
19-Feb-97	9		9.6									1.11			
20-Feb-97	10	315	12	1.23	66.5	3	6	0.3	-5.2	1	0.66	1.23	1.40	1.44	0.94
21-Feb-97	11		8									1.19			
22-Feb-97	12		2.4									1.27			
23-Feb-97	13		0.4									1.35			
24-Feb-97	14	283	0	1.12	60	6	6	0.1	-5.3	0.5	1.72	1.51	1.93	1.58	1.74
25-Feb-97	15		0									1.56			
26-Feb-97	16		0.4									1.47			
27-Feb-97	17		8									1.42			
28-Feb-97	18		0									1.28			
01-Mar-97	19	305	4	1.64	61	1	3	0.8	-6.3	0.5	2.43	1.55	2.57	2.15	1.92
02-Mar-97	20		7									1.66			
03-Mar-97	21		5									1.90			
04-Mar-97	22		24									2.26			
05-Mar-97	23	275	0	1.52	86	1	3	0.4	-5.7	0.3	2.77	1.58	3.08	1.96	2.29
06-Mar-97	24		9.6									2.10			
07-Mar-97	25		16									2.15			
08-Mar-97	26	355	12	1.96	116	1	4	0.1	-5.3	0.3	2.27	2.67	3.46		2.14

Mt. St. Anne Plot Surface hoar layer buried 30-December-1999

Date	Age (days)	HS (cm)	24 hr load (mm)	Slab load (kPa)	H (cm)	Emin (mm)	Emax (mm)	TG (deg C/m)	T wl (deg C)	Thick (cm)	Measured shear strength (kPa)	Model predicted shear strength		
												Lagged Load (kPa)	Power Law (kPa)	Interval (kPa)
05-Jan-00	6	254	7.6	0.50	48	4	15	0.1	-7.8	2	0.46	0.28	0.50	0.28
06-Jan-00	7		2.3									0.32		
07-Jan-00	8		4.6									0.36		
08-Jan-00	9		16.5									0.40		
09-Jan-00	10		5.3									0.44		
10-Jan-00	11		7									0.48		
11-Jan-00	12		0									0.52		
12-Jan-00	13	285	3.6	1.49	104	10	20	0.5	-6	2	1.46	0.95	1.04	1.37
13-Jan-00	14		2.3									0.90		
14-Jan-00	15		2									0.76		
15-Jan-00	16	290	8.1	1.77	111	10	15	0.6	-6.1	2	1.32	0.80	1.26	1.54
16-Jan-00	17		6.4									0.71		
17-Jan-00	18		23.2									1.25		
18-Jan-00	19		8									1.31		
19-Jan-00	20		0									1.48		
20-Jan-00	21		0									1.22		
21-Jan-00	22		0.762									1.45		
22-Jan-00	23	270	0	2.23	119	10	10	0.5	-5.5	1.8	1.88	1.42	1.78	2.34
23-Jan-00	24		0.1									1.45		
24-Jan-00	25		0.1									1.31		
25-Jan-00	26		0									1.50		
26-Jan-00	27		4.4									1.32		
27-Jan-00	28		0									1.45		
28-Jan-00	29		0.1									1.49		
29-Jan-00	30	269	0	2.21	103	10	15	0.6	-4.7	1.7	2.24	1.45	2.29	2.49